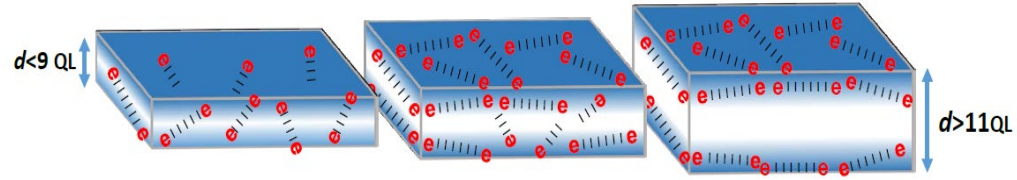
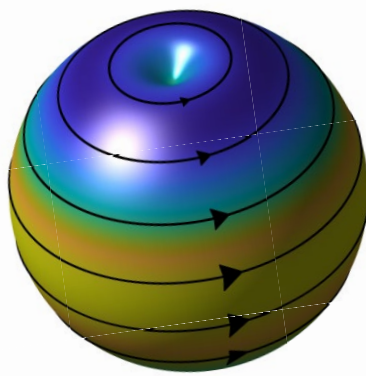


New twists in the research of strongly correlated electronic systems

Chung-Yu Mou
National Tsing Hua University
Taiwan



Outline:



- A recent puzzle from quantum oscillation experiment (Phys. Rev. B 101, 115102, 2020; Phys. Rev. B, 106, 195107, 2022)
- Exotic superconductivity that can arise in topological materials
 - Topological Kondo superconductivity (Communication Physics 7, 253, 2024)
 - Geometry induced topological superconductivity (Phys. Rev. B 103, 014508, 2021)
 - Flat band superconductivity, charge density wave and superconducting pair density wave state (Phys. Rev. B 98, 205103, 2018, Phys. Rev. X 11, 041038, 2021)
- Conclusion and summary

Collaborators:

Theory: Chia-Hsin Chen (NTHU, Taiwan)

Po-Hao Chou (NCTS, Taiwan)

Yung-Yeh Chang (NYCTU, Taiwan)

Chung-Hou Chung (NYCTU, Taiwan)

T. K. Lee (Academia Sinica, Taiwan)

Feng Xu (Shaanxi Univ. of technology, China)

Experiment:

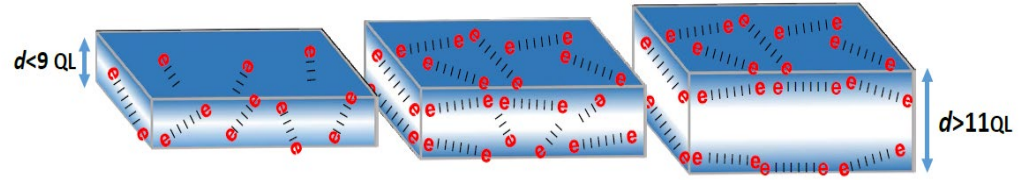
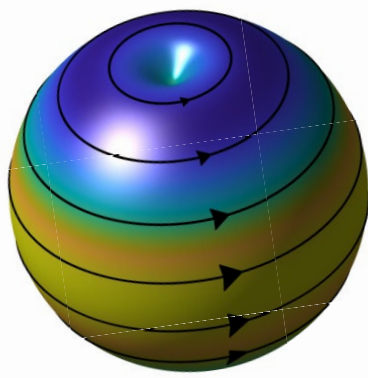
M.N. Ou, Yang-Yuan Chen (Academia Sinica, Taiwan)

Sergey R. Harutyunyan (Institute for Physical Research,
NASRA, Armenia)

W.H. Tsai, F.Y. Chiu C.H. Chien, P.C. Lee, Y.C. Chang
(Academia Sinica, Taiwan)

Di-Jing Huang (NSRRC), Atsushi Fujimori (U. of Tokyo)

Outline:



- A recent puzzle from quantum oscillation experiment (Phys. Rev. B 101, 115102, 2020; Phys. Rev. B, 106, 195107, 2022)

Outline:

- A recent puzzle: quantum oscillation experiment

PHYSICS TODAY

[HOME](#)

[BROWSE](#)▼

[INFO](#)▼

[RESOURCES](#)▼

[JOBS](#)

DOI:10.1063/PT.5.7188

20 Jul 2015 in [Research & Technology](#)

An insulator with conducting electrons?

[View Article Online](#) | [Download Full Text](#) | [View Article PDF](#) | [View Article HTML](#)

Quantum oscillation

-- has long been known as an experimental technique to map out **the Fermi surface in metals**.

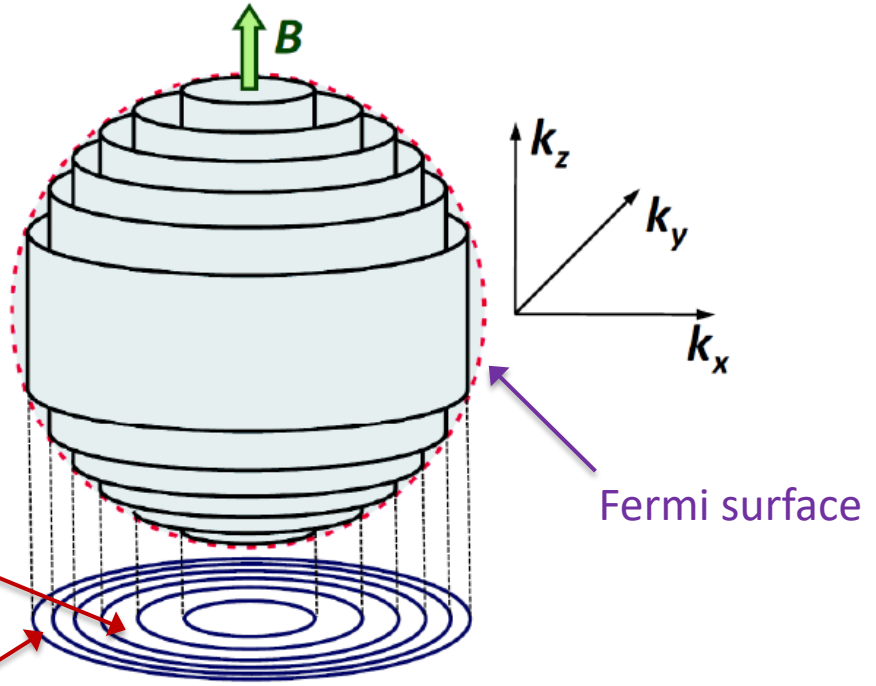
$$\epsilon_n = \left(n + \frac{1}{2} \right) \hbar\omega_c + \frac{\hbar^2}{2m_e} k_{\parallel}^2$$

$$\frac{\hbar^2}{2m_e} (k_x^2 + k_y^2)$$

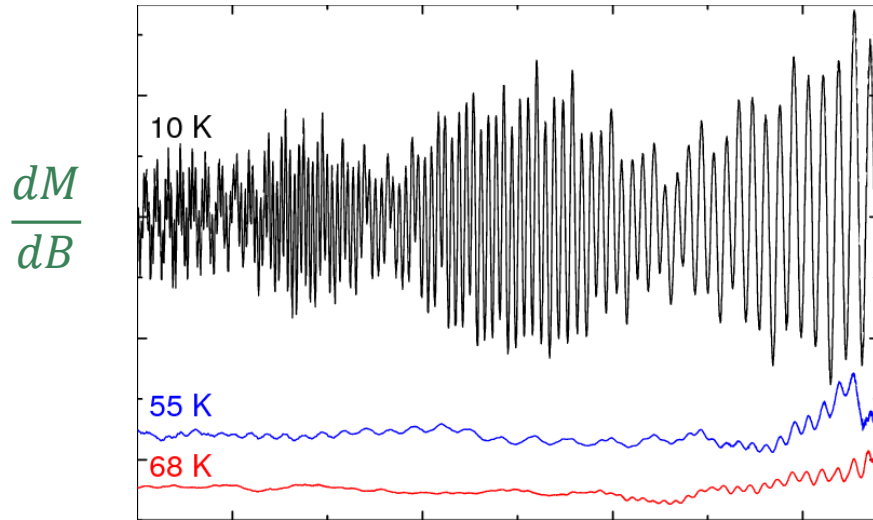
$$S_n = (n + \gamma) \frac{2\pi e}{\hbar} B$$

$$S_{n+1}(B) = S_n(B') = S_F$$

$$\rightarrow \Delta \frac{1}{B} = \frac{1}{B} - \frac{1}{B'} = \frac{2\pi e}{\hbar S_F}$$



de Haas–van Alphen oscillation

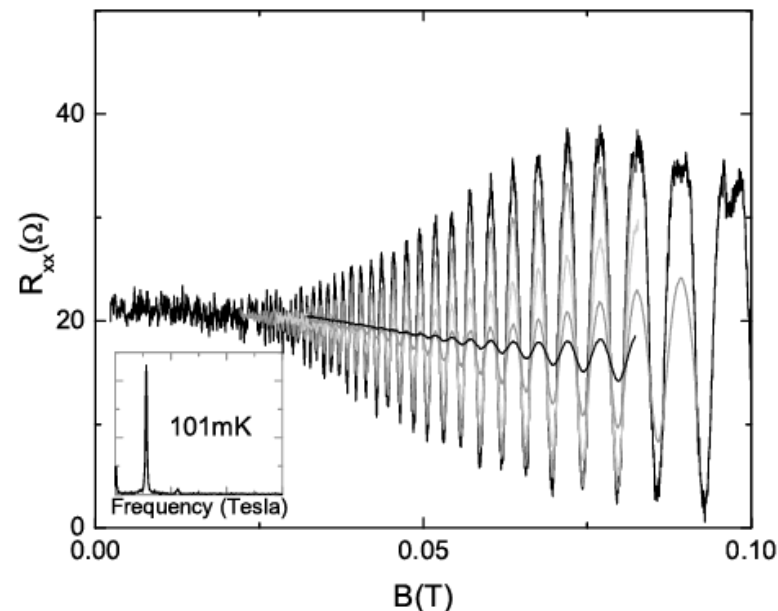


shape-memory alloy AuZn
PRL **94**, 116401 (2005)

Lifshitz-Kosevich (LK) theory

$$M \propto \frac{eFk_BTV}{\sqrt{2\pi HA''}} \sum_{p=1}^{\infty} p^{-\frac{3}{2}} R_T(p) R_D(p) R_s(p) \times \sin \left[2\pi p \left(\frac{F}{H} - \frac{1}{2} \right) \pm \frac{\pi}{4} \right]$$

Shubnikov-de Haas oscillation



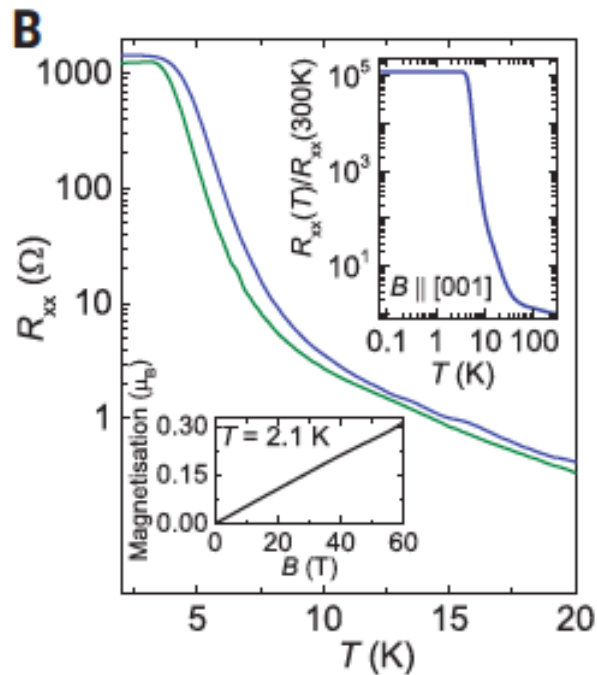
$$A'' = \left| \frac{\partial^2 A}{\partial k_z^2} \right|_{k_z=k_{extr}}$$

$$R_T(p) = \frac{\pi\kappa}{\sinh \pi\kappa} = \frac{2\pi^2 p k_B T / \beta^* H}{\sinh (2\pi^2 p k_B T / \beta^* H)}$$

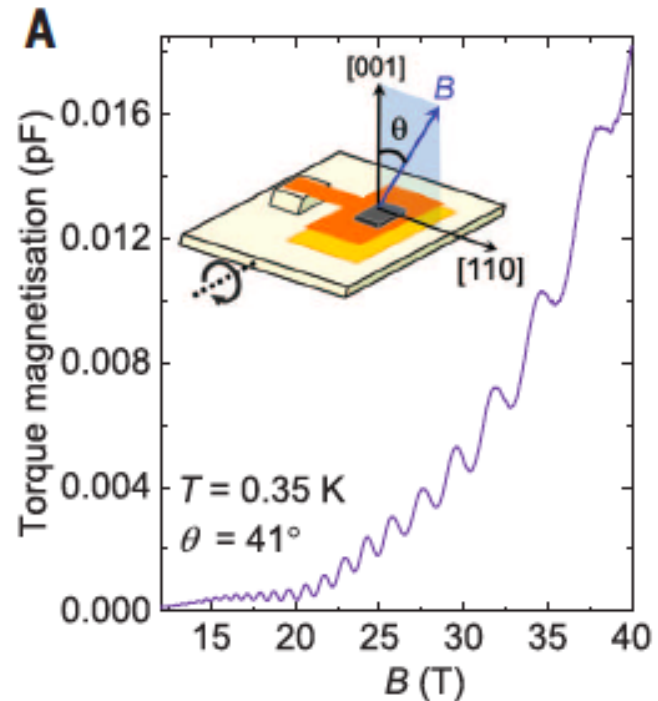
2DEG in GaAs/AlGaAs at different T
(101mK, 180mK...)
PRL **94**, 016405 (2005)

Quantum Oscillations in Kondo insulator SmB_6

They were, however, observed in Kondo insulators. This poses as a great challenge to explain it.

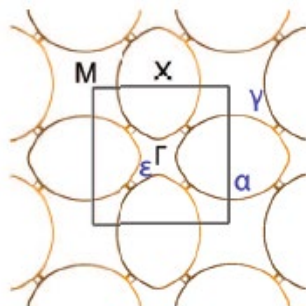
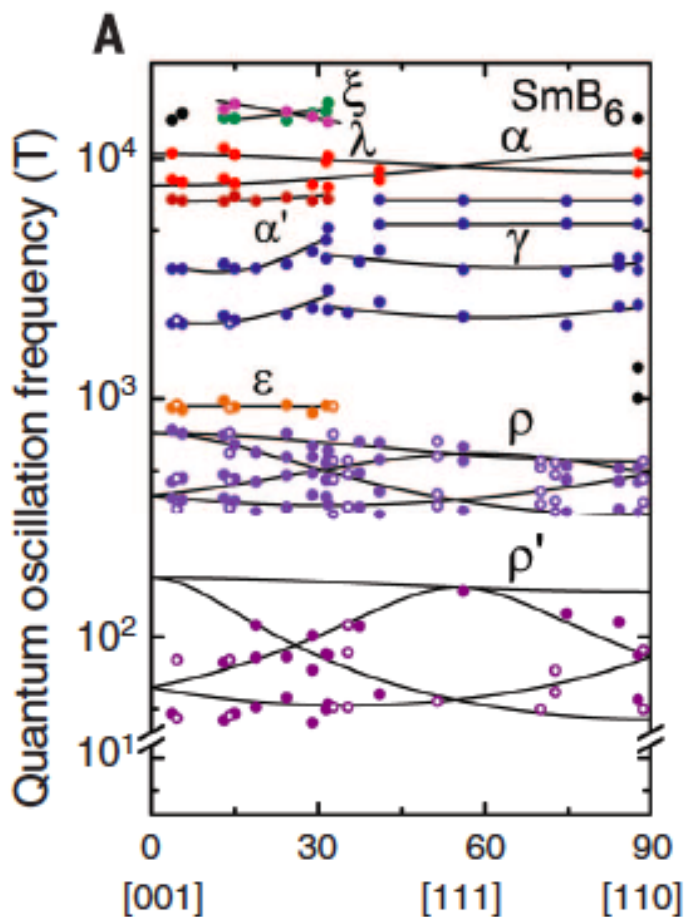


Insulator!



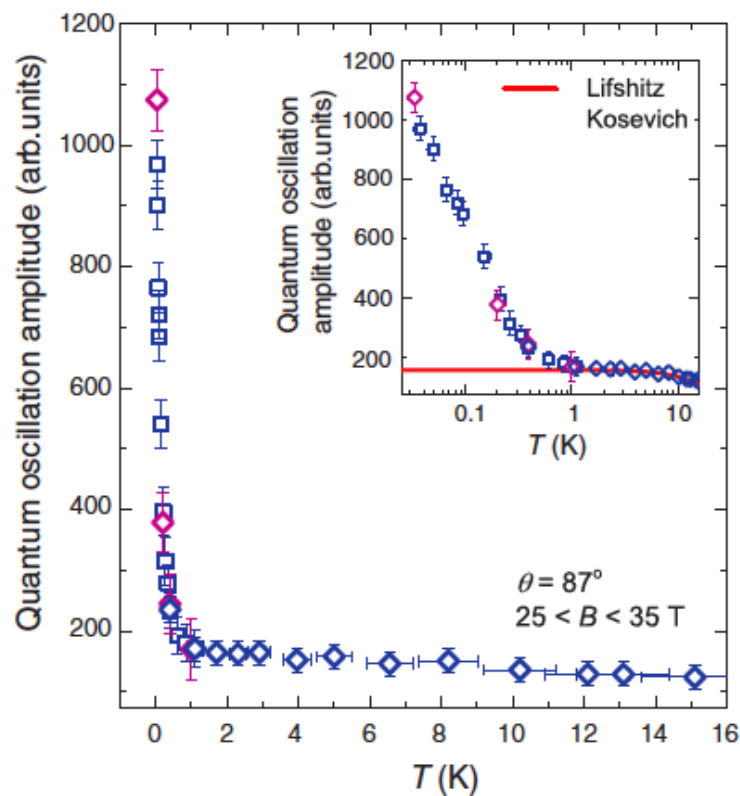
S. E. Sebastian et al,
Science 349, 287(2015)

Fermi Surface and unconventional temperature dependence



DFT calculation

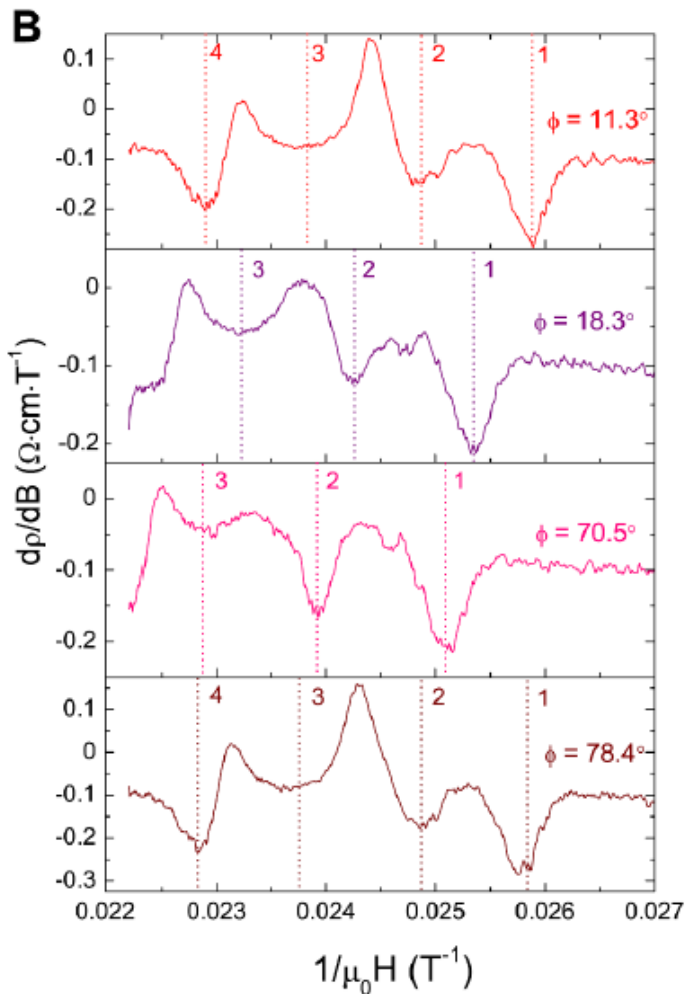
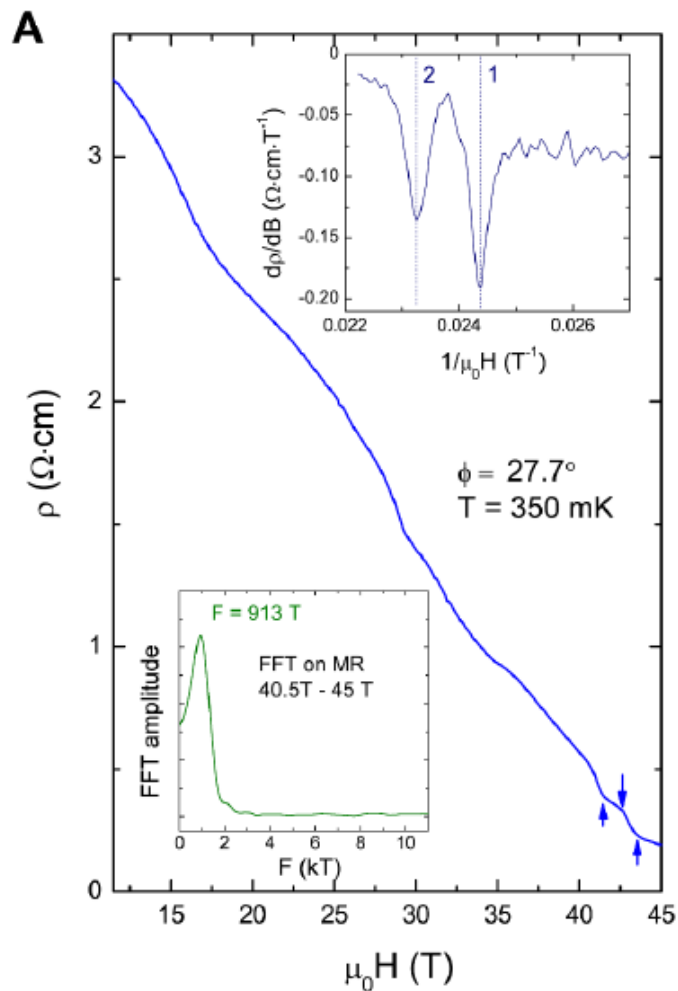
S. E. Sebastian et al,
Science 349, 287(2015)



Observed Fermi Surface

Quantum Oscillations in resistivity derivative

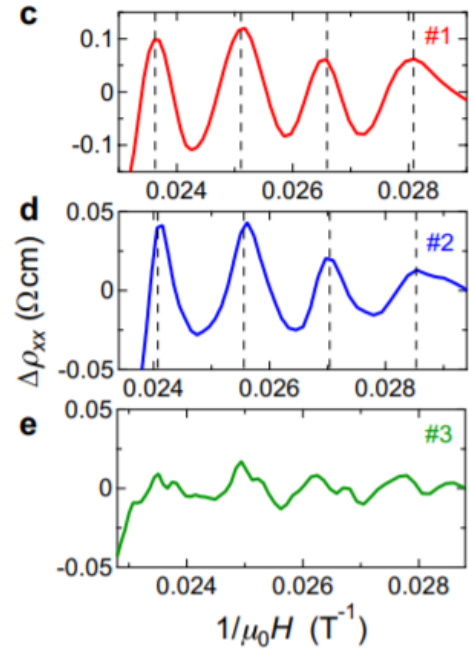
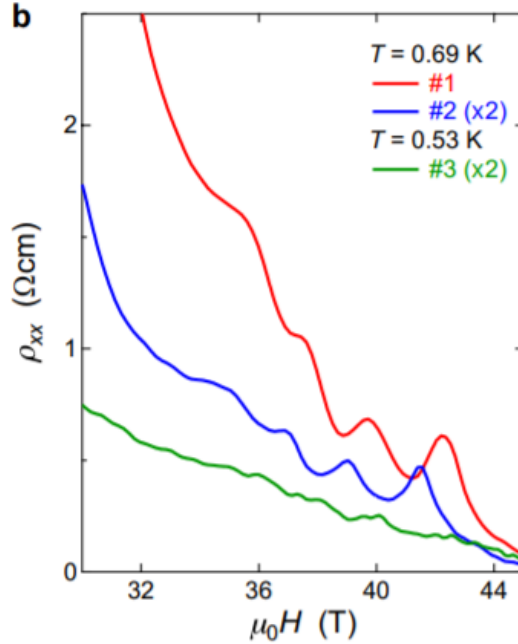
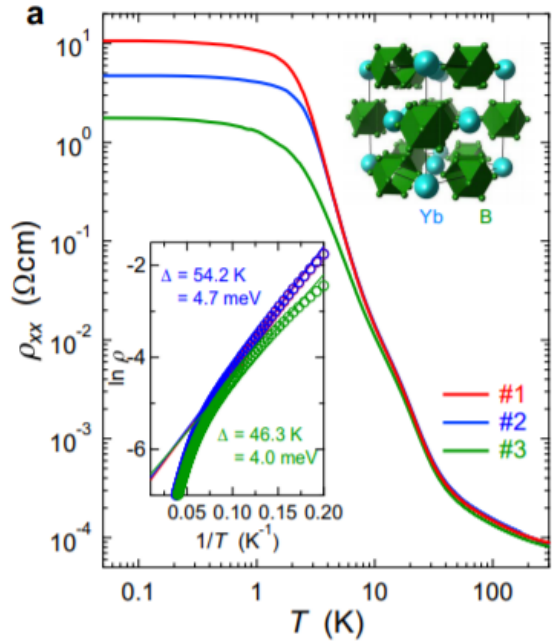
Y. Matsuda, and L. Li etc, Science 362, 65 (2018).



Kondo insulator YbB_{12}

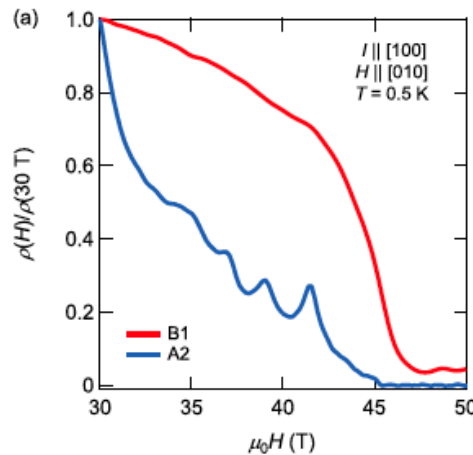
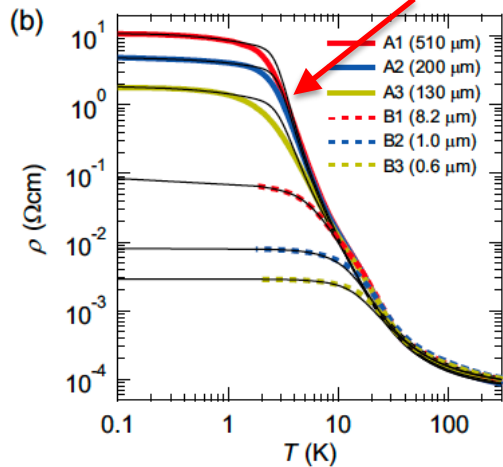
(ytterbium
dodecaboride)

Kondo Insulator YbB_{12}



ρ is larger, oscillation amplitude is larger

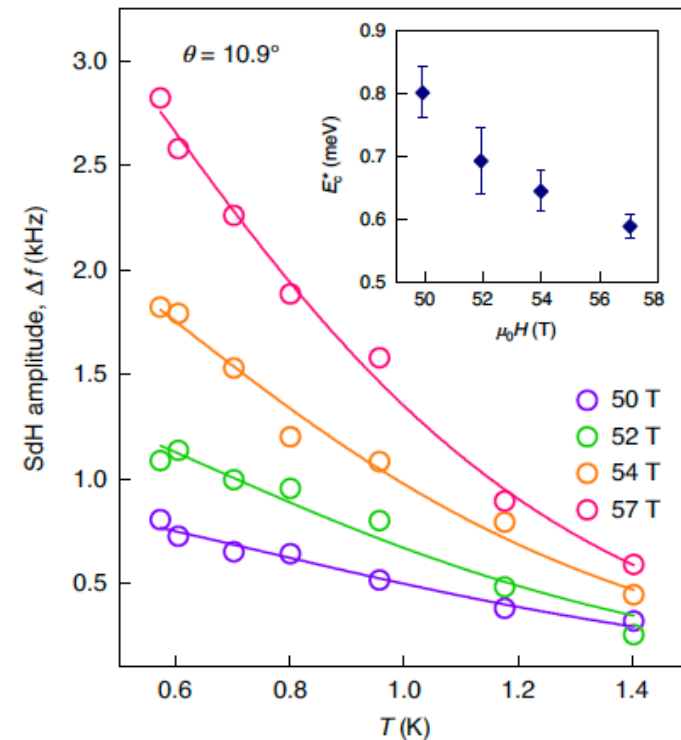
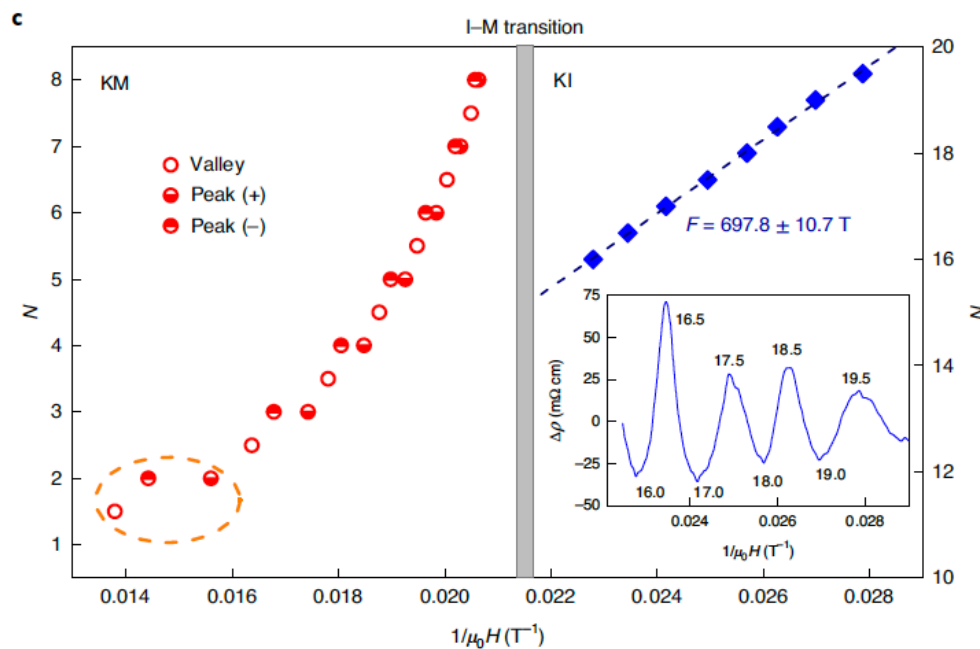
Sato, Y. et al. *Nat. Phys.* **15**, 954–959 (2019).



J. Phys. D: Appl. Phys. **54**, 404002 (2021)

A2=single crystal

More recent data on Kondo insulator YbB_{12} : Pulse Magnetic field up to 75T



Under strong fields, it's like a metal in
agree with the LK theory

Many theories are proposed

*Due to narrow gap

J. Knolle and N. R. Cooper, Phys. Rev. Lett. 115, 146401 (2015); L. Zhang, X. Y. Song, and F. Wang, Phys. Rev. Lett. 116, 046404 (2016).

*Due to surface state

Kondo breakdown, O. Erten, P. Ghaemi, and P. Coleman, Phys. Rev. Lett. 116, 046403 (2016).

*Due to neutral Fermion

Inti Sodemann, Debanjan Chowdhury, T. Senthil, Phys. Rev. B 97, 045152 (2018)

Neutral fermions in mixed-valence insulators

C. M. Varma, Phys. Rev. B 102, 155145, 2020

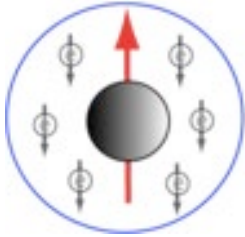
*Bulk scalar Majorana Fermi Liquid

arXiv:1507.03477, G. Baskaran

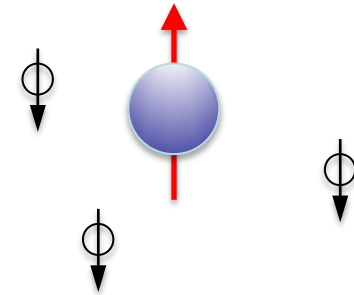
but none can explain all features observed in expt.

Our theory (Phys. Rev. B 101, 115102, 2020)

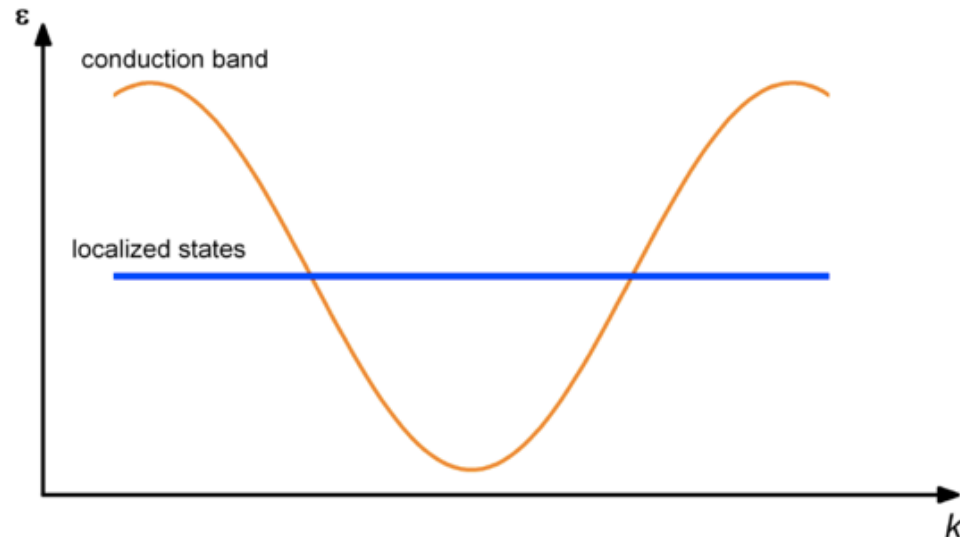
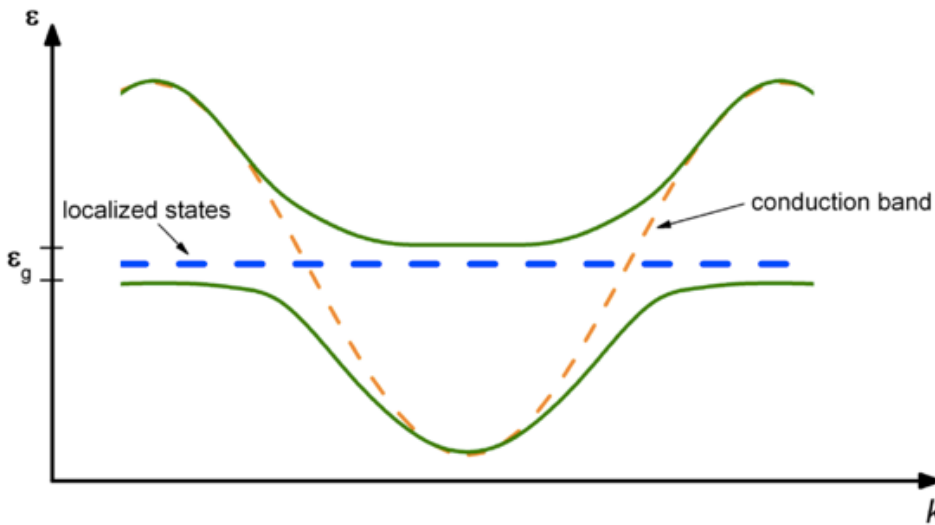
Kondo screening itself under **goes oscillation**
- non-rigidity of band enables **the oscillations**



$$T < T_K$$



$$T > T_K$$



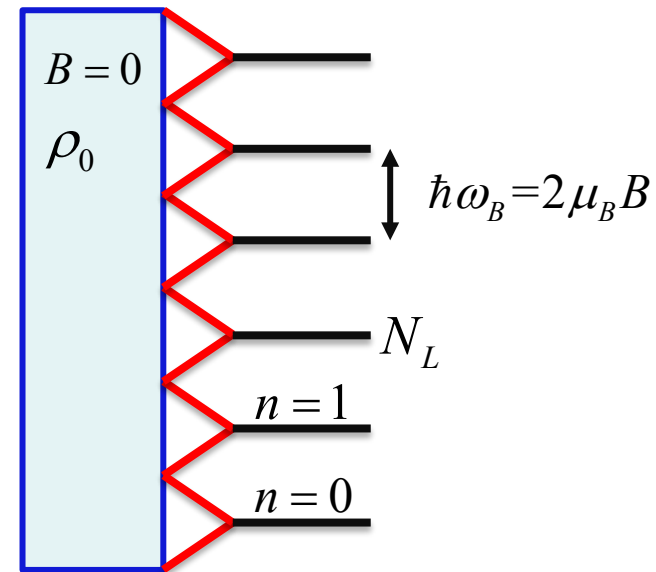
New ingredient: Landau quantization (2D), DOS is discrete

$$\frac{\vec{p}^2}{2m} \rightarrow \frac{(\vec{p} + e\vec{A}/c)^2}{2m}.$$

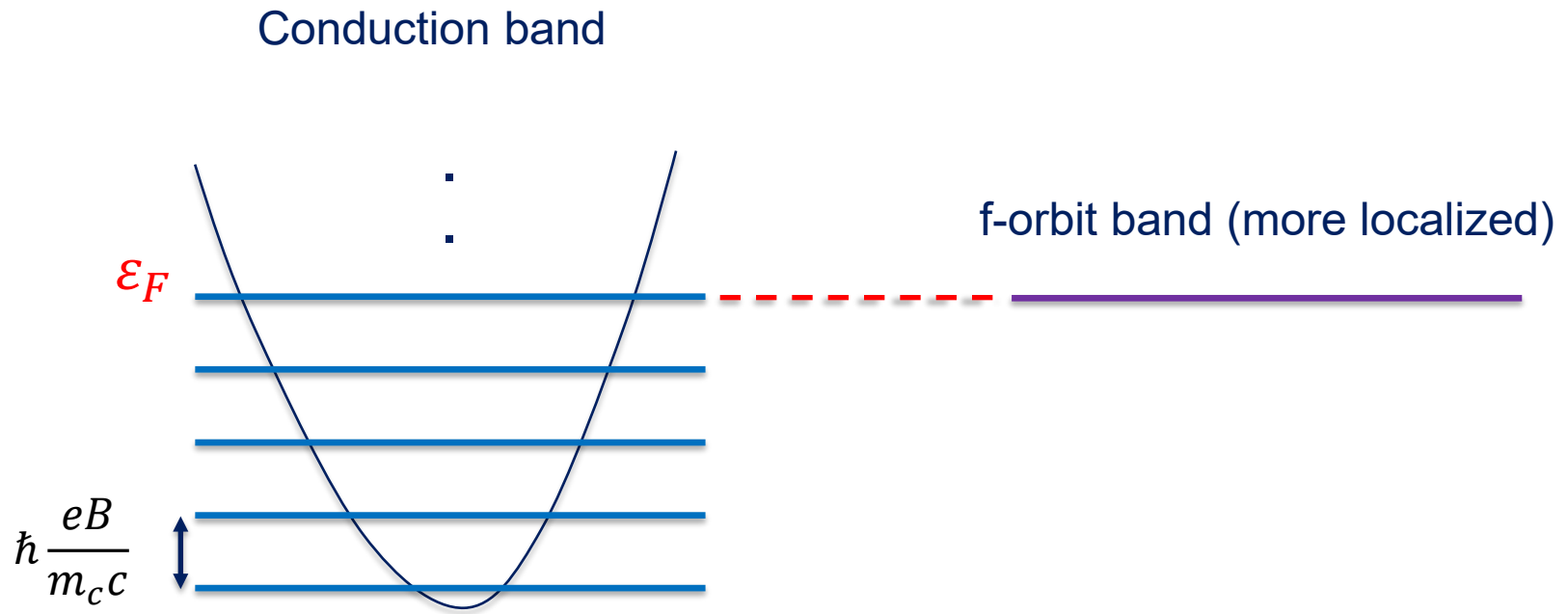
$$\varepsilon_k = \frac{k^2}{2m} \rightarrow \varepsilon_n = \hbar\omega_B \left(n + \frac{1}{2}\right), \hbar\omega_B = \frac{eB}{mc}.$$

$$\text{density of states per volume : } \rho_0 = \frac{m}{2\pi\hbar^2}$$

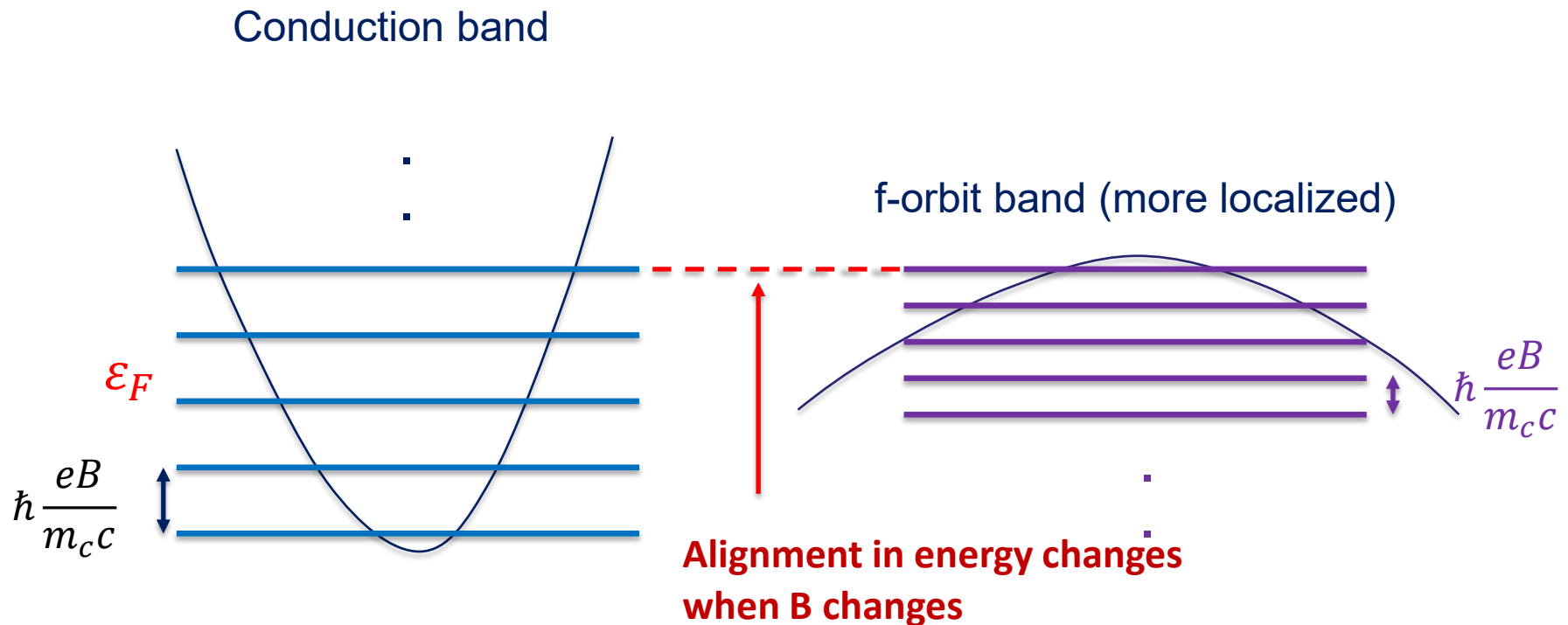
$$\rightarrow \text{Landau degeneracy per volume : } N_L / L^2 = \rho_0 \hbar\omega_B$$



Kondo screening itself under goes oscillation
-- due to periodical alignment of Landau levels
with f orbit when magnetic field B changes



More realistic model with finite band width f-orbit band



Slave-boson mean field theory

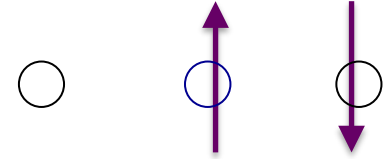
$$H = \sum_{k\sigma} \xi_k c_{k\sigma}^\dagger c_{k\sigma} + \sum_{k\sigma} \xi_k^d d_{k\sigma}^\dagger d_{k\sigma} + \sum_{k\sigma} V_k^{\sigma\sigma'} c_{k\sigma}^\dagger d_{k\sigma'} + h.c. + U \sum_i n_{i\uparrow}^d n_{i\downarrow}^d$$

$$V_{\mathbf{k}} = v_0 I \text{ (even parity) or } 2\lambda_{so} \sum_{i=x,y,z} \sigma_i \sin k_i$$

$$d_{i\sigma}^\dagger = f_{i\sigma}^\dagger b_i$$

$$1 = \sum_{\sigma} f_{i\sigma}^\dagger f_{i\sigma} + b_i^\dagger b_i$$

$\langle b_i \rangle = r$ (holon condensate)



$f_{i\sigma}^\dagger =$ spinon

Lagrangian multiplier:

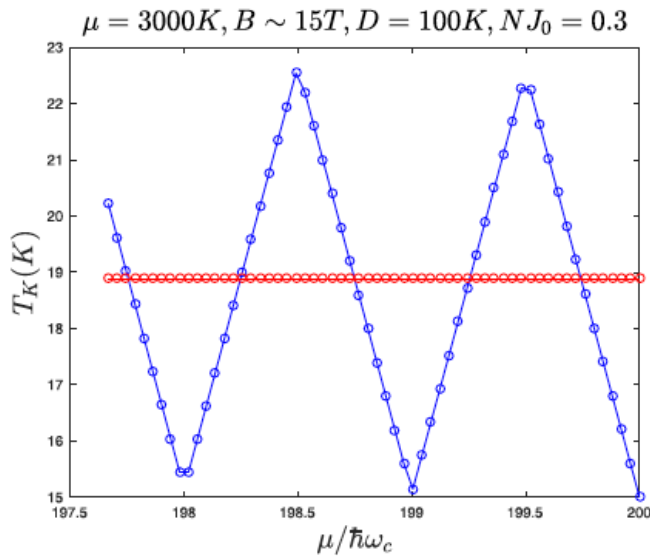
$$\sum_{i\sigma} \lambda_i (f_{i\sigma}^\dagger f_{i\sigma} + b_i^\dagger b_i - 1), \lambda$$

$$\xi_k \rightarrow -\mu_c(k_z) + \hbar\omega_c(n + \frac{1}{2})$$

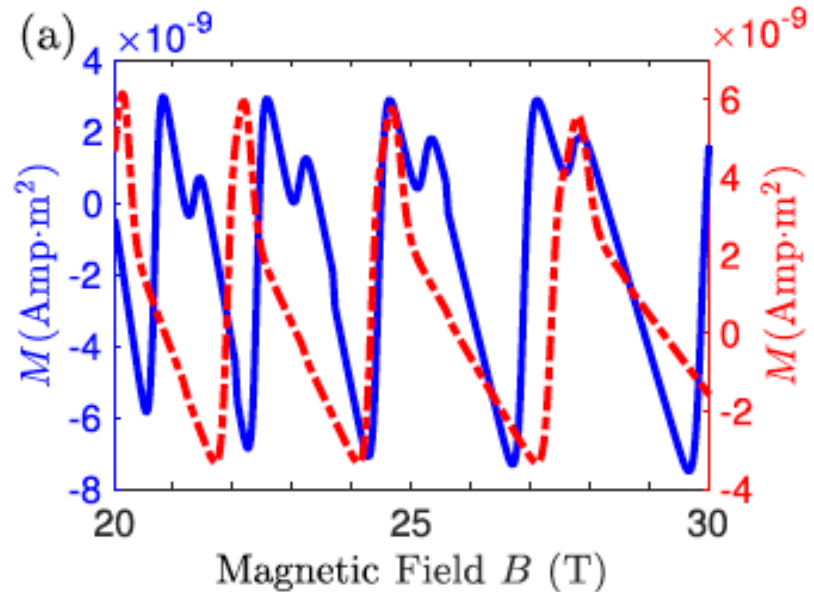
$$\xi_k^d \rightarrow -\mu_f(k_z) - \hbar\omega_f(m + \frac{1}{2})$$

Solve λ and r self-consistently

Explain important features observed in Experiments



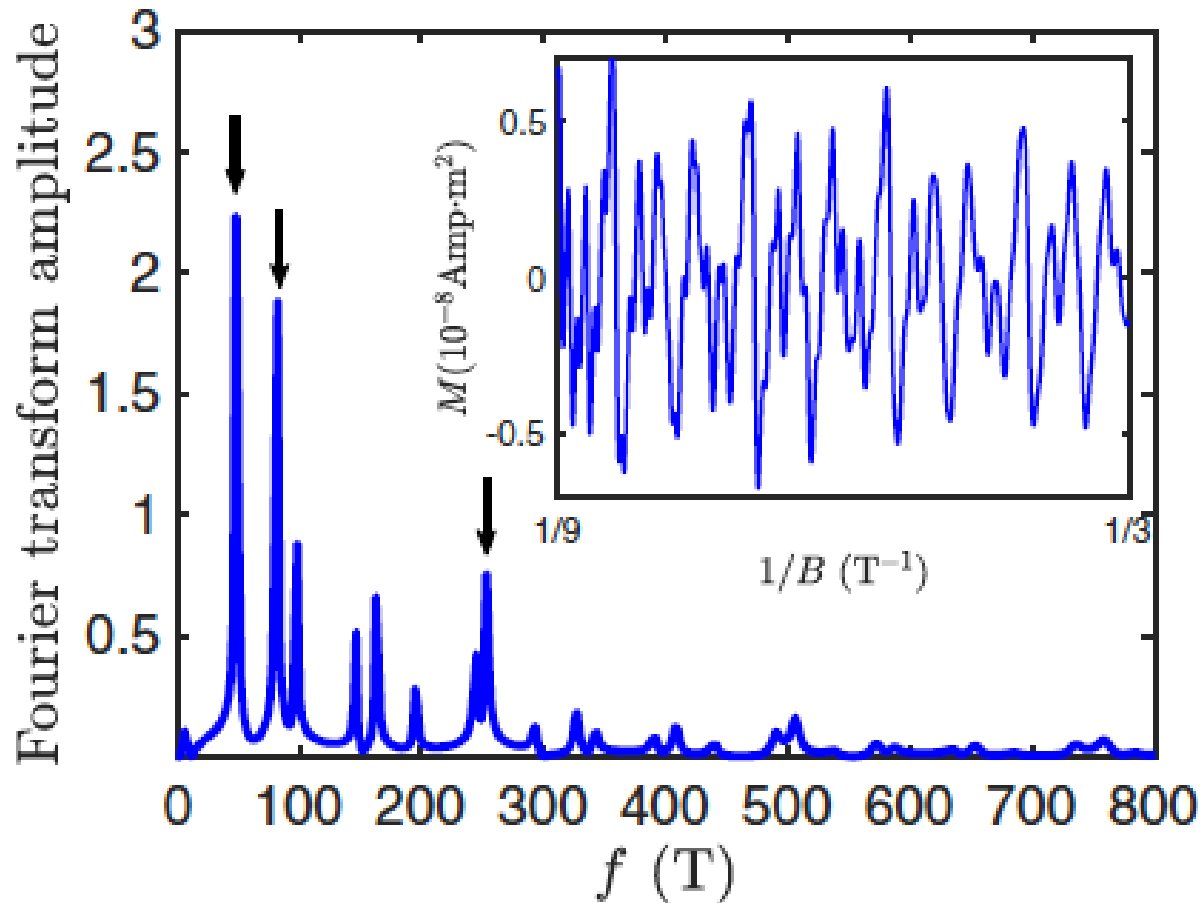
Oscillation of Kondo screening for a single impurity



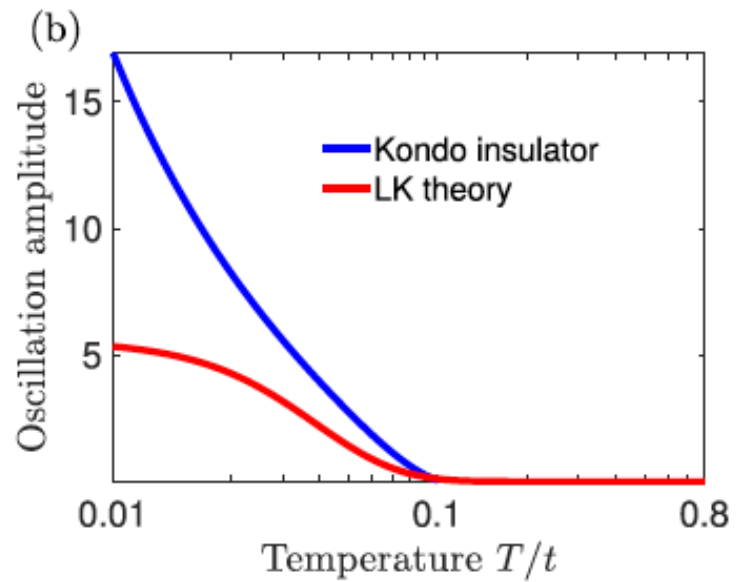
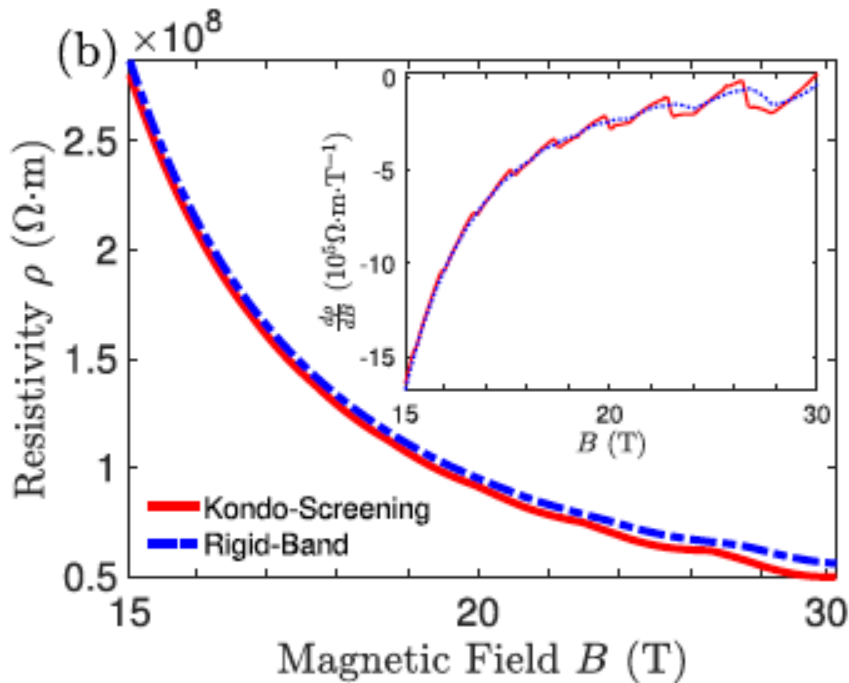
Quantum oscillation in magnetization (moment) for odd (blue)/even (red) parity hybridization.

amplitude $\sim 10^{-8} \text{ Am}^2$ consistent with 0.001pF observed in Cantilever magnetometer

Exhibiting Fermi surface



Fourier transformation of quantum oscillation in M when there are **3 conduction-band sections**, denoted by α , β , and γ . **Arrows** indicate frequencies that correspond to **Fermi surface areas: 55.2T, 92T, and 276T**.
Inset: quantum oscillations of M versus $1/B$

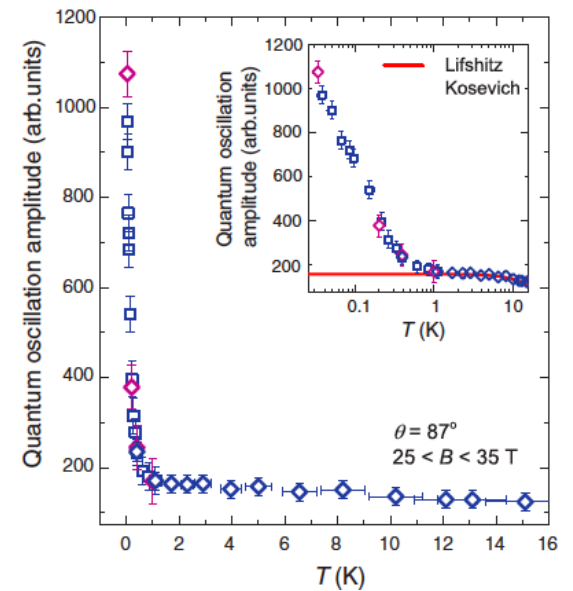


Temperature dependence

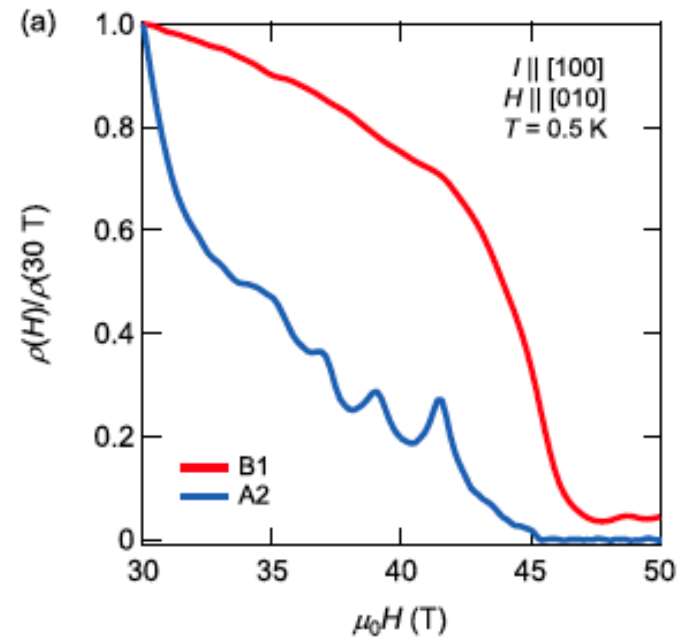
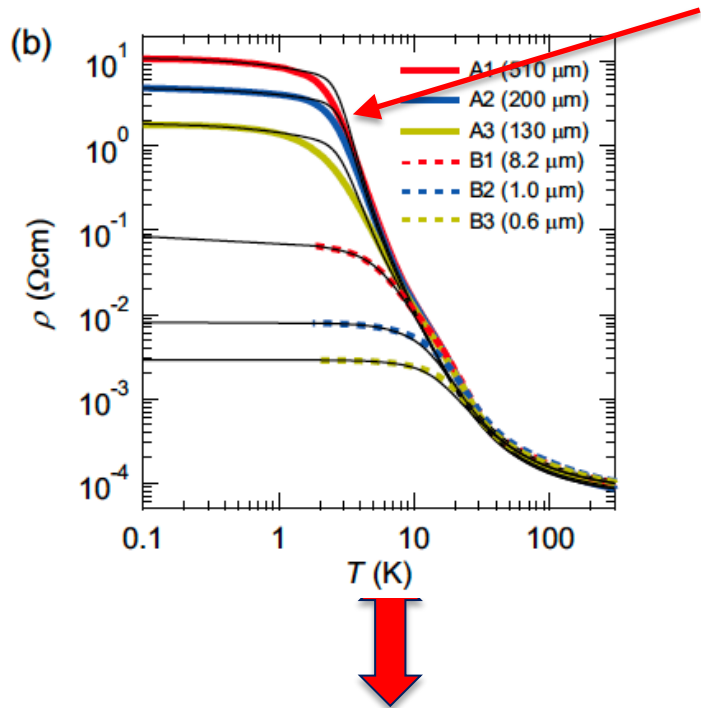


expt

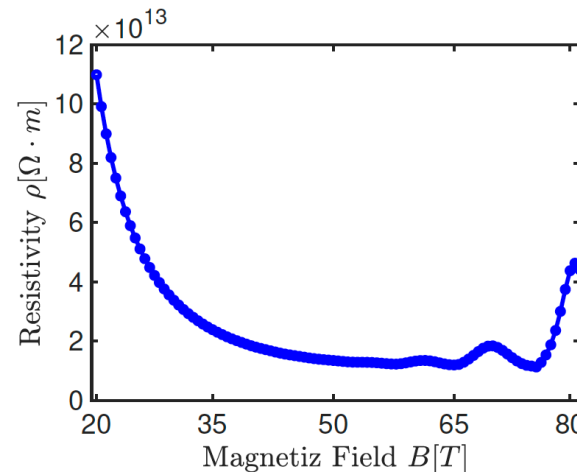
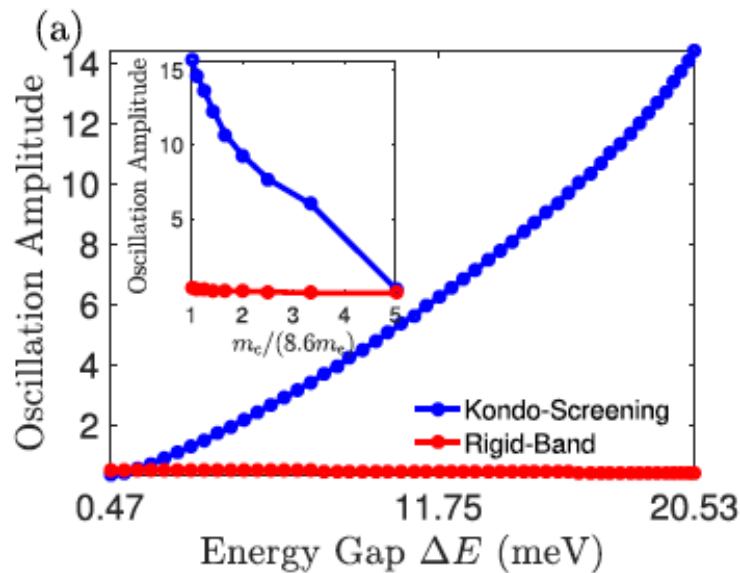
Derivative of resistivity shows oscillation



ρ is larger, oscillation amplitude is larger



Our interpretation: it indicates Kondo break down around 45 T ($r \rightarrow 0$ seen in our numerical result)



Nor exactly the same
 But in the right
 direction

What are phases that oscillate?

(Phys. Rev. B, 106, 195107, 2022)

What is the ground state for dilute magnetic impurities in Landau quantized system?

(Previous researches for Kondo impurities in magnetic field focus on the Zeeman splitting interaction of impurity, where the conduction band is still treated as continuous band.)

Model Hamiltonian

$$H = H_c + H_V + H_d$$

$$H_c = \sum_{\sigma} \int C_{\bar{r}\sigma}^{\dagger} \frac{1}{2m_e} \left(\bar{p} + \frac{e\vec{A}}{c} \right)^2 C_{\bar{r}\sigma} d\bar{r} + g_c \mu_B B \int s_{c,r}^z d\bar{r}$$

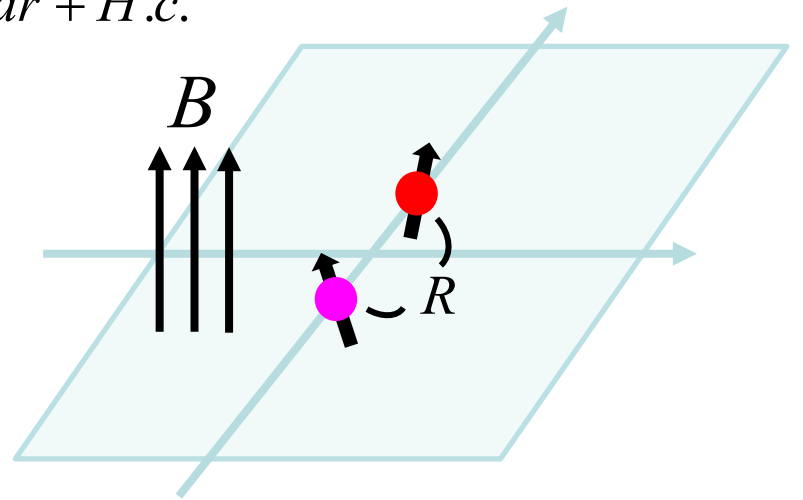
$$H_d = \xi_d \sum_{\sigma} \left(d_{1\sigma}^{\dagger} d_{1\sigma} + d_{2\sigma}^{\dagger} d_{2\sigma} \right) + U \left(n_{1\uparrow}^d n_{1\downarrow}^d + n_{2\uparrow}^d n_{2\downarrow}^d \right) + g_d \mu_B B (s_{d_1}^z + s_{d_2}^z)$$

$$H_{hyb} = Va \sum_{\sigma} \int C_{\bar{r}\sigma}^{\dagger} \left(\delta(\bar{r} - \bar{r}_1) d_{1\sigma} + \delta(\bar{r} - \bar{r}_2) d_{2\sigma} \right) d\bar{r} + H.c.$$

$$\vec{A} = (0, Bx, 0)$$

$$\bar{r}_1 = (0, R/2)$$

$$\bar{r}_2 = (0, -R/2)$$



Model Hamiltonian in basis of Landau level

Hybridization term

$$H_V = \frac{\tilde{V}}{\sqrt{L}} \sum_{\{n\}, k_y \sigma} \phi_n(x_k) e^{ik_y R} d_\sigma^\dagger c_{nk_y \sigma} + \text{H.c.} \quad \Rightarrow \quad \left(\frac{\Gamma \varepsilon_B}{\pi} \right)^{1/2} \left(\sum_{\{n\}, \sigma} d_\sigma^\dagger A_{n\sigma} + \text{H.c.} \right), \quad L \gg l_B$$

$$A_{n\sigma} = \sqrt{\frac{L}{N_L}} \sum_{k_y} e^{ik_y R} \phi_n(x_k) c_{nk_y \sigma}$$

$$H_1 = U d_\uparrow^\dagger d_\uparrow d_\downarrow^\dagger d_\downarrow + \sum_{\sigma} \xi_\sigma^d d_\sigma^\dagger d_\sigma + \sum_{\{n\}, \sigma} \xi_{n\sigma}^c A_{n\sigma}^\dagger A_{n\sigma} + \left(\frac{\Gamma \varepsilon_B}{\pi} \right)^{1/2} \left(\sum_{\{n\}, \sigma} d_\sigma^\dagger A_{n\sigma} + \text{H.c.} \right)$$

$$\rho J = \frac{\Gamma}{\pi} \left(\frac{1}{|U + \xi_d|} + \frac{1}{|\xi_d|} \right)$$

Landau Level $\hbar \omega \left(n + \frac{1}{2} \right) - \mu$

$$\Gamma = \rho \pi V^2$$

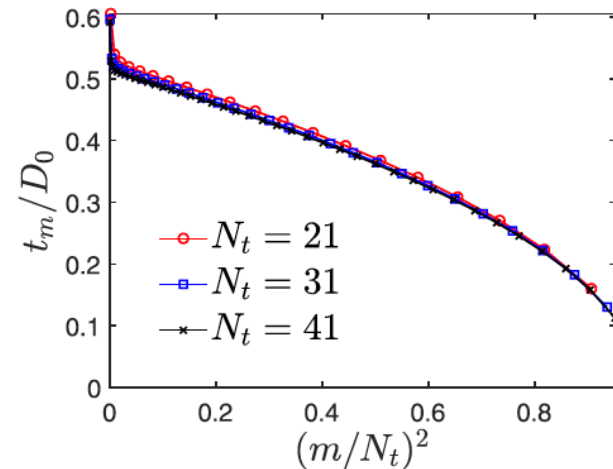
Reduction to a universal 1D chain

$$\sum_{n\sigma} \xi_{n\sigma}^c A_{n\sigma}^\dagger A_{n\sigma} \quad \Rightarrow \quad \sum_{m=1,\sigma}^{N_t} \epsilon_m f_{m\sigma}^\dagger f_{m\sigma} + t_m (f_{m\sigma}^\dagger f_{m+1\sigma} + \text{H.c.})$$

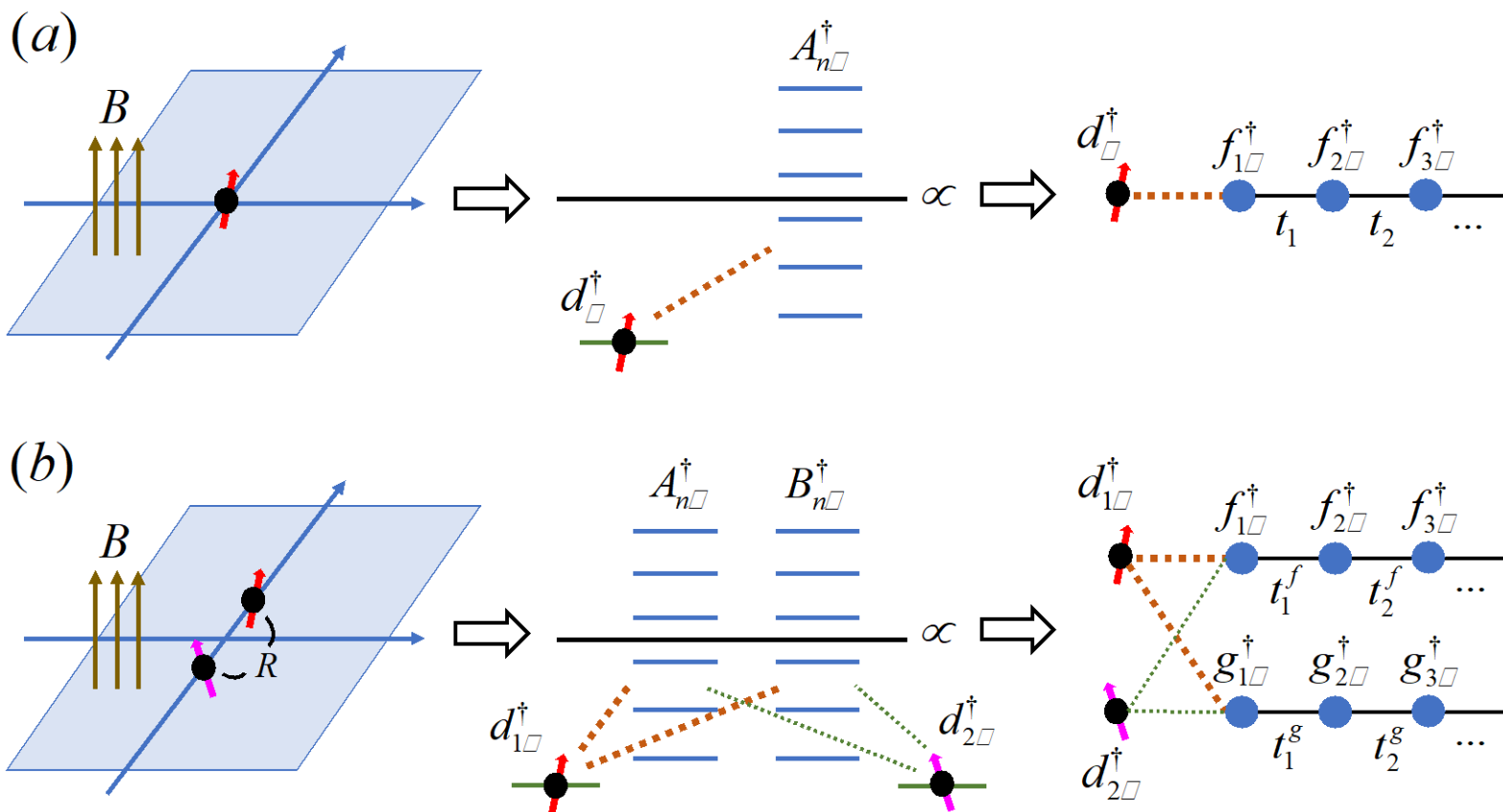
Transformation matrix from $A_{n\sigma}$ to $f_{m\sigma}$: $v_{n,m}$

$$\begin{pmatrix} \epsilon_1 & t_1 & & \\ t_1 & \epsilon_2 & t_2 & \\ & t_2 & \dots & \end{pmatrix} \begin{pmatrix} v_{1,n} \\ v_{2,n} \\ \dots \end{pmatrix} = \xi_n \begin{pmatrix} v_{1,n} \\ v_{2,n} \\ \dots \end{pmatrix}$$

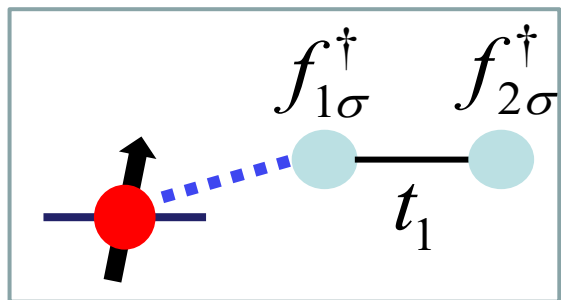
Scaling form of solution



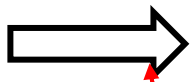
Universal 1D chains



Schematic NRG procedure



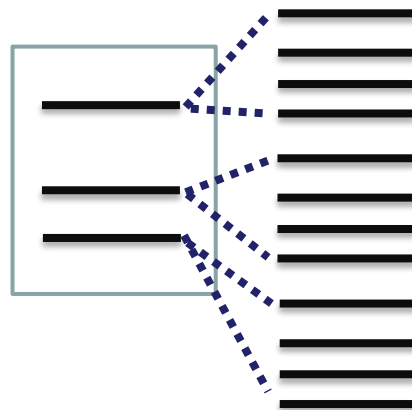
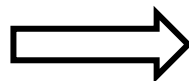
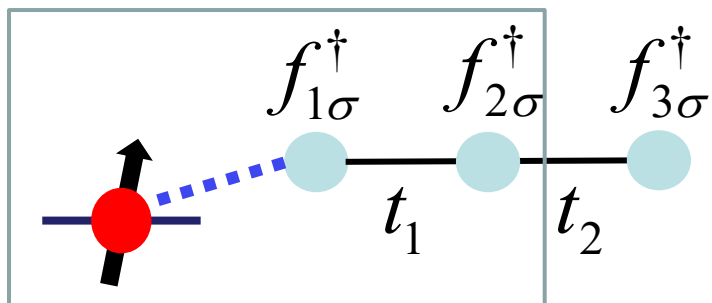
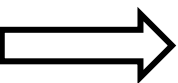
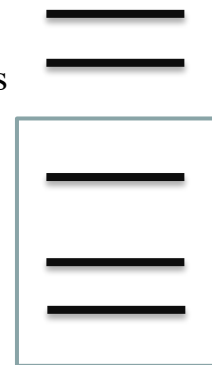
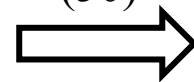
Exact diagonalization



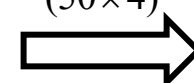
Exact eigen-energies and states (4^3)



drop high energy states (50)



Exact diagonalization (50×4)

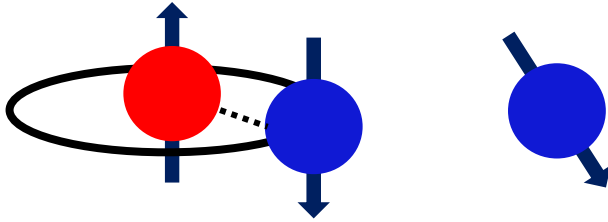


Results: Zero field

Zero field

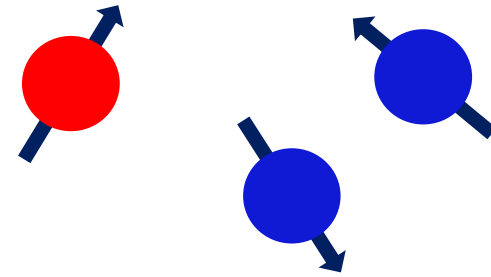
Singlet

(Screened states):



Doublet

(Unscreened state):



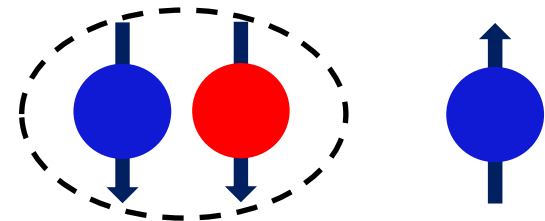
In the presence of Zeeman splitting and non-vanishing B field

Initial state before screening $S_z = -1$

or $S_z = -1/2$

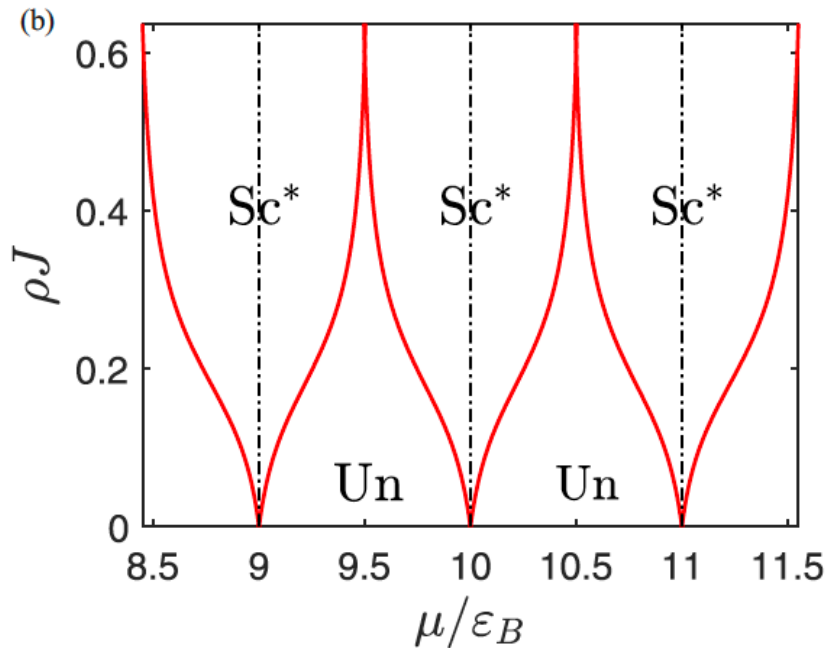
($S_{z,imp} = -1/2$, $S_{z,c} = 0$ or $-1/2$,

depending on whether the Fermi energy is between Zeeman splitting or not)

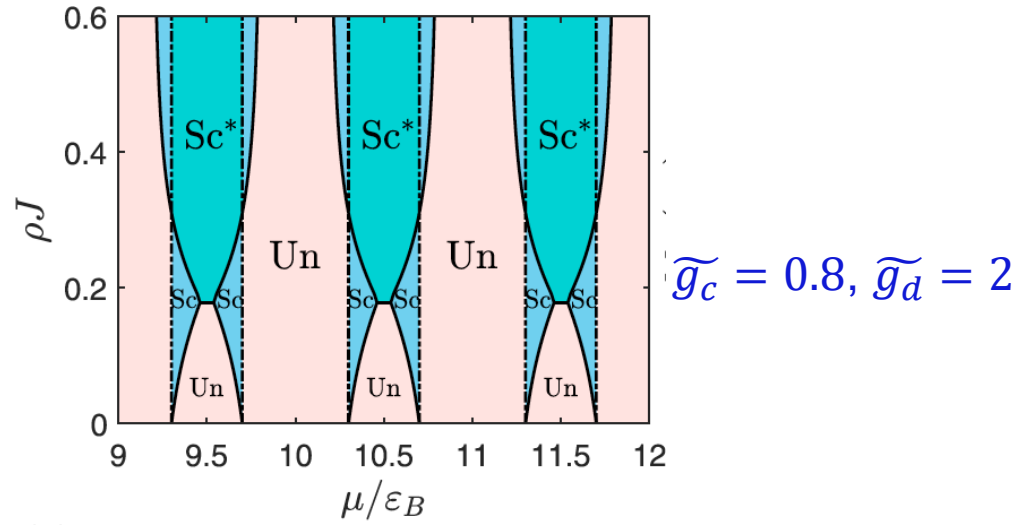


Screening $\Delta S_z = 1/2$ (Sc) or $\Delta S_z = 1$ (Sc*)

Typical Phase diagram



$$\tilde{g}_c = g_c \frac{\mu_{BB}}{\varepsilon_B} = 2, \quad \tilde{g}_d = g_d \frac{\mu_{BB}}{\varepsilon_B} = 2$$



$$\Delta s^z \equiv \langle s_{tot}^z \rangle_{\Gamma} - \langle s_{tot}^z \rangle_{\Gamma=0}$$

$$Un : \Delta s^z = 0$$

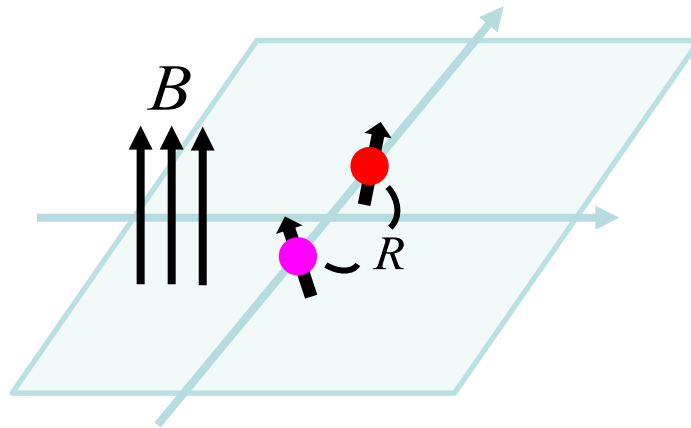
$$Sc : \Delta s^z = 1/2$$

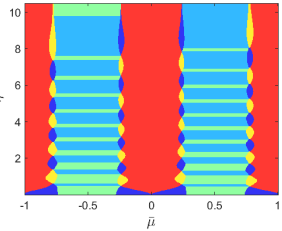
$$Sc^* : \Delta s^z = 1$$

Sc (Screened)

Un (Unscreened)

Two impurities





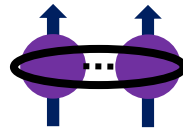
$R / l_B :$

∞

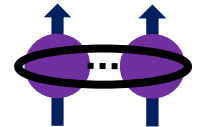
\rightarrow

0

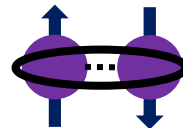
Two-impurity Triplet



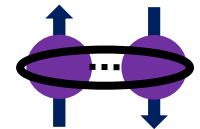
\rightarrow



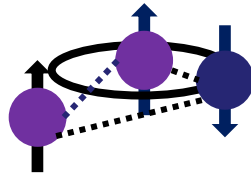
Two-impurity Singlet



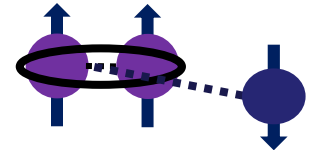
\rightarrow



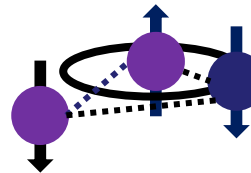
FM $S=1/2$ Mixing state



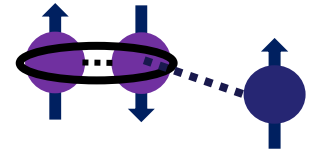
\rightarrow



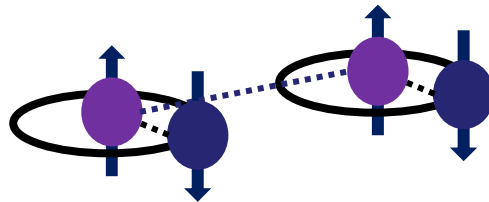
AFM $S=1/2$ Mixing state



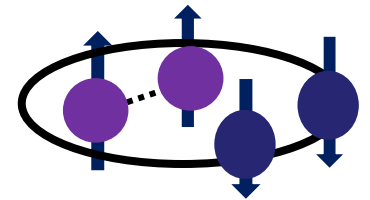
\rightarrow



Kondo Singlet



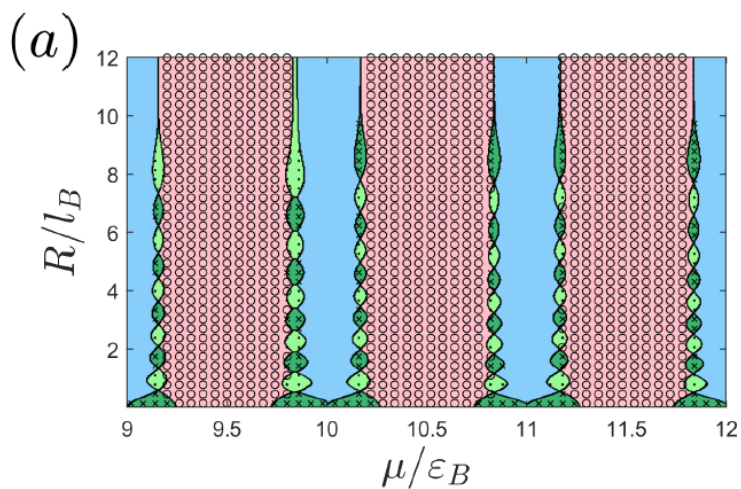
\rightarrow



$$\tilde{g}_c = \tilde{g}_d = 2$$

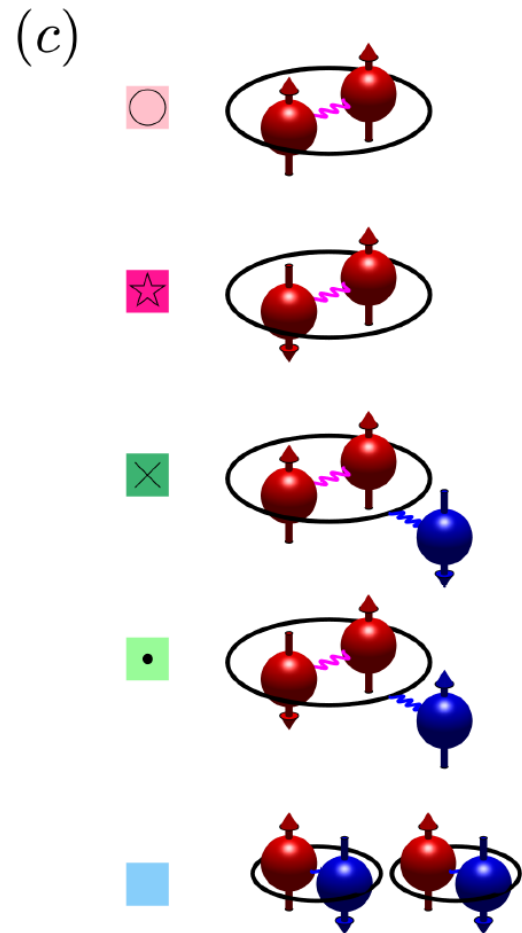
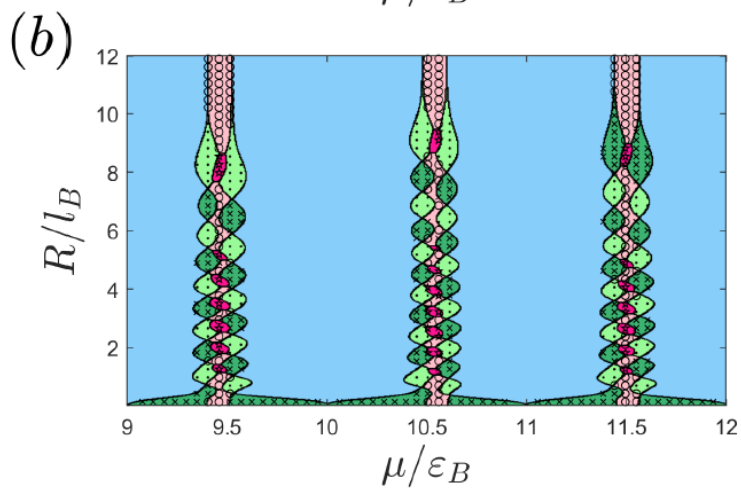
weak ρJ :

$$\rho J = 0.18$$



strong ρJ :

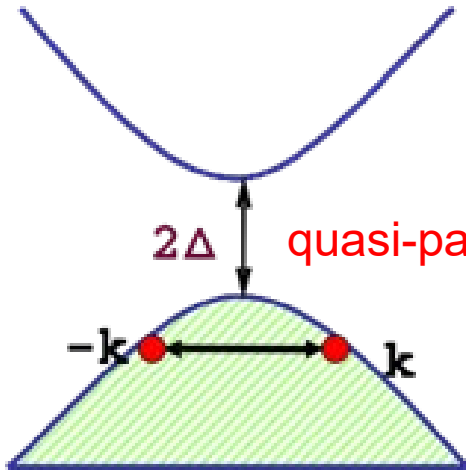
$$\rho J = 0.45$$



Outline:

- Exotic superconductivity that can arise in topological materials
 - Topological Kondo superconductivity
(Communication Physics 7, 253, 2024)
 - Geometry induced topological superconductivity
(Phys. Rev. B 103, 014508,2021)
 - Flat band superconductivity, charge density wave and superconducting pair density wave state
(Phys. Rev. B 98, 205103, 2018, Phys. Rev. X 11, 041038,2021)
 - Emergence of $O(4)$ symmetry in cuprate superconductors
(Submitted to Nature Communication, 2024)

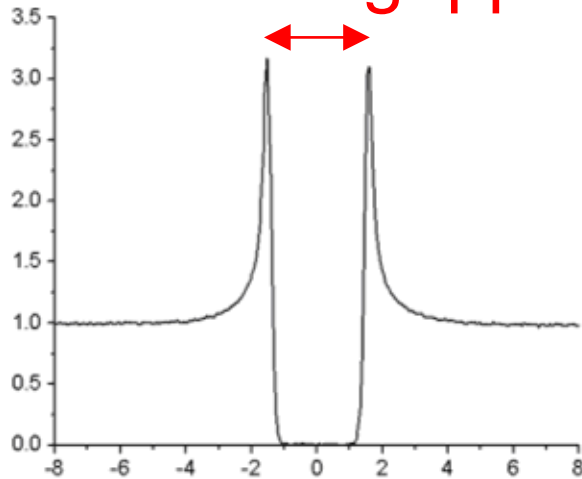
BCS theory – conventional s-wave



$$\Delta_k = - \sum_{k'} V_{k,k'} \langle c_{-k'\downarrow} c_{k'\uparrow} \rangle$$

pairing symmetry:
s-wave, $\Delta_k = \Delta$

density of state **gapped, 2Δ**



$$\Delta_k = - \sum_{k'} V_{k,k'} \frac{\Delta_{k'}}{2E_{k'}} \tanh \beta E_{k'}$$

$$\Delta = 0 \rightarrow k_B T_c = 1.13 \hbar \omega_D e^{-1/Ng} \lesssim k_B \Theta_D$$

E $N(\varepsilon_F) = \text{density of state}, \Theta_D \propto 1/\sqrt{M_{ion}}$

What can other forms of superconductivity exist?

Two electrons: **relative motion**

+ **center of mass motion**

$$\langle c_{-k+Q/2\downarrow} c_{k+Q/2\uparrow} \rangle = \phi(k) \psi(Q)$$

Relative motion: pairing symmetry $\phi(k)$ (non s-wave?)

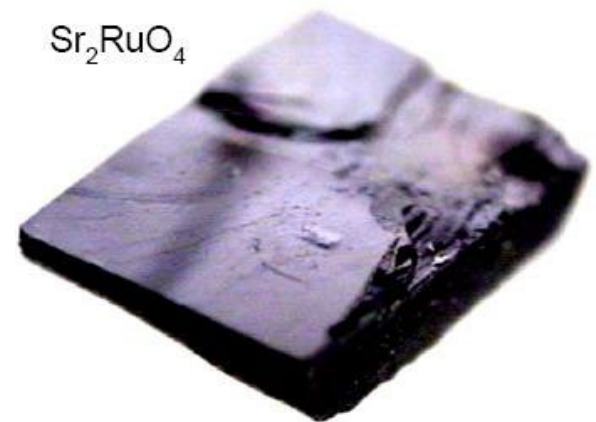
CM momentum: pair density waves $\psi(Q)$

Condensate at finite momentum ($\frac{\hbar^2 Q^2}{2m}$?)

higher T_c? different mechanism?

Nature odd-parity superconductors

Superfluid ^3He ,
old candidate: Sr_2RuO_4 (?)



Recent proposed candidates: $\text{PrOs}_4\text{Sb}_{12}$,
 $\text{Cu}_x\text{Bi}_2\text{Se}_3$, Bi_2Te_3 & Sb_2Te_3 (under high
pressure), $\beta\text{-PdBi}_2$, $\text{In}_x\text{Sn}_{1-x}\text{Te}$,
 $\text{Cu}_x(\text{PbSe})_5\text{Bi}_2\text{Se}_3$, $\text{Sr}_x\text{Bi}_2\text{Se}_3$, Sb_2Te_3

Confirmed candidates are rare!

Outline:

- Exotic superconductivity that can arise in topological materials
 - Topological Kondo superconductivity
(Communication Physics 7, 253, 2024)

Topological Kondo Superconductors

Yung-Yeh Chang, Khoe Van Nguyen, Kuang-Lung Chen,
Yen-Wen Lu, Chung-Yu Mou, and Chung-Hou Chung

Offer a qualitative and some quantitative understanding of the spin-triplet superconductivity recently observed in UTe_2

Key idea:

spin-orbit hybridization between d-orbit electrons and f-orbit electrons

- 5d conduction band + 4f more localized band

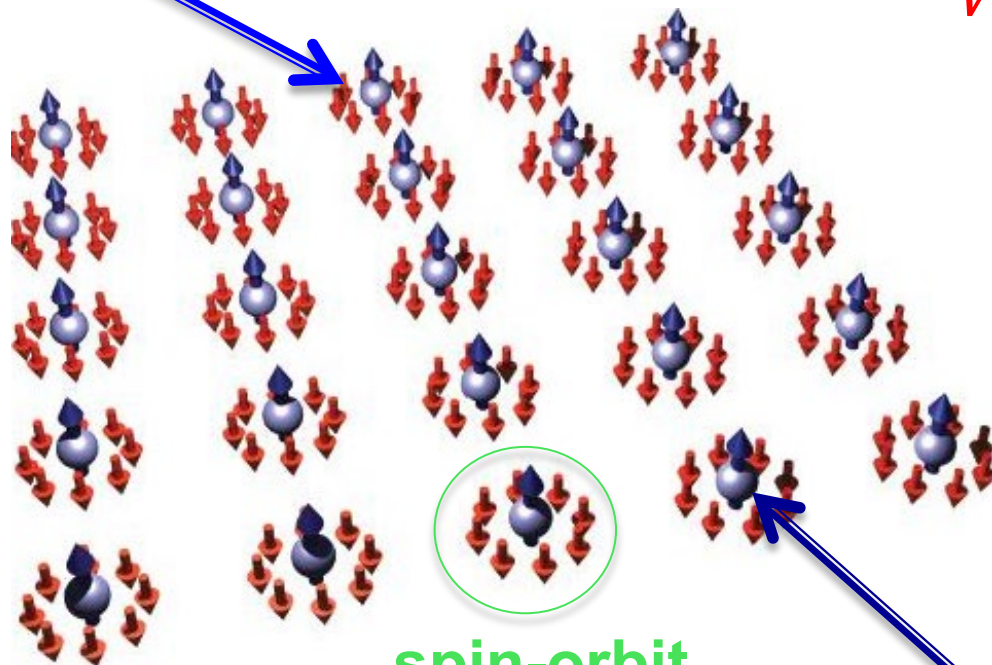
(due to difference in $l = 2$ and $l = 3$)

Kondo lattice with spin-orbit hybridization

$$H = \sum_{k\sigma} \xi_k c_{k\sigma}^\dagger c_{k\sigma} + \xi_k^d d_{k\sigma}^\dagger d_{k\sigma} + \sum_{k\sigma} V_k^{\sigma\sigma'} c_{k\sigma}^\dagger d_{k\sigma'} + h.c. + U \sum_i n_{i\uparrow}^d n_{i\downarrow}^d$$

conduction e⁻ $c_{k\sigma}$

$$V_k = 2\lambda_{SO} \sum_o \sigma_i \sin k_i$$



spin-orbit
interaction

f-orbit e⁻ $d_{k\sigma} \rightarrow f_{k\sigma}$

Kondo-Heisenberg Model with spin-orbit hybridization

U term is replaced by two magnetic interactions:

Kondo spin interaction

$$H_K = J_K \sum_i \vec{S}_{ic} \cdot \vec{S}_{if}$$

Ferromagnetic RKKY ($J_R > 0$)

$$H_{RKKY} = J_R \sum_{\langle i,j \rangle} \vec{S}_{if} \cdot \vec{S}_{jf}$$

Kondo-Heisenberg Lattice with $p \pm ip$ pairing

Pure Kondo phase

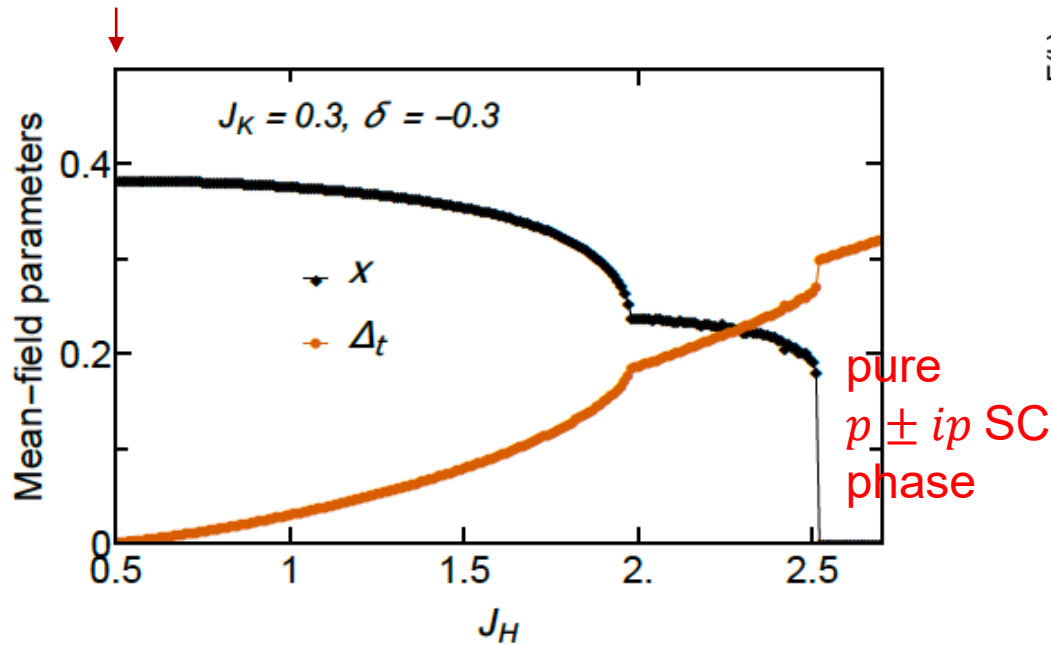


Fig. 2. The zero-temperature mean-field solutions of t -RVB order parameter Δ_t (brown) and the Kondo correlation x (black) as a function of J_H . We fix $J_K = 0.3$ and doping of the conduction band $\delta = -0.3$ (30 percent hole doping). Without loss of generality, we set $t = 1$. This plot reveals a (co-existing) superconducting ground state with $x \neq 0, \Delta_t \neq 0$ for $0 < J_H \lesssim 2.5$ and a pure t -RVB phase where $x = 0, \Delta_t \neq 0$ when $J_H \gtrsim 2.52$. A pure Kondo phase ($x \neq 0, \Delta_t = 0$) only exists at $J_H = 0$.

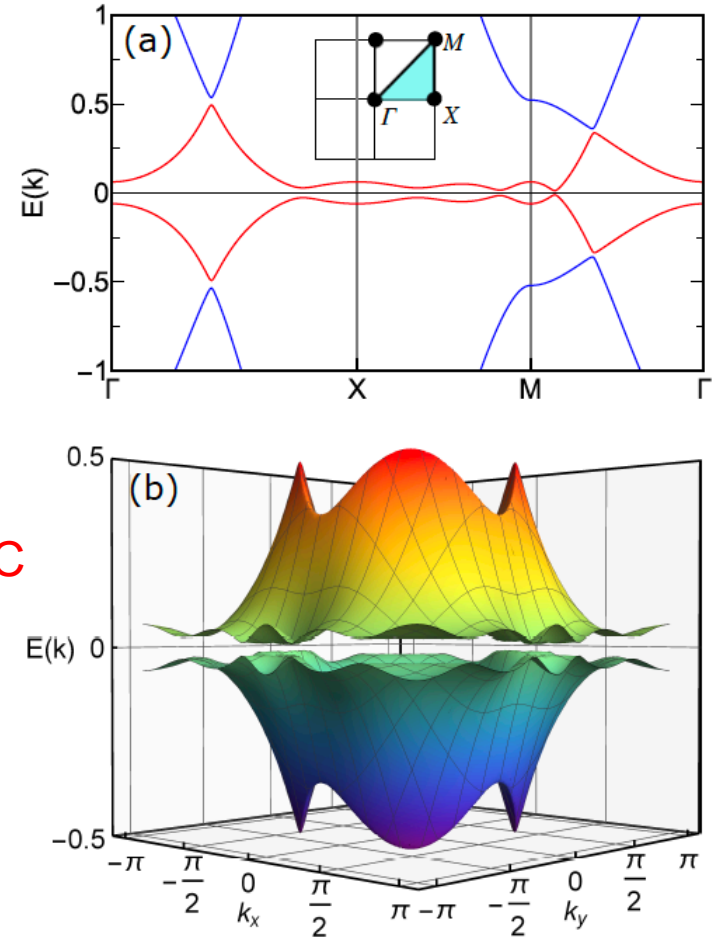
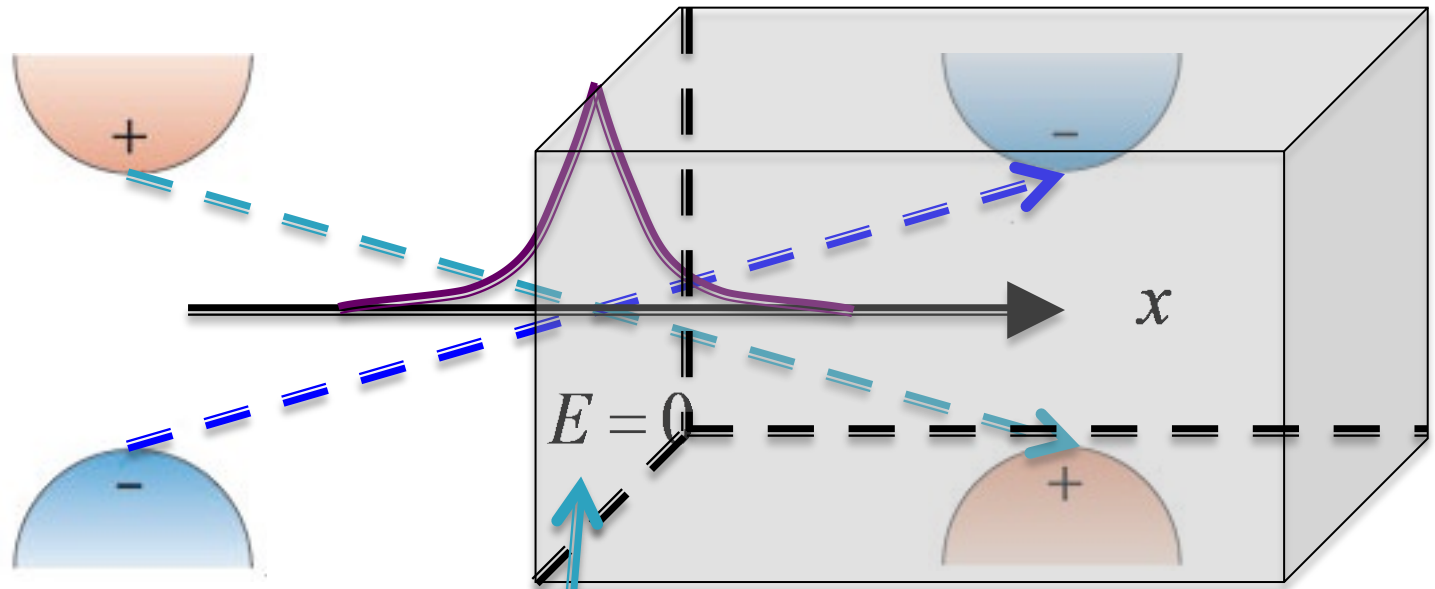


Fig. 3. Figures (a) (red curves) and (b) show the bulk energy spectrum of the co-existing superconducting state near the Fermi level μ . The Fermi level locates at $E(\mathbf{k}) = 0$. The coupling constants are $J_K = 0.3$ and $J_H = 1.0$. Inset of (a) displays the First Brillouin zone of a square lattice with indications of high-symmetry points Γ, X, M .

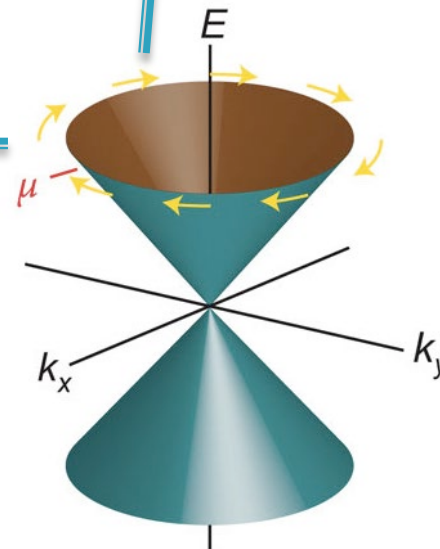
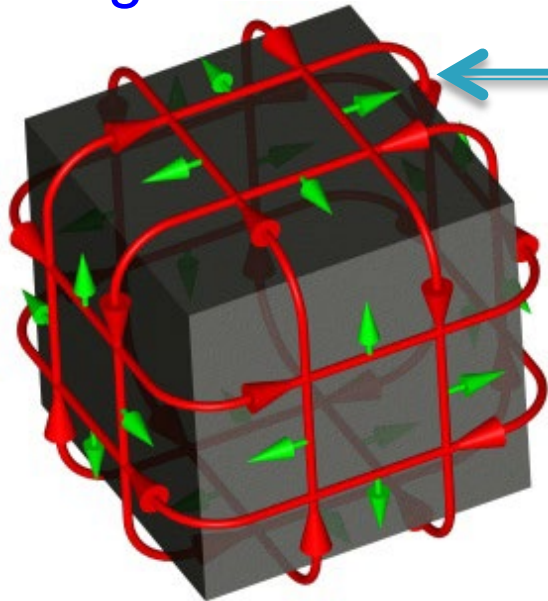
Outline:

- Exotic superconductivity that can arise in topological materials
 - Geometry induced topological superconductivity
(Phys. Rev. B 103, 014508,2021)

New Twist from consideration of topology



3D topological insulator

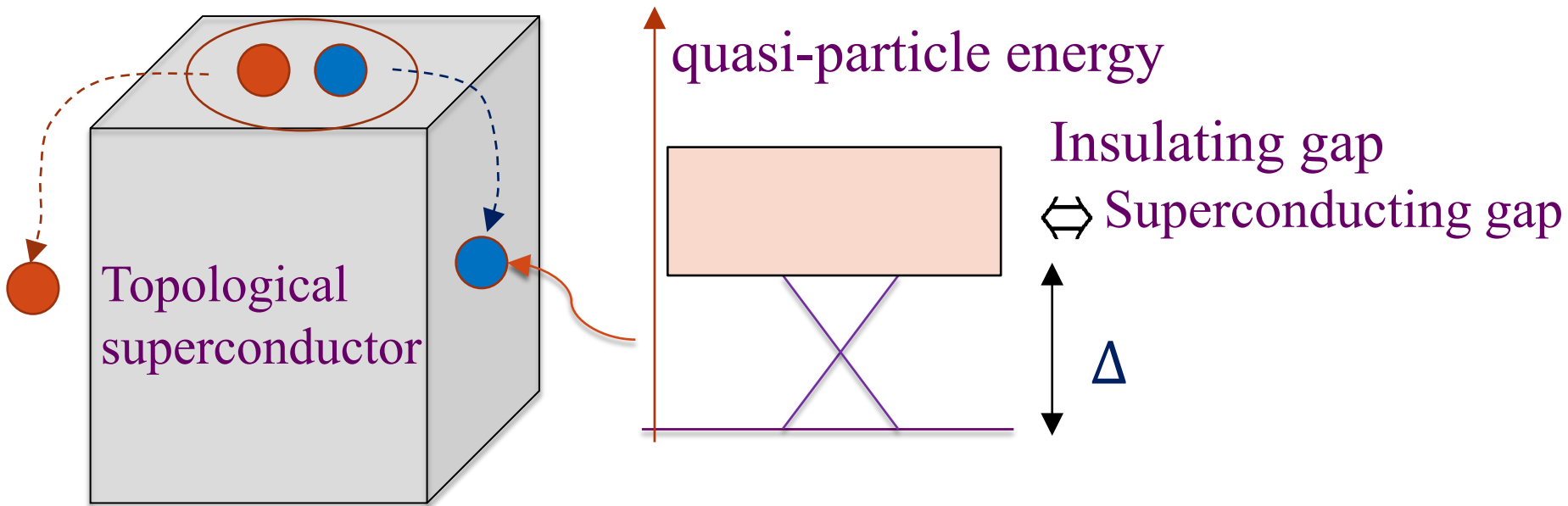


Topological invariant Z_2 :

Odd number inversion
Even number inversion

Liang Fu, C. L. Kane, and E. J. Mele, 2007

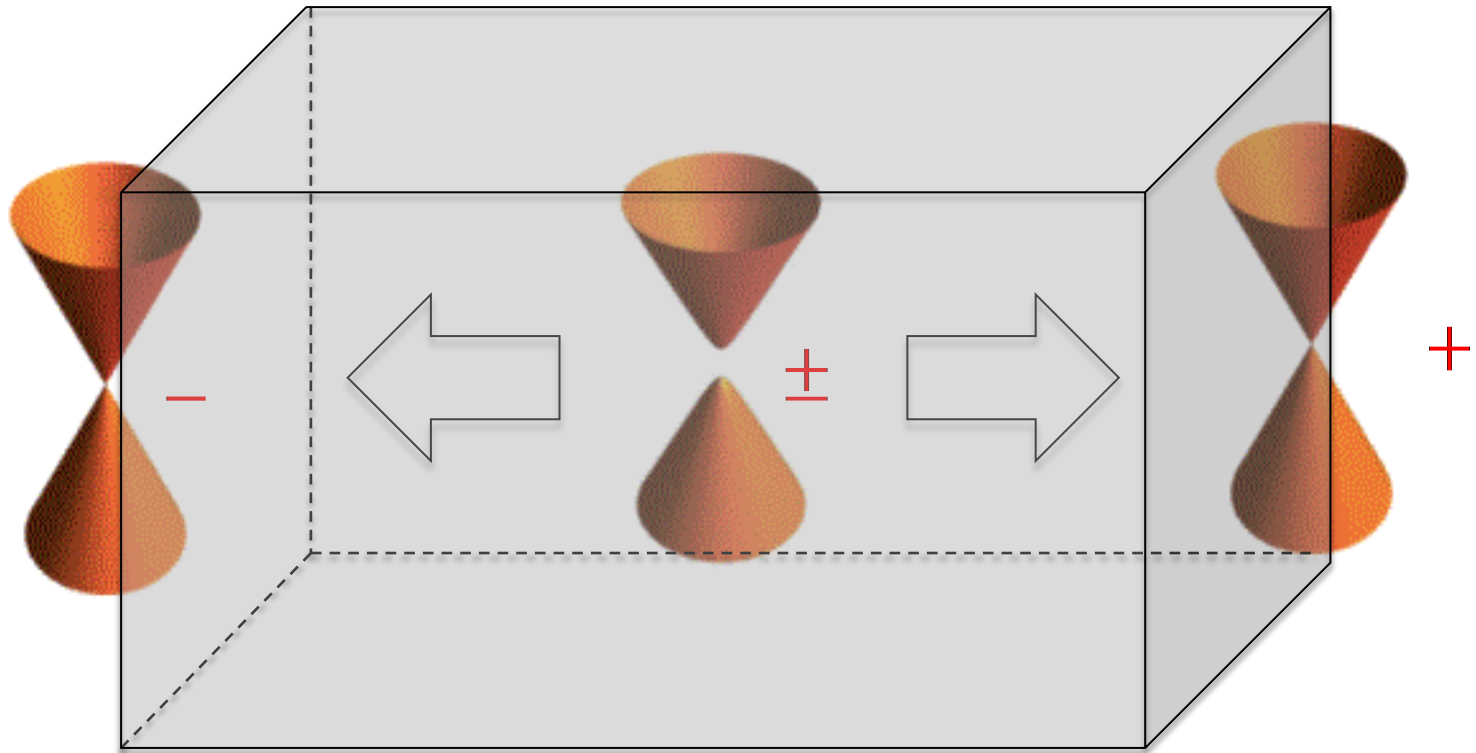
Topological superconductivity



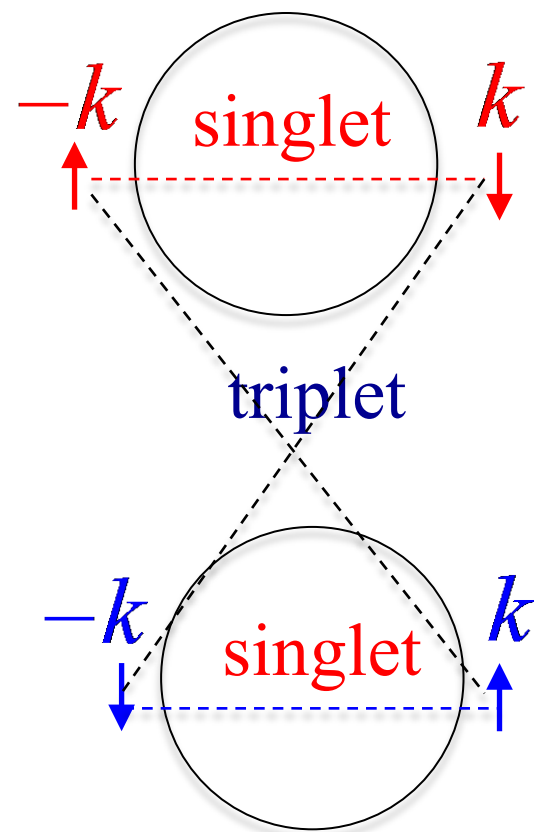
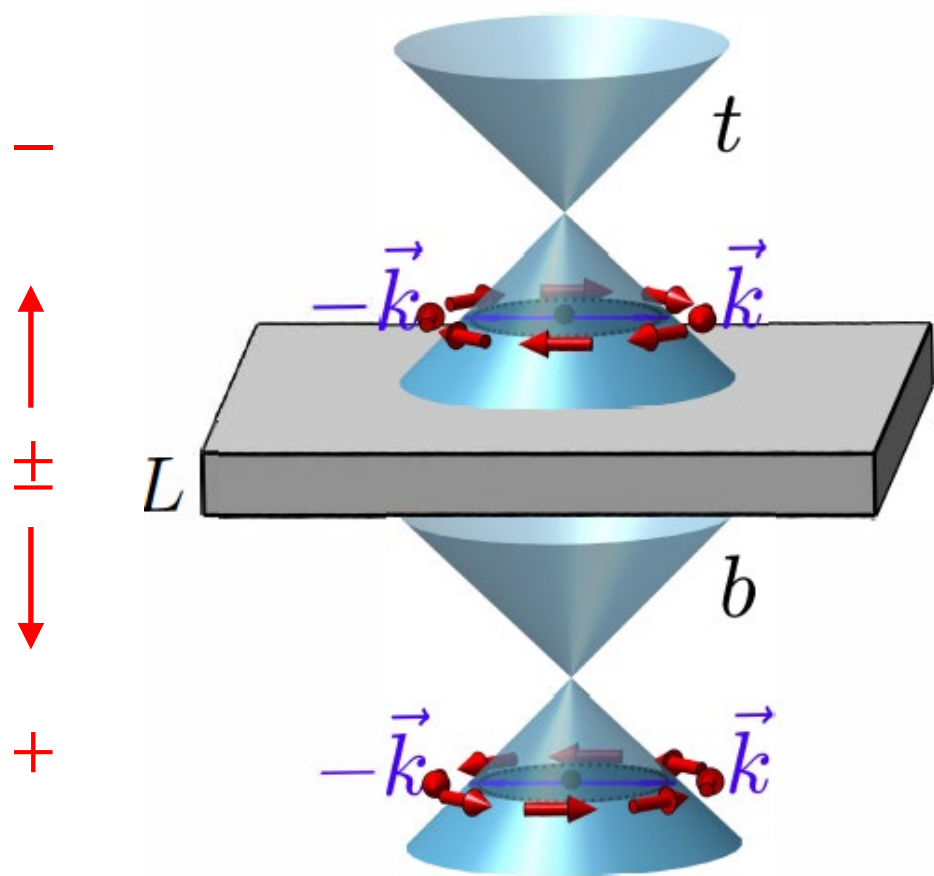
$$H_{SC\uparrow}(k) = \begin{pmatrix} \Lambda_k - \mu & T_k & 0 & \Delta_k \\ T_k^* & -\Lambda_k - \mu & -\Delta_{-k} & 0 \\ 0 & -\Delta_{-k}^* & -\Lambda_k + \mu & T_k \\ \Delta_k^* & 0 & T_k^* & \Lambda_k + \mu \end{pmatrix} \quad \psi_{FM} = \begin{pmatrix} C_{Ak\uparrow} \\ C_{Bk\uparrow} \\ C_{Ak\downarrow} \\ C_{Bk\downarrow} \end{pmatrix} \quad \text{or} \quad \psi_{FM} = \begin{pmatrix} C_{Ak\uparrow} \\ C_{Bk\uparrow} \\ C_{Ak\downarrow} \\ C_{Bk\downarrow} \end{pmatrix}$$

Qi & Zhang, Rev. Mod. Phys. 83, 1057 (2011); Hasan & Kane 82, 3045 (2010).

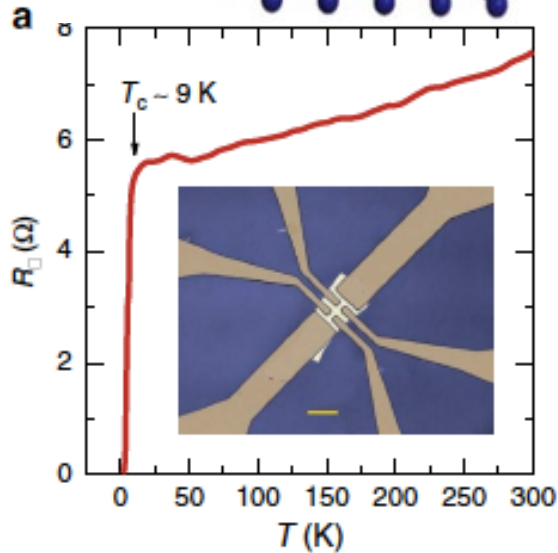
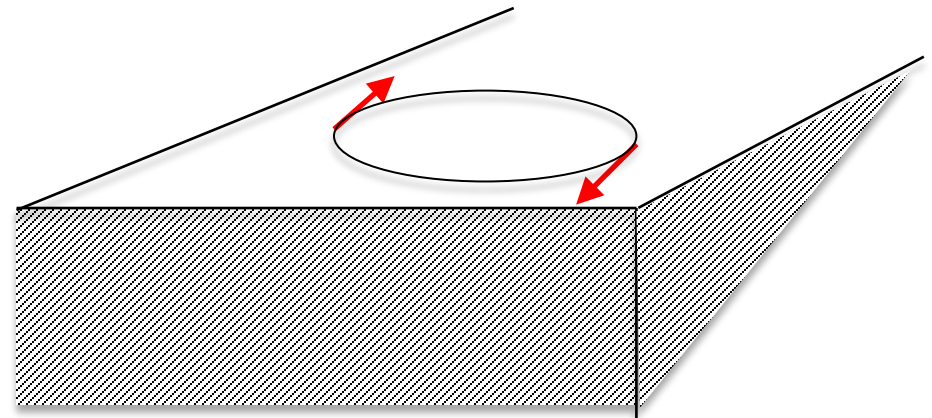
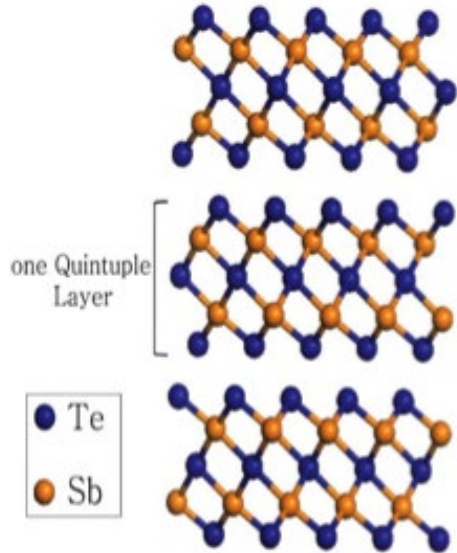
Unique feature of topological Insulators:
chirality separation in real space without
invoking symmetry breaking



Thin film geometry:
competition of intra-surface (singlet) and inter-
surface (triplet) through thickness dependence of
interaction



Feasibility: surface superconductivity on flat surface of Sb_2Te_3 (hole-doped single Weyl cone)



$$= \frac{1}{2} \left[e^{-i\phi} |\uparrow\uparrow\rangle - e^{i\phi} |\downarrow\downarrow\rangle \right] - \frac{1}{2} \left[|\uparrow\downarrow\rangle - |\downarrow\uparrow\rangle \right]$$

Equal strength of singlet and triplet pairing

Marginal topological superconductivity!

L. Zhao et al, Nat. Commun. 6, 8279 (2015).

Additional effect on curved space: spin connection effect

$$\partial_\mu \rightarrow \partial_\mu + igA_\mu \quad A_\mu = \frac{1}{4} \omega_\mu^{ab} \sigma_{ab} \quad \nabla \times \vec{A} = \vec{B}_{eff}$$

$$\sigma_{ab} = -\frac{i}{2} [\gamma_a, \gamma_b] \quad \omega_\mu^{ab} = \text{spin connection}$$

$\int gA_\mu dx^\mu = \text{Berry phase}$ due to different orientation of Dirac cone

Sphere:

A. A. Abrikosov, Int. J. Mod. Phys. A17, 885, (2002)

D.-H. Lee, Phys. Rev. Lett. 103, 196804 (2009).

Local spin up

$-1/2$

Local spin down

$+1/2$

Only $\uparrow\uparrow$ or $\downarrow\downarrow$ sees \vec{B}_{eff} !

Our extension:

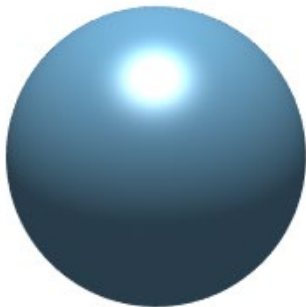
$$\vec{B}_{eff} = \pm \frac{1}{2} K \hat{n}$$

K = Gauss curvature

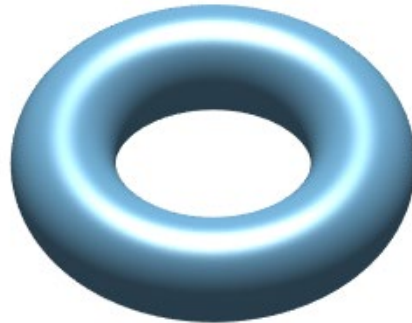
\hat{n} = unit normal vector to the surface

Gauss-Bonnet theorem: $\oint_S \vec{B}_{eff} \cdot d\vec{a} = \pm 2\pi(1 - g)$

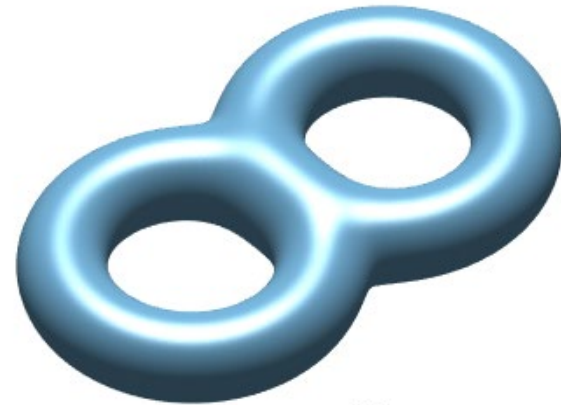
$S =$



$g = 0$



$g = 1$



$g = 2$

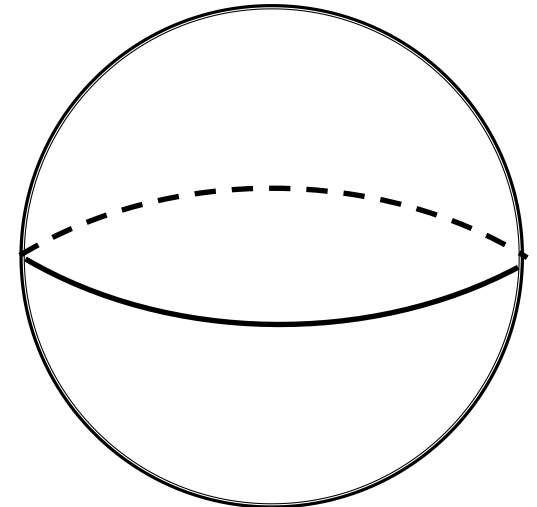
...

Illustration on two $g = 0$ surfaces

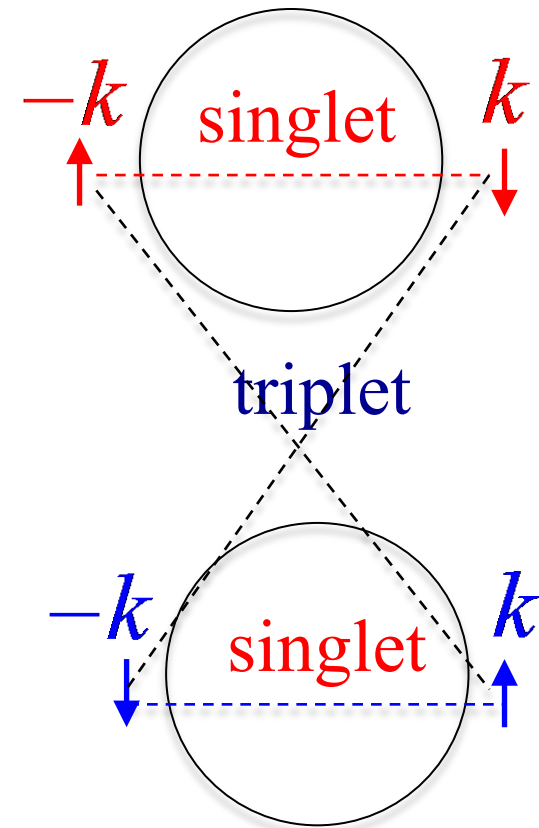
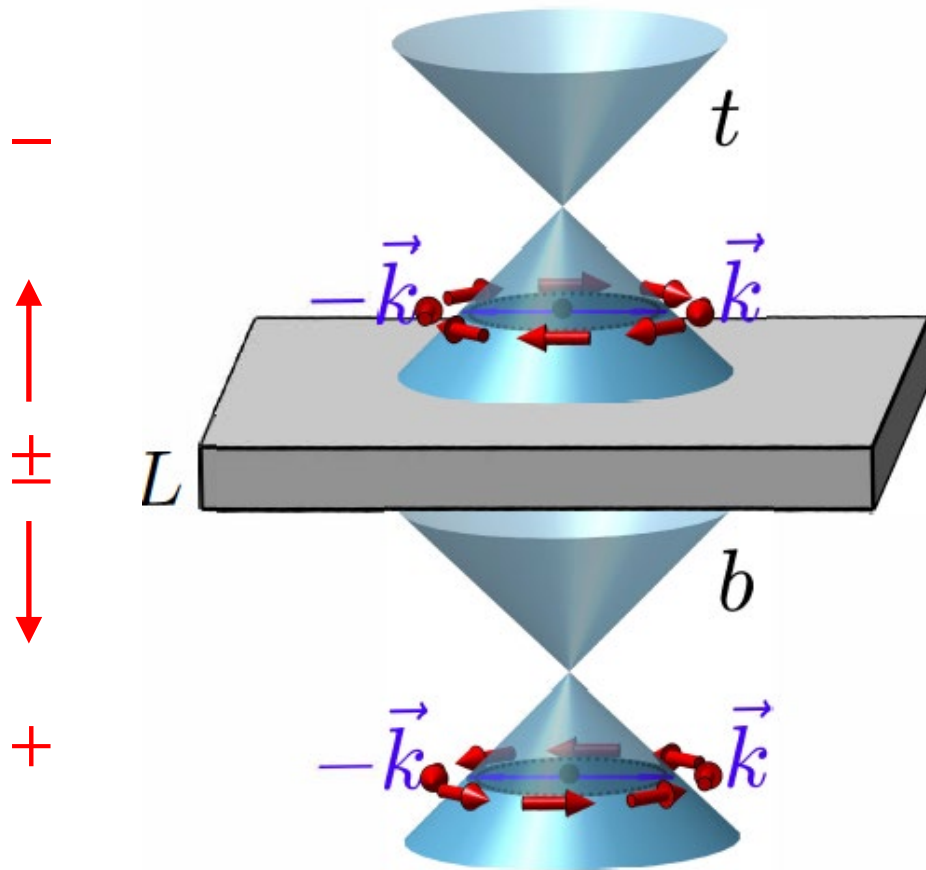
(i) thin film geometry
(two surfaces,
thickness can be tuned)



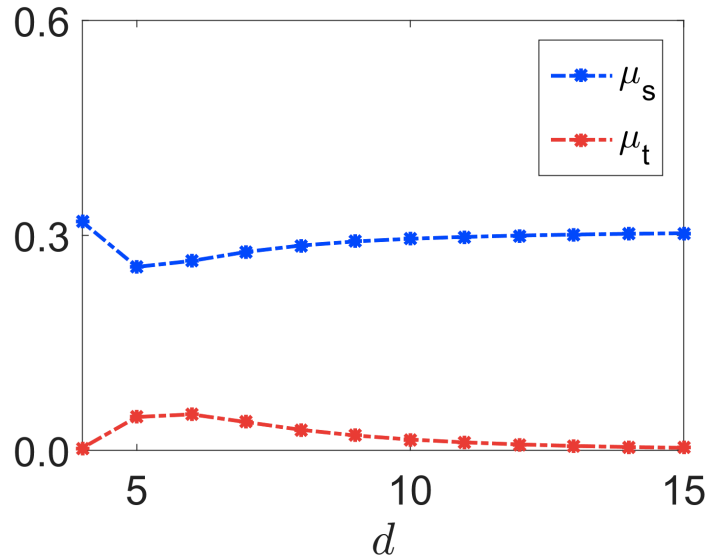
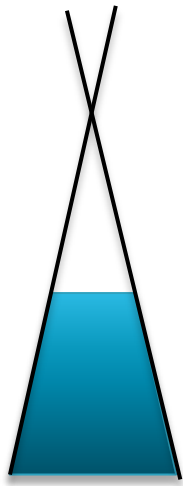
(ii) spherical geometry
(curvature can be tuned)



Thin film geometry: competition of **intra-surface (singlet)** and **inter-surface (triplet)** through thickness dependence of interaction

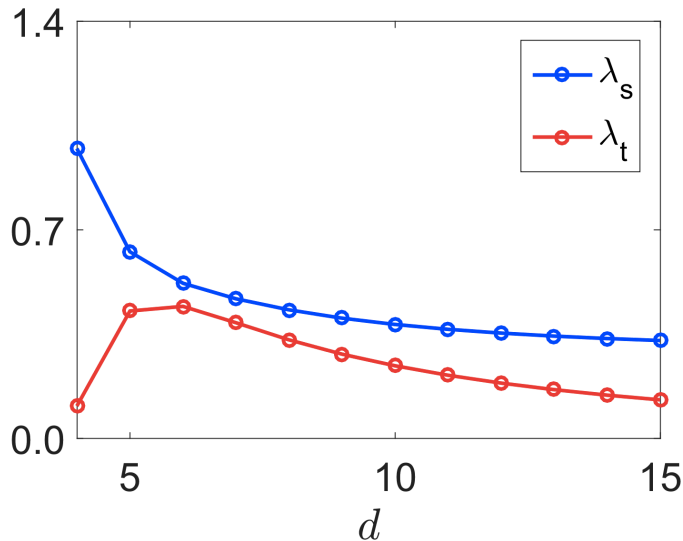
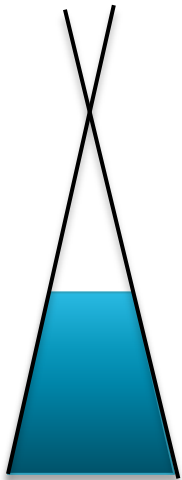


Coulomb interaction (average over Fermi surface)



$$\mu_\alpha = \oint g_\alpha^C(k_F, k_F)$$

Electron-phonon coupling



$$\lambda_\alpha = \oint g_\alpha^P(k_F, k_F)$$

Exclusive singlet and triplet pairing

$$H_{\Delta} = \sum_k \Delta_s(k) e^{-i\phi_k} (c_{kt}^{\dagger} c_{-kt}^{\dagger} - c_{kb}^{\dagger} c_{-kb}^{\dagger}) + \Delta_t(k) e^{-i\phi_k} (c_{kt}^{\dagger} c_{-kb}^{\dagger} + c_{kb}^{\dagger} c_{-kt}^{\dagger}) + h.c.$$

Both singlet and triplet pairing are determined by the same quasi-particle energy

$$E(k) = \sqrt{\xi_k^2 + \Delta_s^2(k) + \Delta_t^2(k)}$$

$$\Delta_s(k) = \sum_{k'} g_s(k, k') \frac{\Delta_s(k')}{2E_{k'}} \tanh(\beta E_{k'})$$

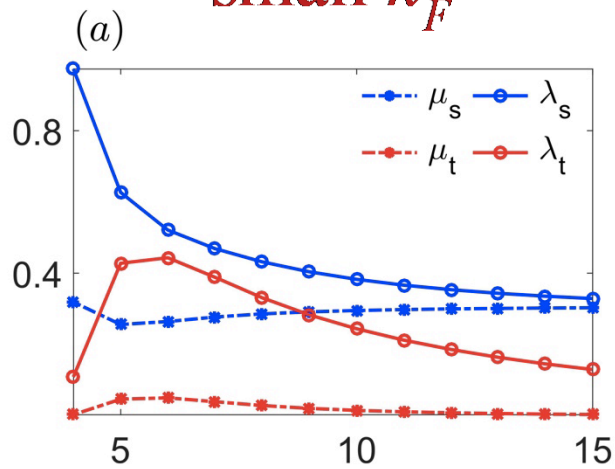
$$\Delta_t(k) = \sum_{k'} g_t(k, k') \frac{\Delta_t(k')}{2E_{k'}} \tanh(\beta E_{k'})$$

\Rightarrow can not be satisfied simultaneously!

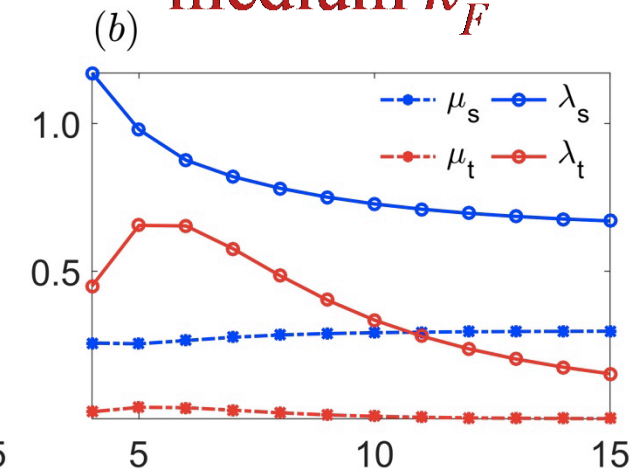
Theoretical results for Sb_2Te_3 films

McMillan formula: $T_c = \frac{\theta_D}{1.45} \exp\left[-\frac{1.04(1+\lambda)}{\lambda - \mu^*(1+1.62\lambda)}\right], \mu^* = \mu[1 + \ln(\Lambda/\omega_c)]$

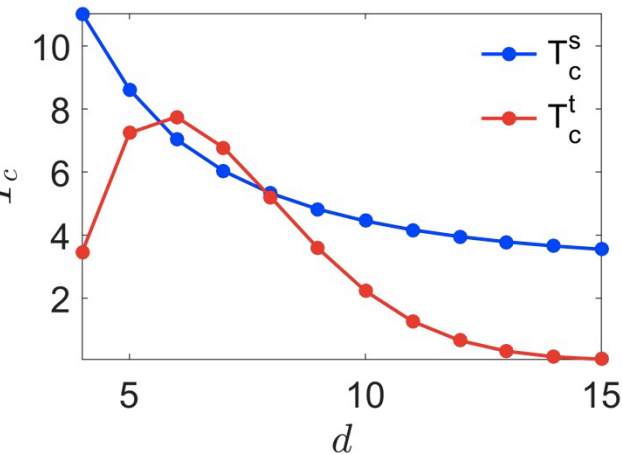
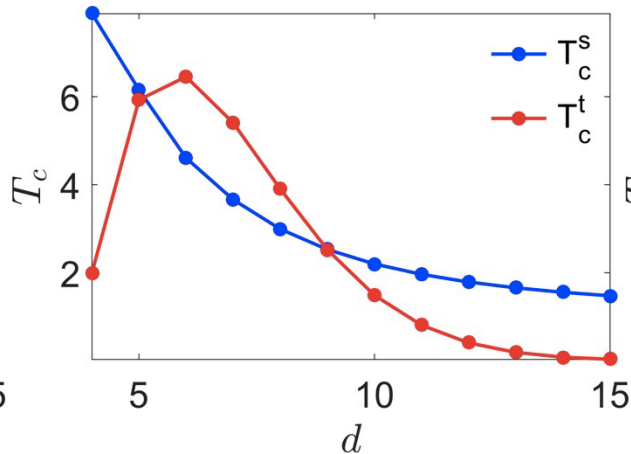
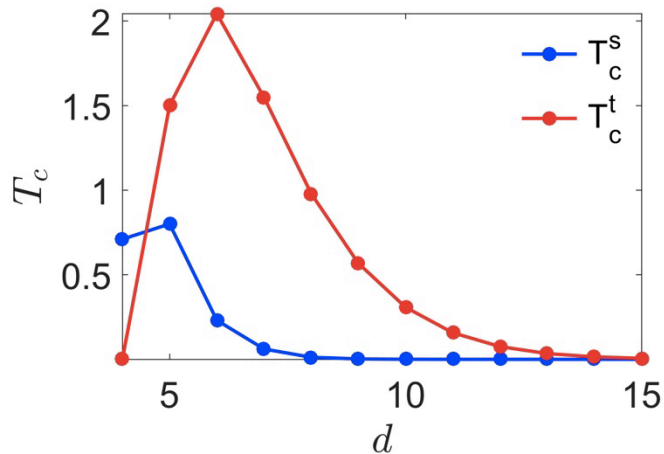
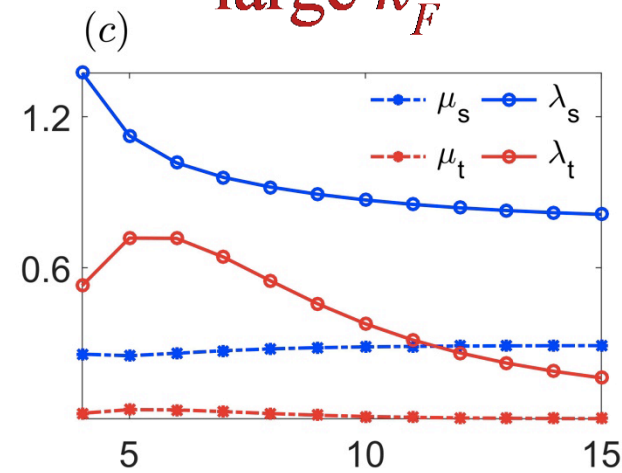
small k_F



medium k_F

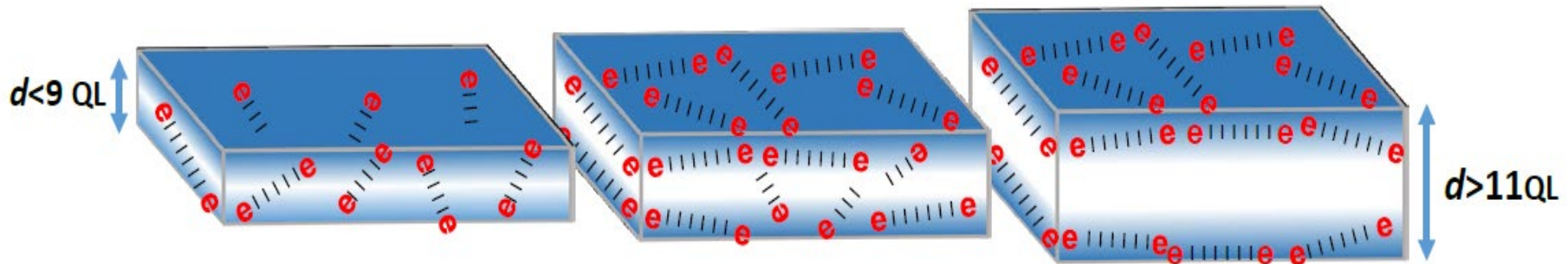


large k_F

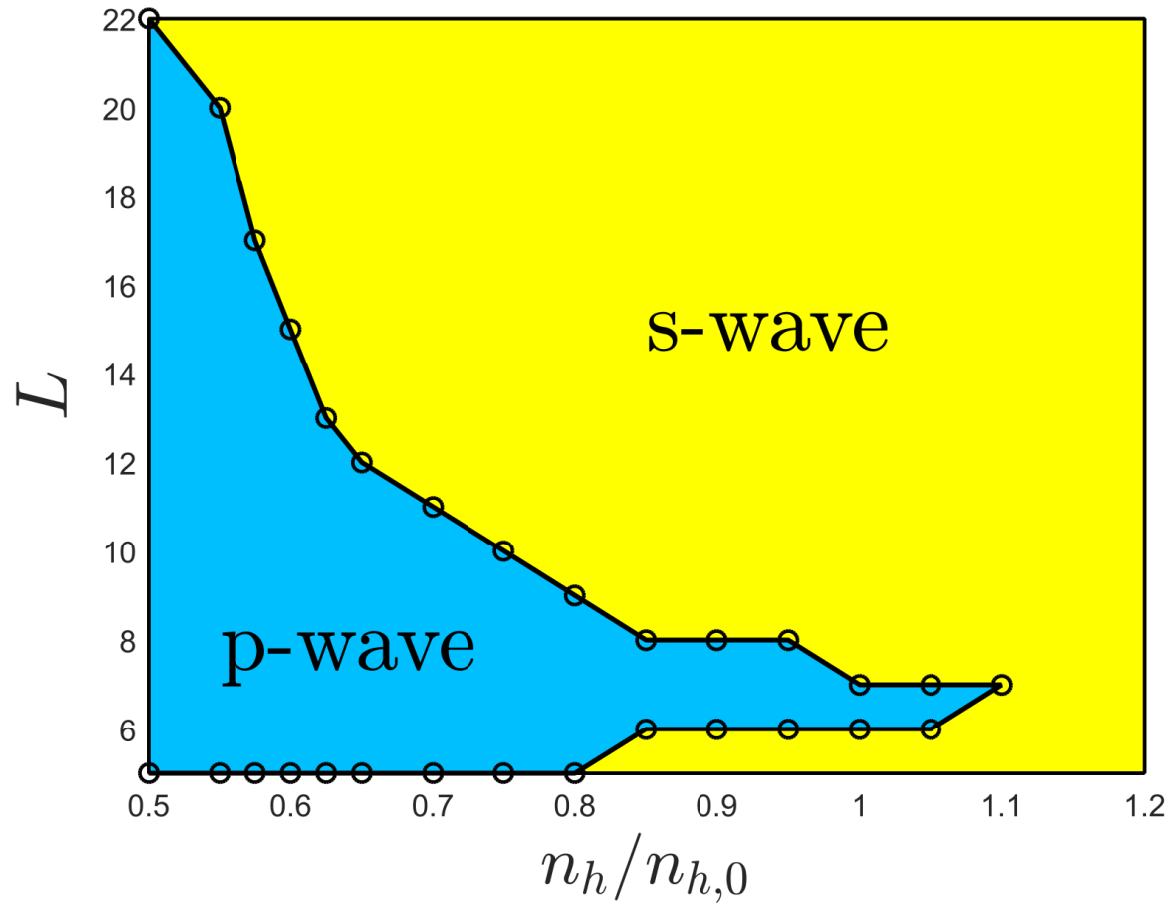


Experimental observations on superconductivity in Sb_2Te_3 nanoflakes

-- Yang-Yuan Chen's group Academia Sinica

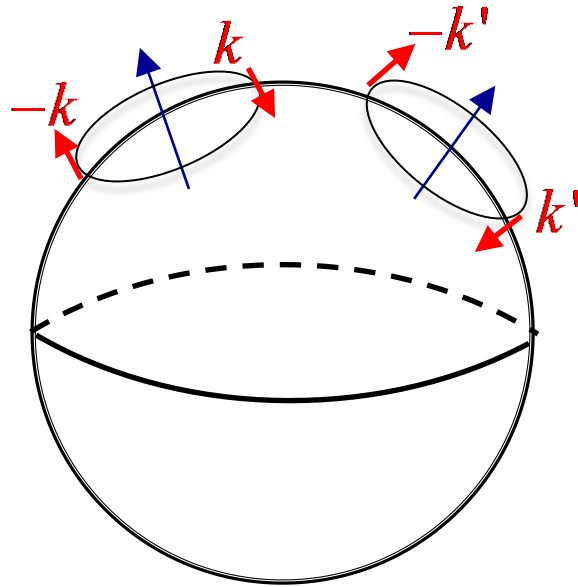


Phase diagram



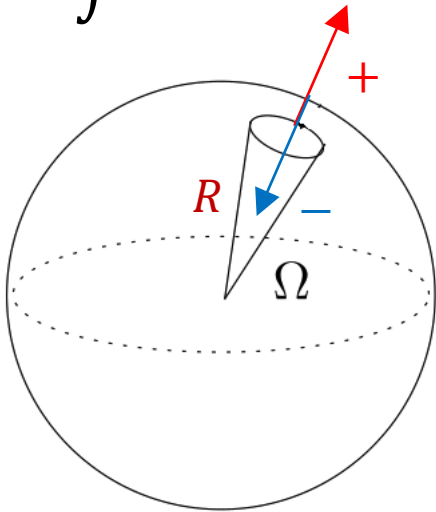
Spherical geometry:

Competition of **singlet pairing at same site** and **triplet pairing at different sites** through change of **curvature**



General Hamiltonian for superconductivity on sphere

$$H = \int d\Omega \Psi_{\Omega}^{\dagger} (h - \mu) \Psi_{\Omega} + \frac{1}{2} \iint d\Omega d\Omega' V(\Omega, \Omega') (\Psi_{\Omega}^{\dagger} \Psi_{\Omega}) (\Psi_{\Omega'}^{\dagger} \Psi_{\Omega'})$$



Local spinor $\Psi_{\Omega}^{\dagger} = (c_{\Omega,+}^{\dagger}, c_{\Omega,-}^{\dagger})$

$$h = \frac{\lambda_{so}}{R} \begin{pmatrix} 0 & D_- \\ D_+ & 0 \end{pmatrix}$$

$$D_{\pm} = e^{\pm i\phi} \left(\pm \partial_{\theta} + \frac{i}{\sin \theta} \partial_{\phi} \mp \frac{1}{2} \tan \frac{\theta}{2} \right)$$

$$V(\Omega, \Omega') = V_c(\Omega, \Omega') + V_{ph}(\Omega, \Omega') \quad V_{ph}(\Omega, \Omega') = -V_{ph} \exp(-\alpha_{ph} \Delta\Omega^2)$$

$$V_c(\Omega, \Omega') = \frac{V_c}{2R \left| \sin \frac{\Delta\Omega}{2} \right|} \exp(-\alpha_c \left| \sin \frac{\Delta\Omega}{2} \right|)$$

$$\Delta\Omega = \Omega - \Omega'$$

Mean field theory

$$H = \int d\Omega \Psi_{\Omega}^{\dagger} (h - \mu) \Psi_{\Omega} + \frac{1}{2} \iint d\Omega d\Omega' \Delta_{\Omega, \Omega'}^{s, s'} C_{\Omega, s}^{\dagger} C_{\Omega', s'}^{\dagger} + h. c.$$

$$\Delta_{\Omega, \Omega'}^{s, s'} = V(\Omega, \Omega') \langle C_{\Omega, s} C_{\Omega', s'} \rangle$$

Cooper pair: Center of Mass $\bar{\Omega} = \frac{\Omega + \Omega'}{q}$

$$\Delta_{\Omega, \Omega'}^{s, s'} = \Delta_s(\bar{\Omega}) S(\Omega, \Omega') + \Delta_p(\bar{\Omega}) P(\Omega, \Omega') + \dots$$

$$S(\Omega, \Omega') = \text{constant (s-wave)}$$

$$(P + iP)(\Omega, \Omega') = \alpha\beta' - \beta\alpha' \text{ (p+ip wave)}$$

$$(P - iP)(\Omega, \Omega') = \alpha\beta'^* - \beta\alpha'^* \text{ (p-ip wave)}$$

$$s, s' = \pm$$

Local spinor

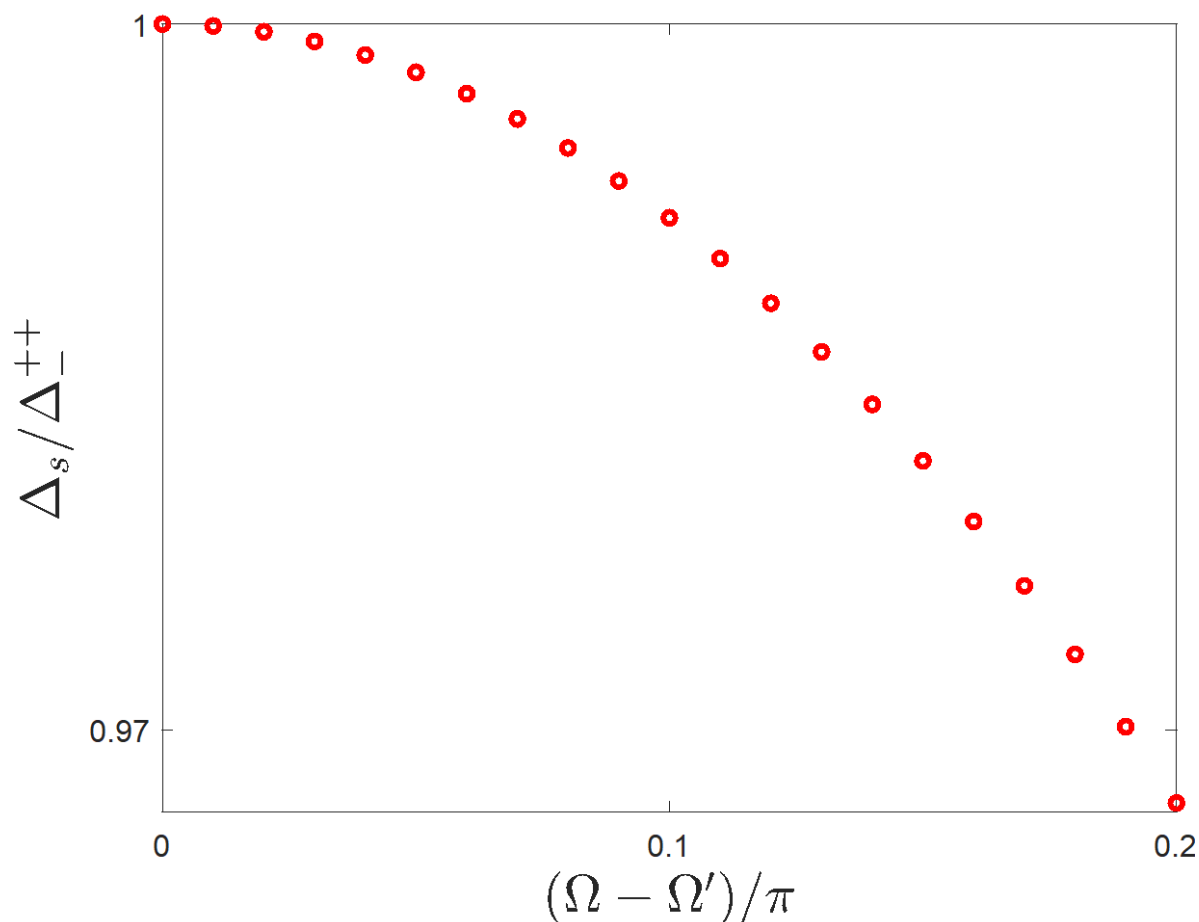
$$|+\rangle = \begin{pmatrix} \alpha \\ \beta \end{pmatrix} \quad |-\rangle = \begin{pmatrix} -\alpha^* \\ \beta^* \end{pmatrix}$$

Meissner Phase : triplet dominates

Singlet: Δ_s

$$\text{Triplet: } \Delta^{++} = \Delta_{-}^{++}(p_x - ip_y) + \Delta_{+}^{++}(p_x + ip_y) = \Delta^{--}$$

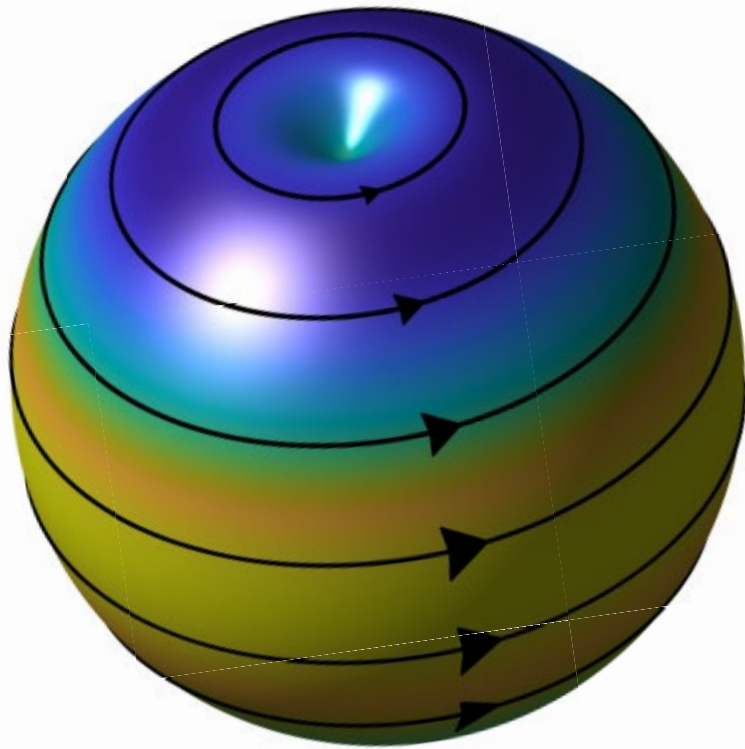
$$\Delta^{--} = \Delta_{-}^{--}(p_x - ip_y) + \Delta_{+}^{--}(p_x + ip_y)$$



Curvature induced vortex states

Vortex phase

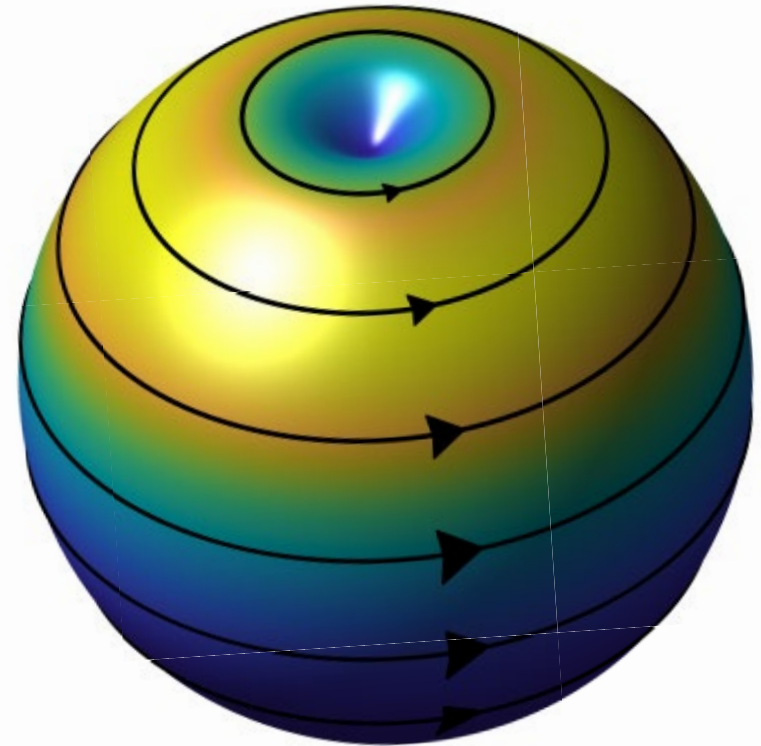
$$Q = 1$$



$$Q = 1$$

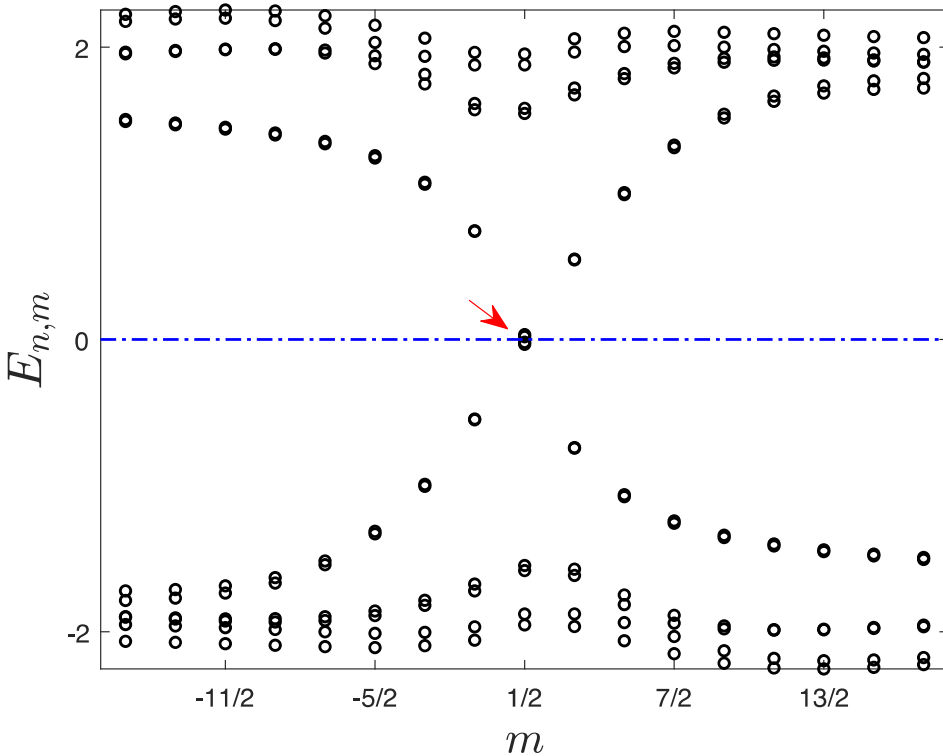
Vortex* phase

$$Q = 2$$

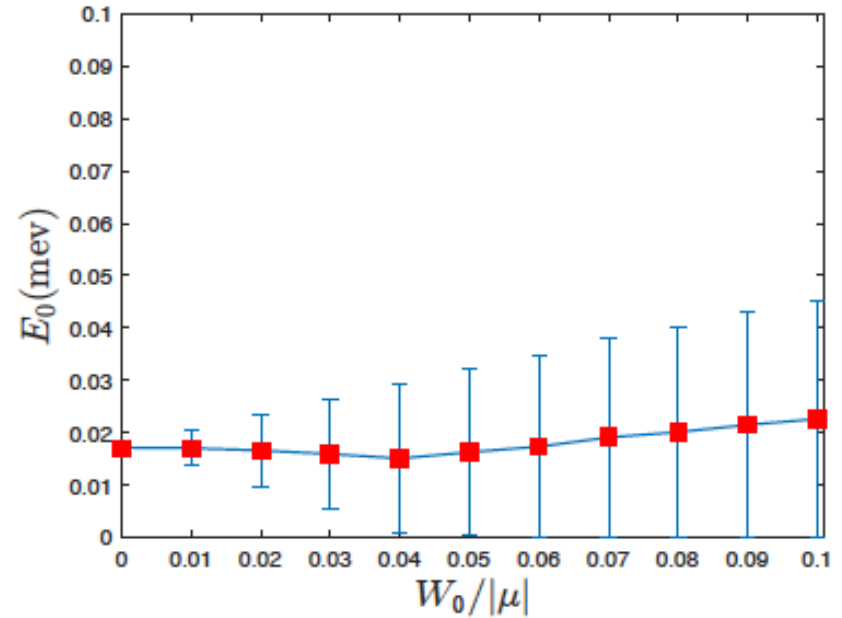


$$Q = 0$$

Majorana zero mode (only for $Q = \pm 1$)



Disorder effect



disorder strength

Majorana mode in the vortex on a sphere:

spinless p+ip, S. Moroz et al. Phys. Rev. B 93, 024521, (2016).

proximity effect, L. H. Hu et al. Phys. Rev. B 94, 224501, (2016)

Poincare-Hopf theorem and vortex formation

Poincare-Hopf theorem

(Hairy ball theorem) :

\vec{v} vector field on a manifold M

\vec{r}_i isolated points that $\vec{v} = 0$



A hair whorl

$\sum_{\vec{r}_i} index(\vec{v}) = \chi(M)$ (Euler characteristic of M)

superconducting state: \vec{v} = supercurrent density

vortex: $index(\vec{v})$ = winding number

general surface: $\chi(M) = 2(1 - g)$

Given a surface with genus g

\Rightarrow Minimum number of vortex: $2(1 - g)$

Vortex formation: curvature + energetics

Example: Sphere $g = 0$

\Rightarrow Minimum number of vortex: 2

$Q = 1$, number of vortices = 2

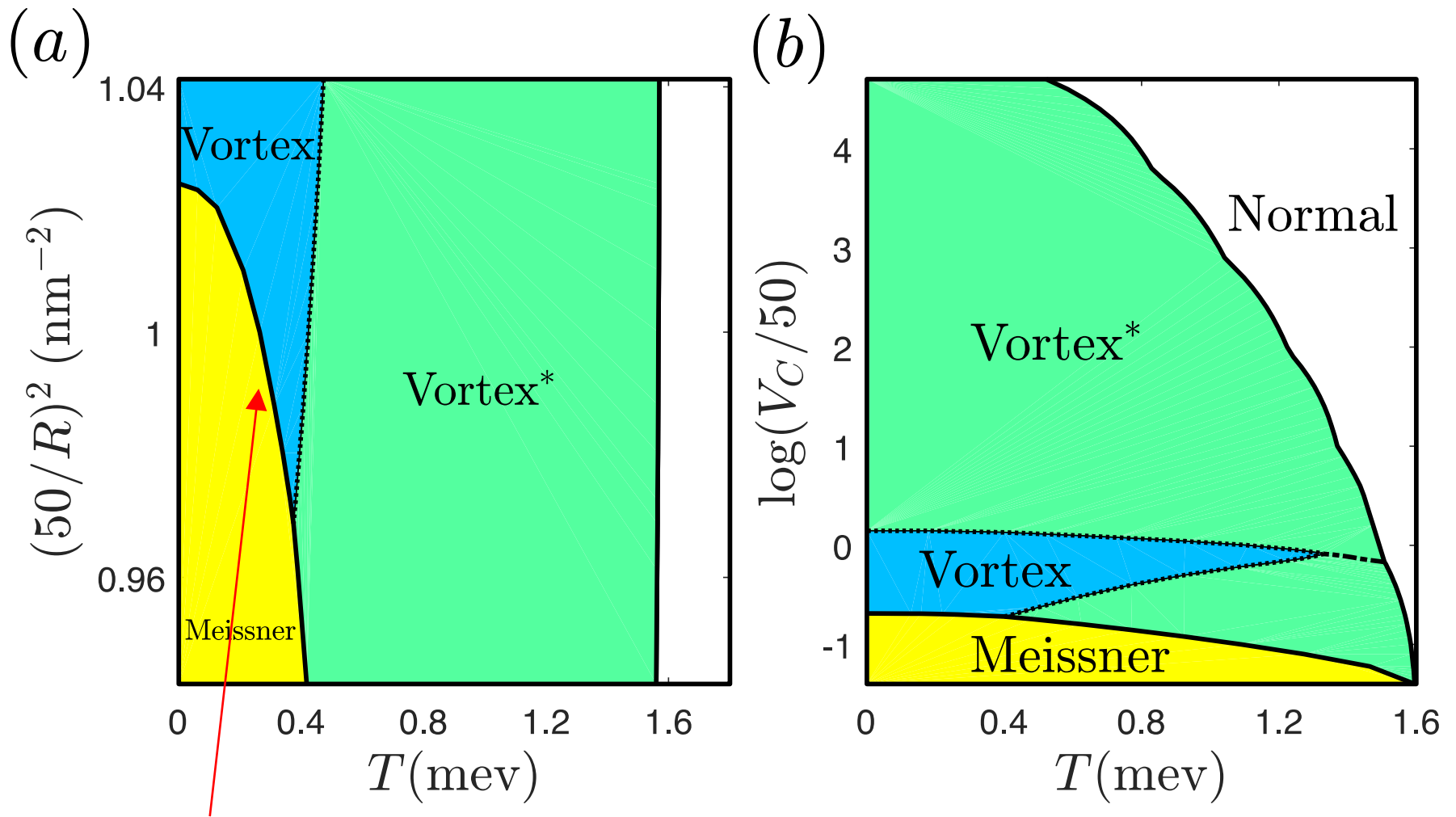
or $Q = 2$, number of vortices = 1

In general, one can add vortex-pairs, $Q = \pm 1$, to satisfy the Poincare-Hopf theorem. However, it costs energy determined by curvature as $\vec{B}_{eff} = \pm \frac{1}{2} K \hat{n}$

threshold curvature: $\epsilon \ell - B_{eff} \int b d^3 r = 0$

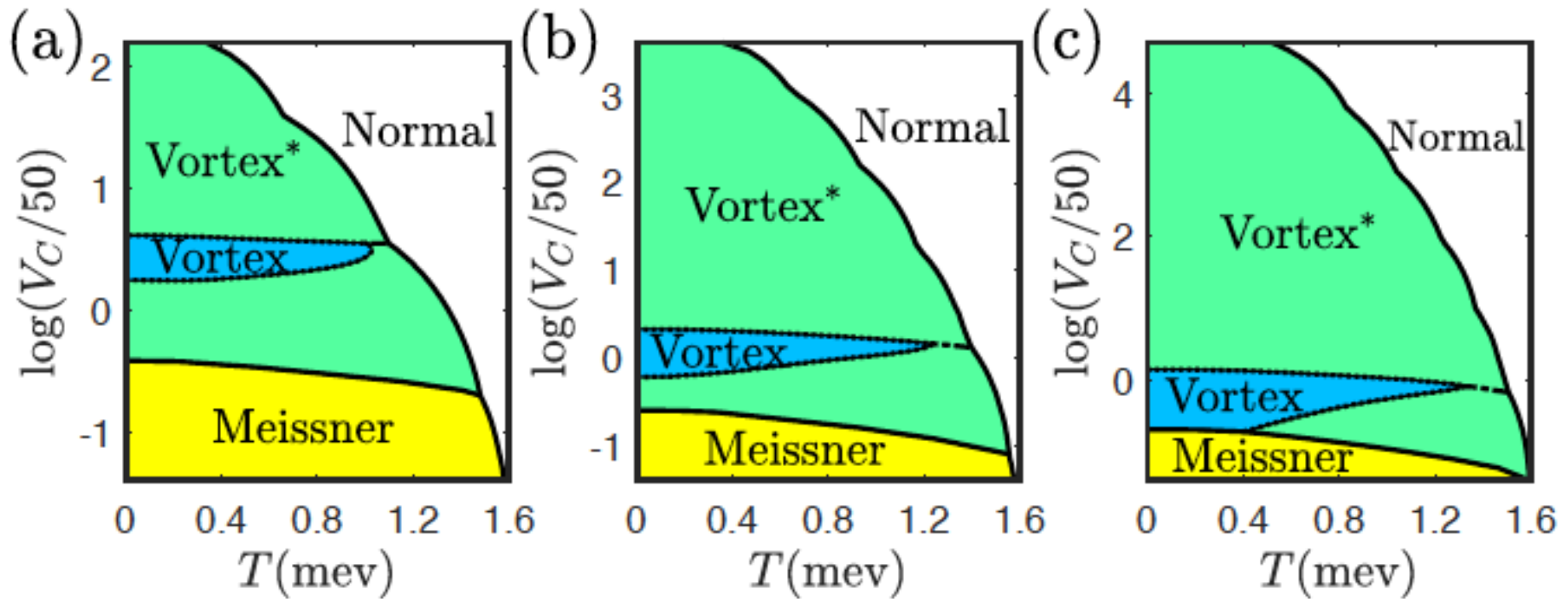
$$K_c = \frac{8\pi\epsilon}{\phi_0}$$

Phase diagram



~ critical (threshold) curvature for forming a vortex

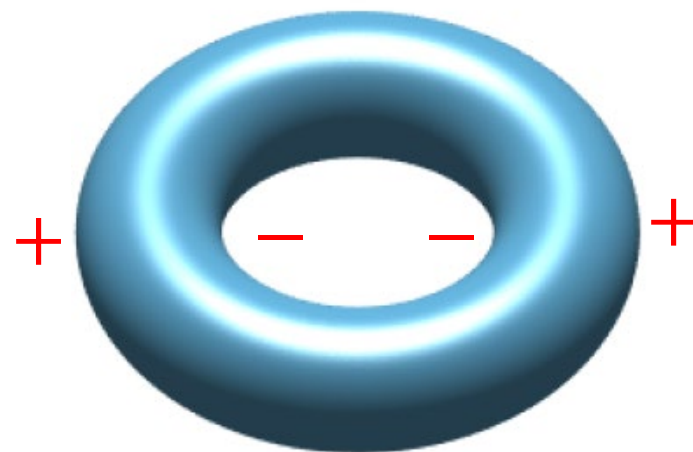
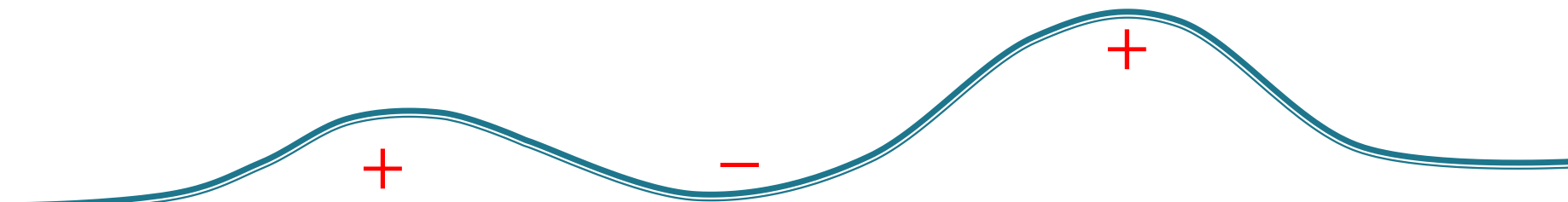
Phase diagram with different phonon strength



(a) $\xi_{ph} = 30\text{nm}, V_{ph} = 9.425\text{meV}$. (b) $\xi_{ph} = 50\text{nm}, V_{ph} = 7.76\text{meV}$ (c) $\xi_{ph} = 70\text{nm}, V_{ph} = 7.2845\text{meV}$.

$\lambda_{so} = 35\text{meV} \cdot \text{nm}$, $\xi_C = 4\text{nm}$, $R = 50\text{nm}$, $V_C = 50 \text{ meV} \cdot \text{nm}$, $\mu = -9.5\text{meV}$.

Extension to surface roughness/bump, ...

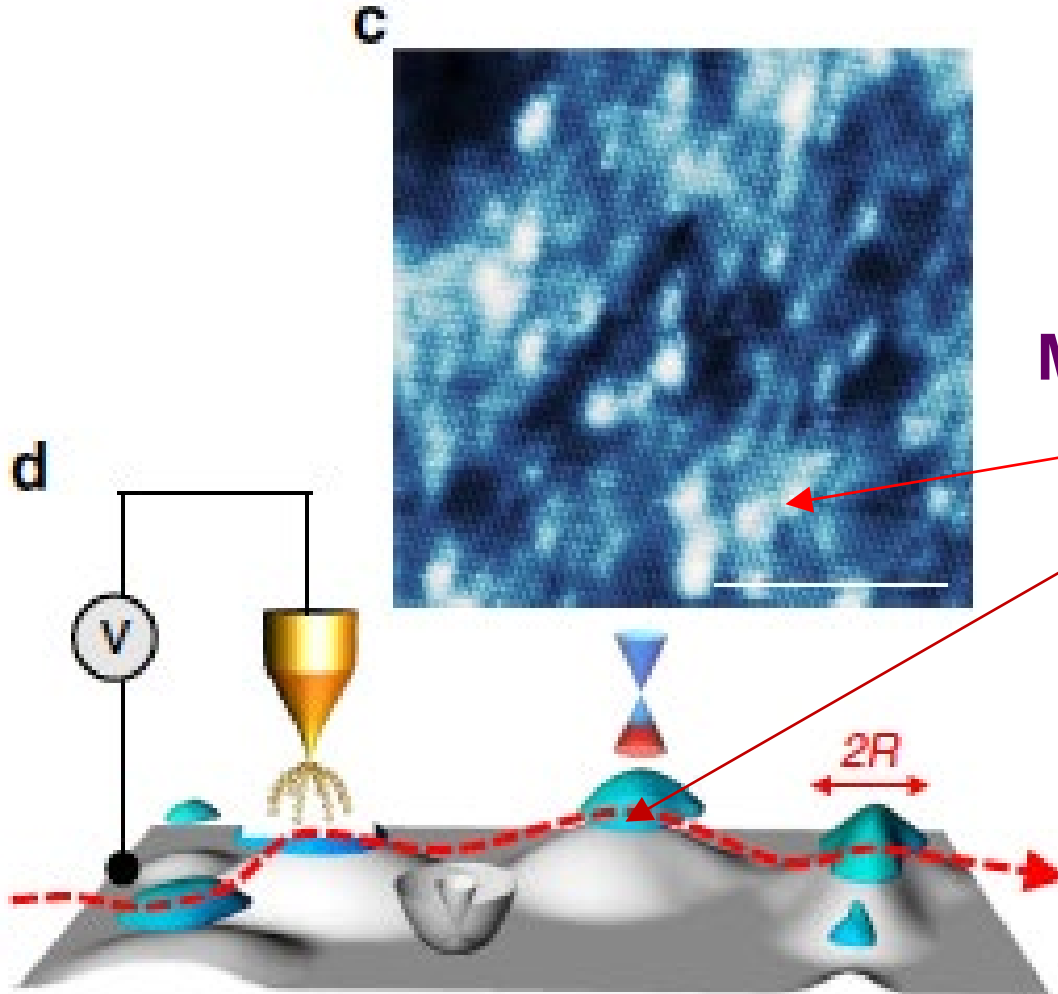


Threshold: $K_c \sim 1/(50\text{nm})^2$

Minimum Free energy:

One vortex occurs at bump with largest curvature

Experimental detection: surface superconductivity in Sb_2Te_3 with surface roughness ($R = 50$ nm or less, below 9K)



Majorana zero mode ?

L. Zhao et al,
Nat .Commun. 6, 8279 (2015).

Outline:

- Exotic superconductivity that can arise in topological materials

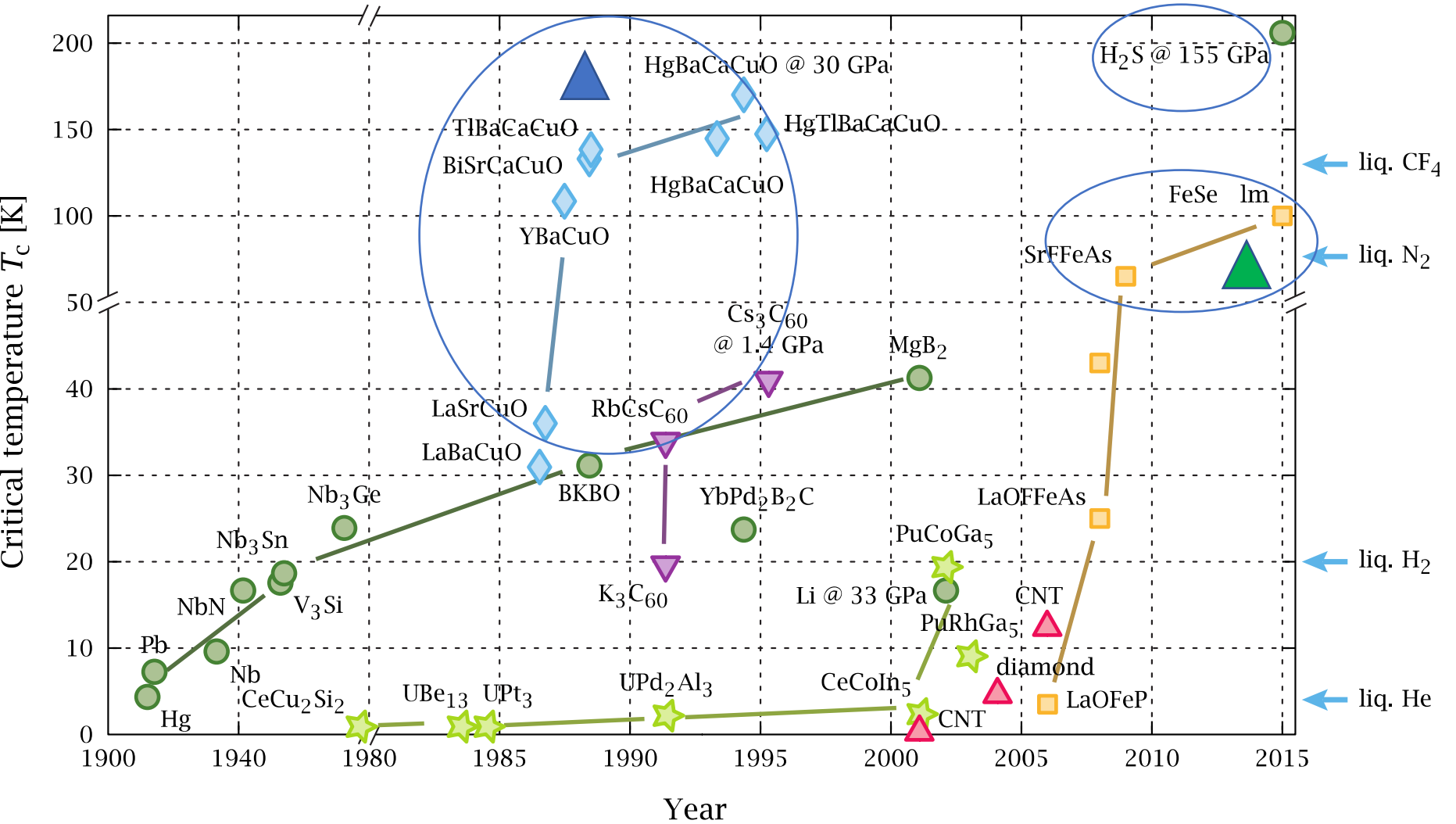
➤ Flat band superconductivity, charge density wave and superconducting pair density wave state

(Phys. Rev. B 98, 205103, 2018)

)

Routes to high T_c

Debye $2-3 \times 10^2$ meV
For metallic hydrogen



By PJRay - Own work, CC BY-SA 4.0,

<https://commons.wikimedia.org/w/index.php?curid=46193149>

T_c due to intermediate boson

$$k_B T_c = \hbar \omega_D e^{-1/Ng}$$

$$\text{or } k_B T_c = \Lambda e^{-1/Ng}$$

$\Lambda \sim$ the bandwidth of **intermediated boson**

T_c is limited by Λ , not by the strength of attractive interaction g !

Flat-band superconductivity

BCS Mean Field Theory:

$$\Delta_k = -\sum_{k'} V_{k,k'} \frac{\Delta_{k'}}{2E_{k'}} \tanh \beta E_{k'} \quad E_k = \sqrt{\xi_k^2 + \Delta_k^2} \quad \xi_k = \varepsilon_k - \mu$$

Flat band at Fermi energy: $\xi_k = \varepsilon_k - \mu = 0$

s-wave: $\Delta_k = \Delta, V_{k,k'} = -g/N$

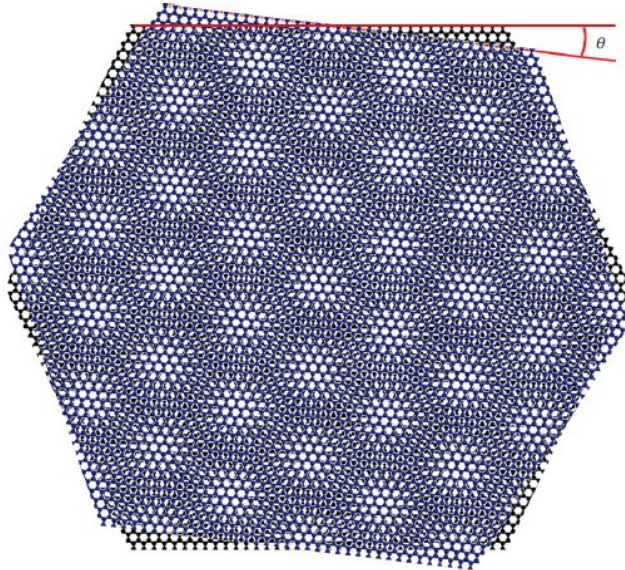
$$\Delta_k = -\sum_{k'} V_{k,k'} \frac{\Delta_{k'}}{2E_{k'}} \tanh \beta E_{k'} \Rightarrow 1 = g \left(\frac{1}{N} \sum_{k'} \right) \lim_{\Delta \rightarrow 0} \frac{\tanh \beta_c \Delta}{2\Delta}$$

$$k_B T_c = \frac{g}{2} \quad \longleftrightarrow \quad k_B T_c = \hbar \omega_D e^{-1/Ng}$$

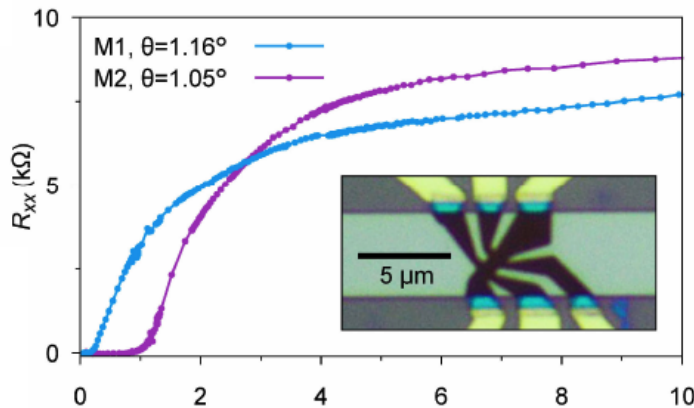
T_c is limited by g ! ($g \lesssim 0.1 \text{ eV}$ for phonon)

Surprised superconductivity in bi-layer graphene

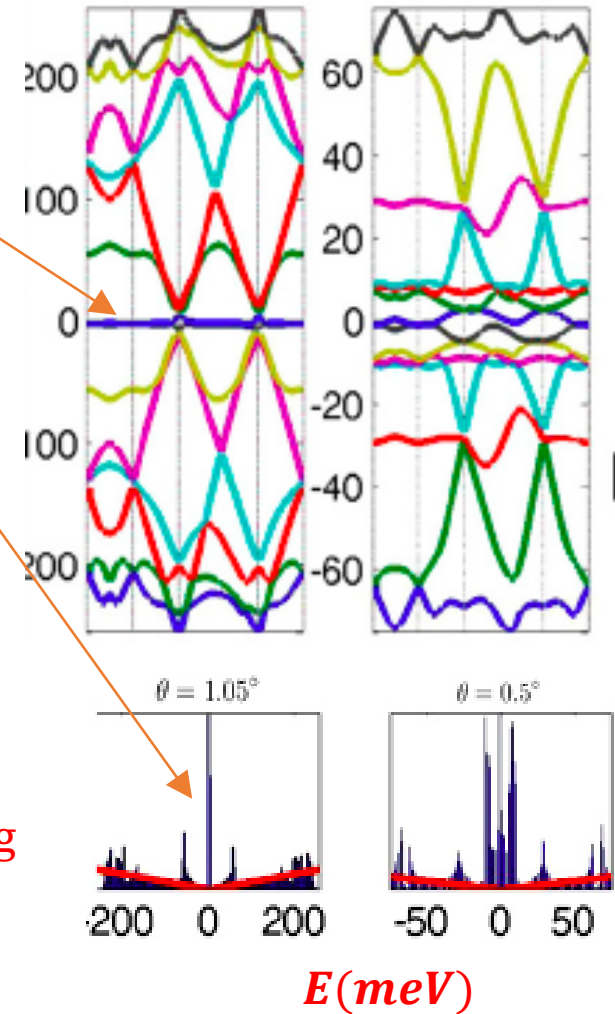
Flat band of bi-layer graphene twisted by $\theta = 1.1^\circ$



(Kinetic energy vanishes due to quantum interference
R Bristritzer, and A. H. MacDonald, PNAS 108, 12233, 2011)

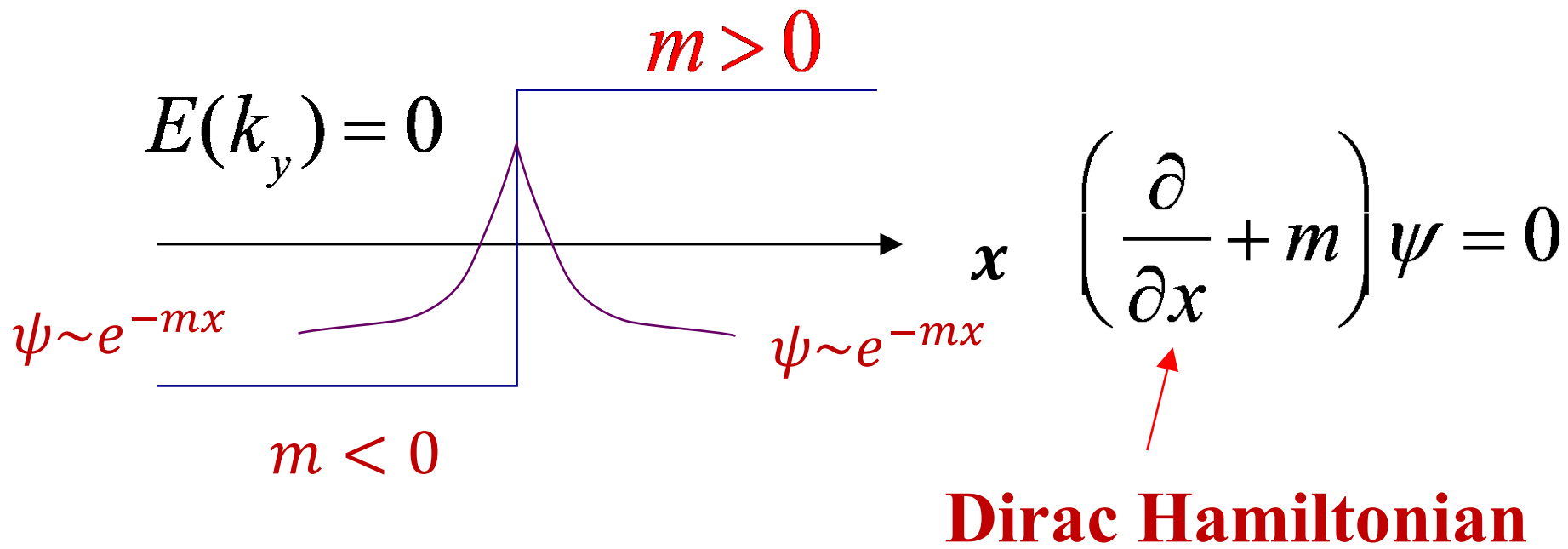


Graphene
non-superconducting
 $\rightarrow T_c = 1.7\text{K}$



(Pablo Jarrillo-Herrero's group),
<http://dx.doi.org/10.1038/nature26160>, 2018)

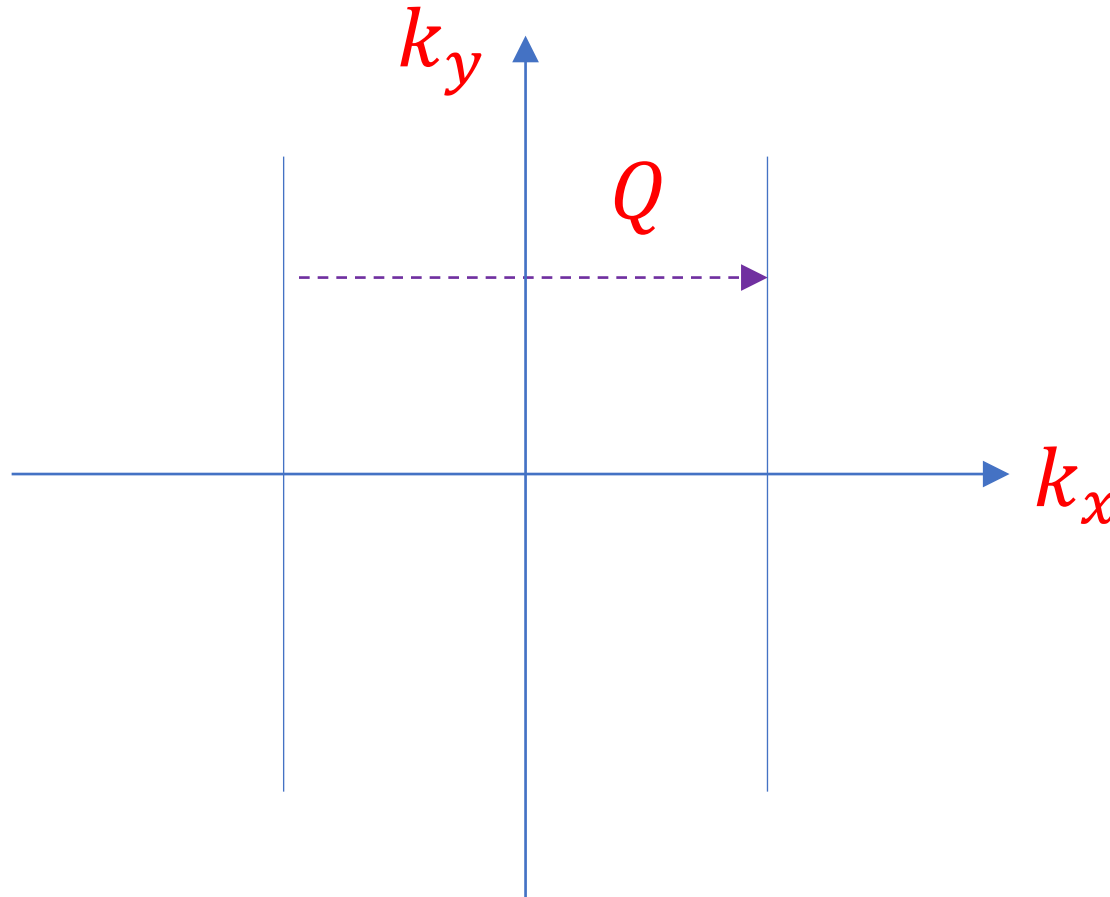
Topological flat band (domain wall Fermi)



Flat band



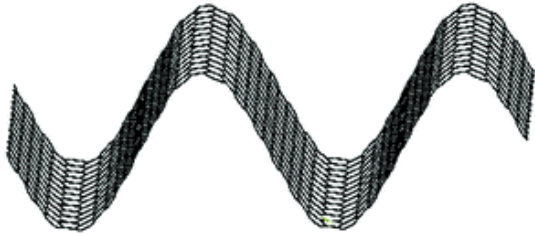
Problems: competing orders ?



charge density wave, spin density wave,

Creating Flat-bands in Strained Graphene ▲

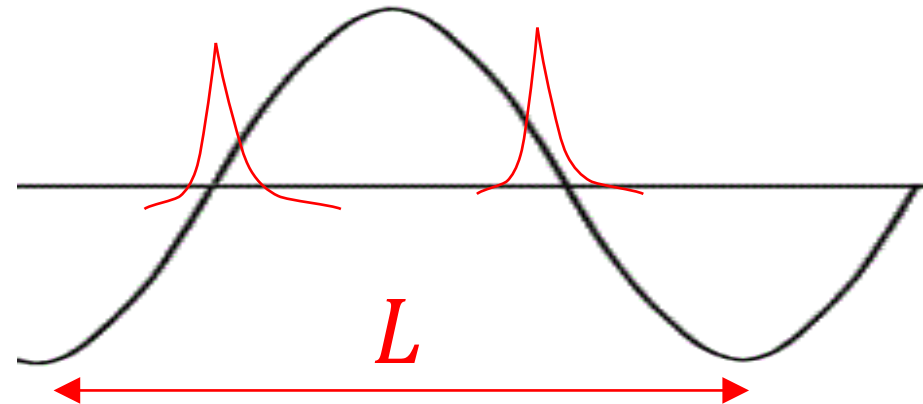
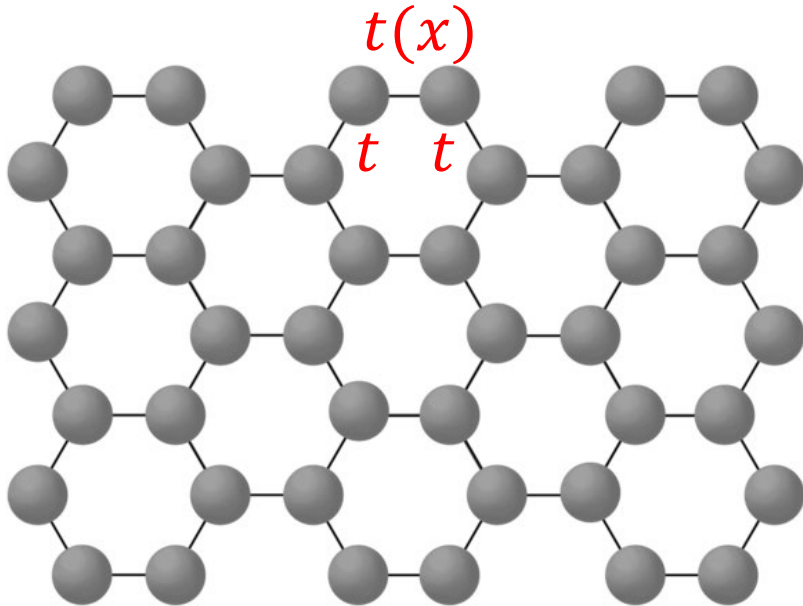
(Phys. Rev. B 98, 205103, 2018)



Strain due to ripples

$$t(x) = t(1 + \alpha \cos Qx)$$

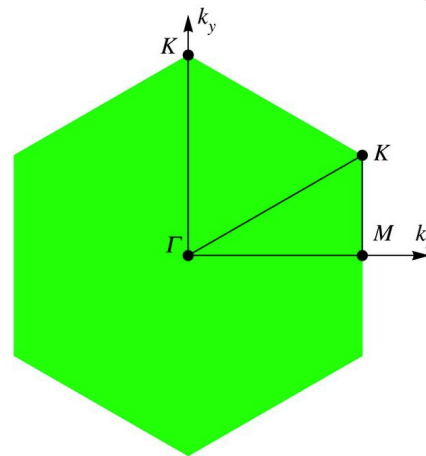
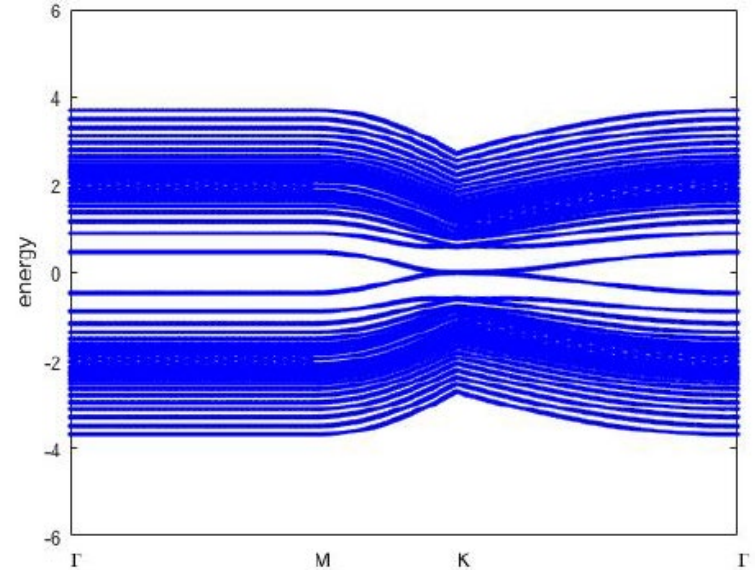
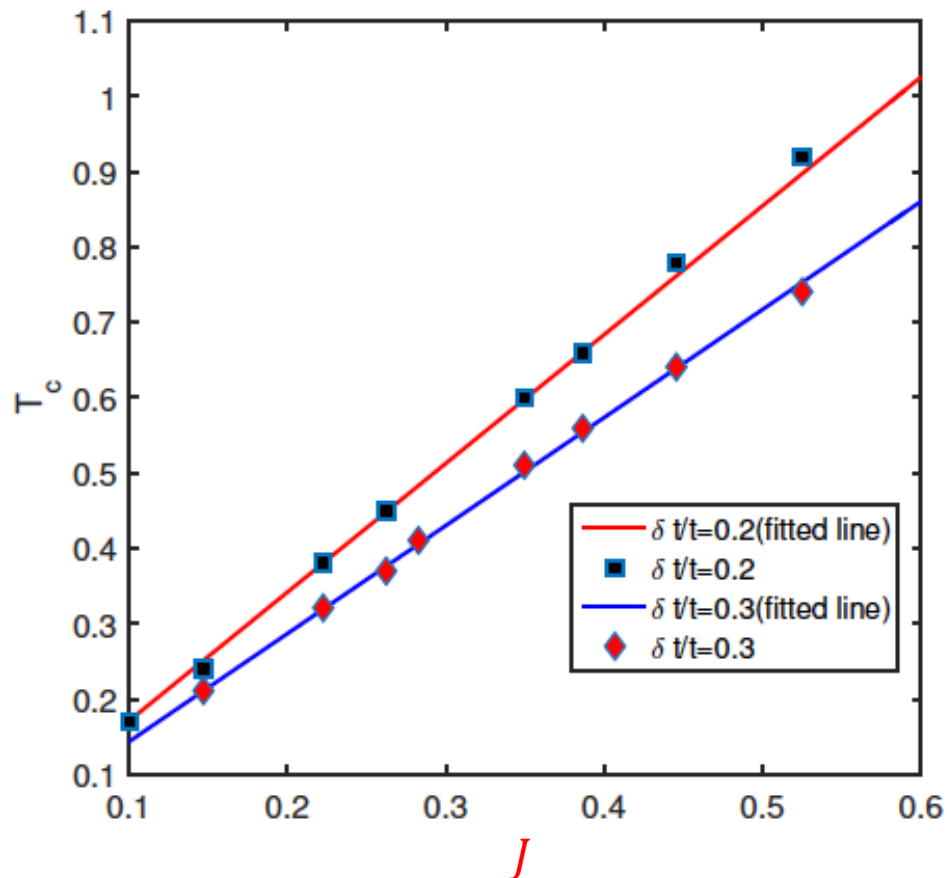
$$Q = 2\pi/L$$



$$H = \sum_{\langle i,j \rangle} -t_{ij} c_{i\sigma}^\dagger c_{j\sigma} + h.c. + J(\vec{s}_i \cdot \vec{s}_j - \frac{1}{4} n_i n_j)$$
$$\sum_{\sigma} c_{i\sigma}^\dagger c_{i\sigma} \leq 1$$

Enhanced T_c due to flat bands in large strain

$\alpha = 0.4$, period = 25

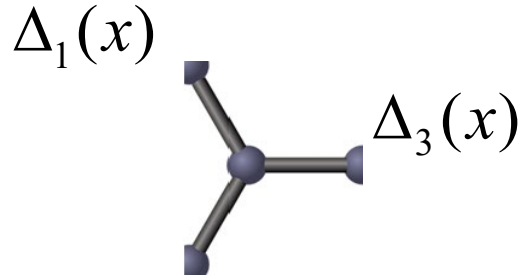


Dirac point

Anomalous density wave state

Mean fields:

$$\chi_{ij} = \sum_{\sigma} \langle c_{j\sigma}^{\dagger} c_{i\sigma} \rangle, \Delta_{ij} = \langle c_{j\downarrow} c_{i\uparrow} - c_{j\uparrow} c_{i\downarrow} \rangle$$



$$\Delta_s(x) \equiv \frac{1}{\sqrt{3}} (\Delta_1(x) + \Delta_2(x) + \Delta_3(x))$$

$$\Delta_{d_{x^2-y^2}}(x) \equiv \frac{-1}{\sqrt{6}} (\Delta_1(x) + \Delta_2(x) - 2\Delta_3(x))$$

$$\Delta_2(x) = \Delta_1^*(x)$$

$$\Delta_{d_{xy}}(x) \equiv \frac{-\text{Im}}{\sqrt{2}} (\Delta_1(x) - \Delta_2(x))$$

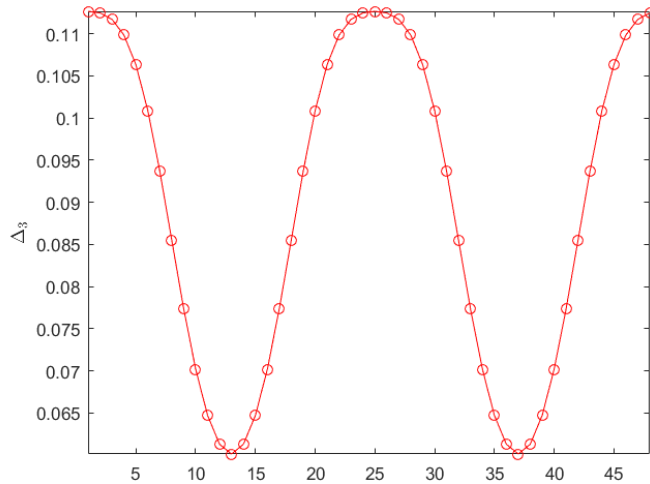
Expected: $Q = 2\pi/L, 2Q, 3Q, \dots$

$\Delta_3(x)$

Anomalous: $Q/2$

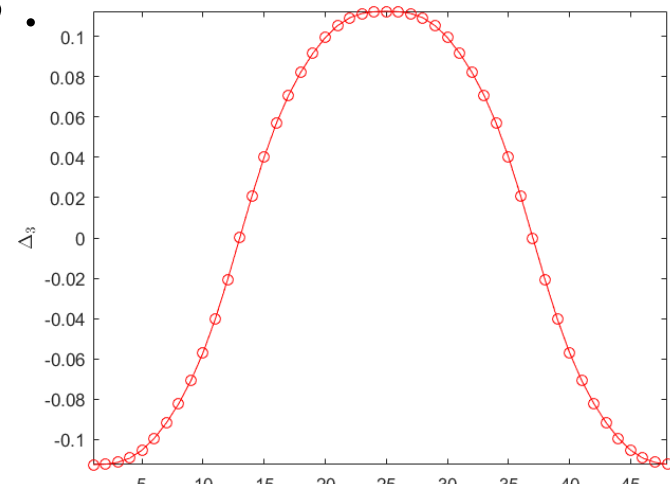
$\Delta_3(x)$

A:



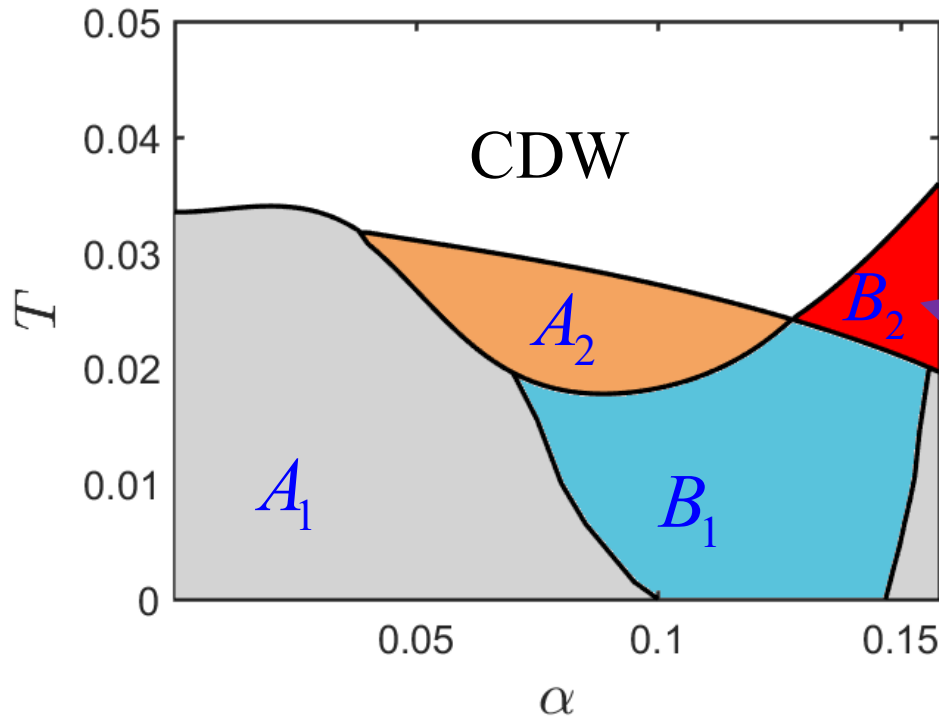
L

B:



$2L$

Typical Phase Diagram (hole doping $\delta = 0.15, L = 16$) --- with complicated density waves



$A_1, A_2,$ and B_1 :
 Non-vanishing uniform SC

B_2 :
 only PDW ($Q/2$)
 +CDW(Q) !

A_1 $S(0, Q), d_{x^2-y^2} + id_{xy}(0, Q)$
 CDW $(0, Q)$

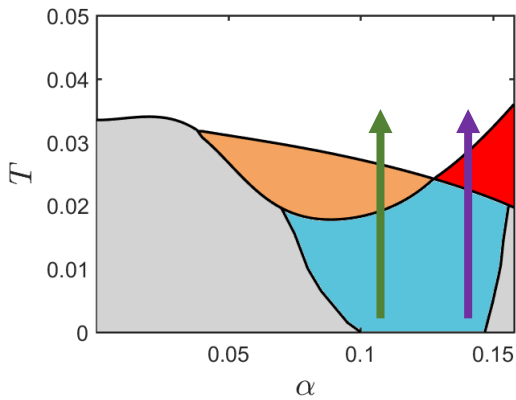
B_1 $S\left(\frac{Q}{2}\right), d_{x^2-y^2}\left(\frac{Q}{2}\right), id_{xy}(0, Q)$
 CDW $(0, Q, Q/2)$

A_2 $d_{xy}(0, Q)$
 CDW $(0, Q)$

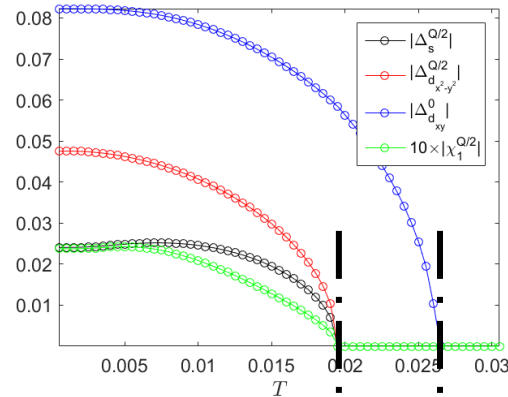
B_2 $S\left(\frac{Q}{2}\right), d_{x^2-y^2}\left(\frac{Q}{2}\right)$
 CDW(Q)

Stablized Cooper pair at finite Q : superconducting pair density wave state

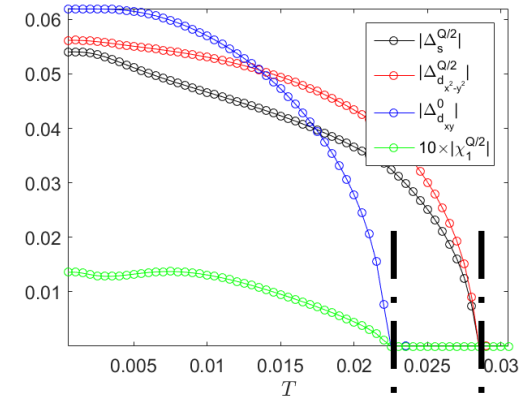
Gain energy through : $-\rho(Q)\Delta(-\frac{Q}{2})\Delta(-\frac{Q}{2})$



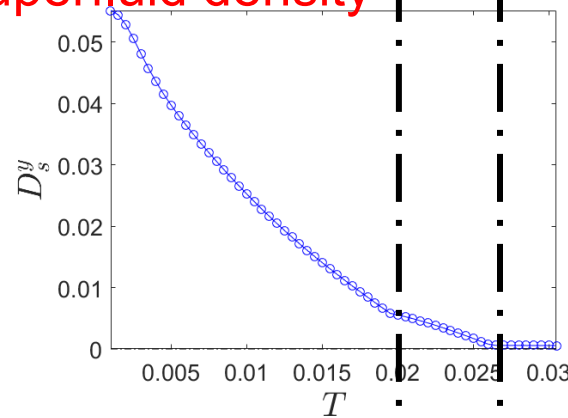
$\alpha = 0.11$



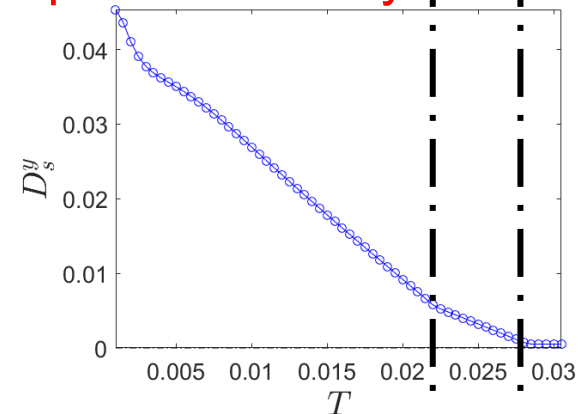
$\alpha = 0.14$



Superfluid density



Superfluid density



Conclusion and Summary

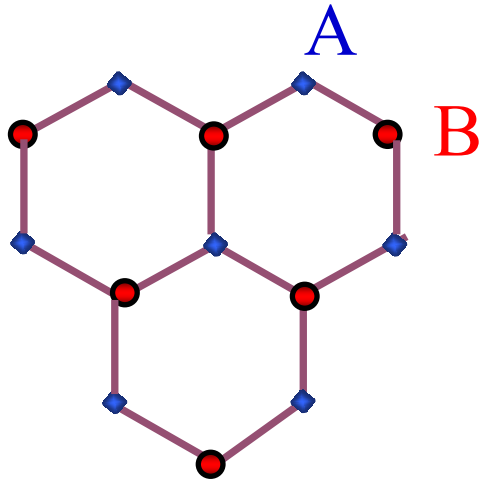
1. Quantum Oscillations in Kondo insulators:

Kondo screening itself undergoes oscillation in the presence of magnetic fields. It explains important features observed in experiments.

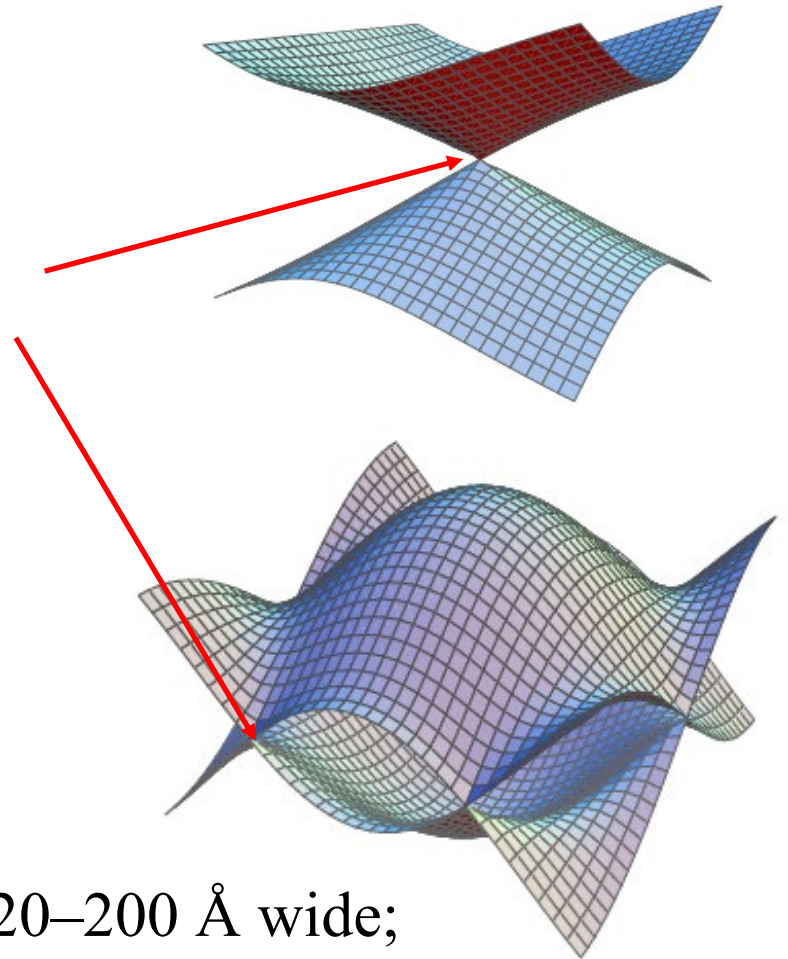
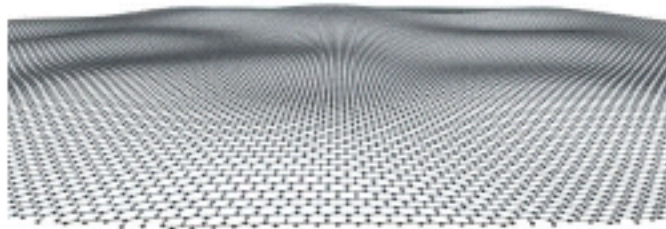
2. Unconventional Superconductivity

1. Spin-orbit hybridization in Kondo lattice provides a route to p-wave superconductivity characterized by Z_2 topological index.
2. A new route to topological superconductivity is possible through inter-surface pairing.
3. Singlet and triplet pairings are differentiated through thickness dependence. The spinfull triplet p+ip pairing dominates for thin films of topological insulators with thickness below 9-10QLs.
4. Experimental evidences of spinfull p-wave for Sb_2Te_3 nanoflakes are observed.
5. Curvature helps in converting surface superconductivity into topological superconductivity
6. Vortices can be spontaneously generated on a sphere and host Majorana zero mode.

2D Dirac Fermions in Graphene



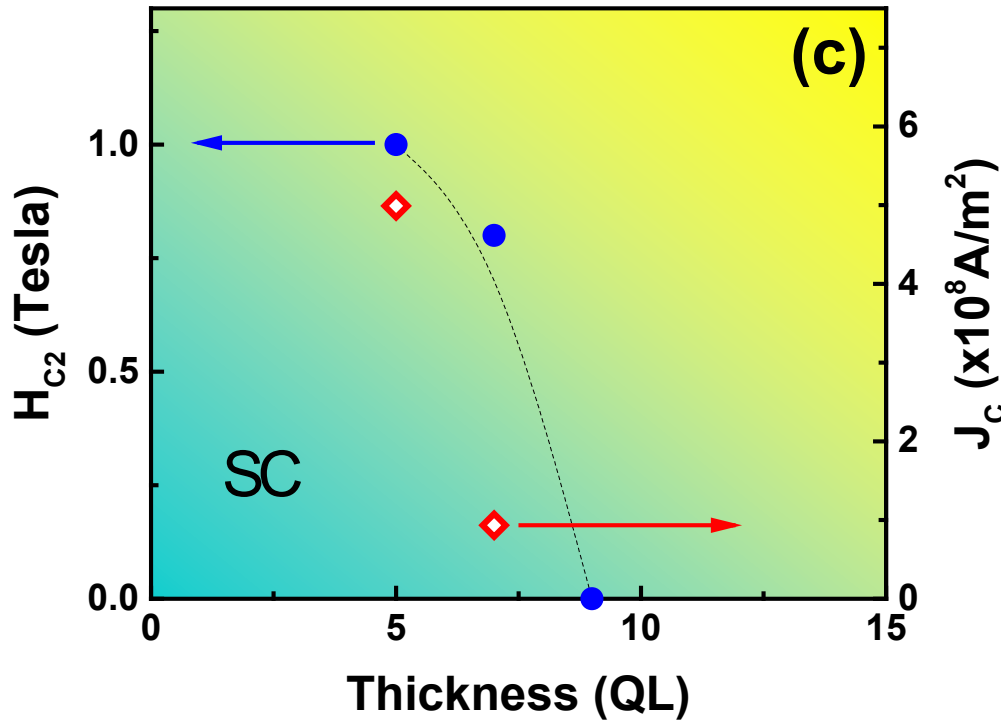
Dirac points



Ripples are of order 2–20 Å high and 20–200 Å wide;
Meyer et al., Nature 446, 60, (2007);
Fasolino et al., Nature Materials 6, 858 (2007)



Strong thickness dependent properties: critical current and fields



$$H_{c_2}^\perp(0) = \frac{\phi_0}{2\pi\xi^2}$$

$$\xi = 0.885\sqrt{\xi_0 l}, \quad l = d$$

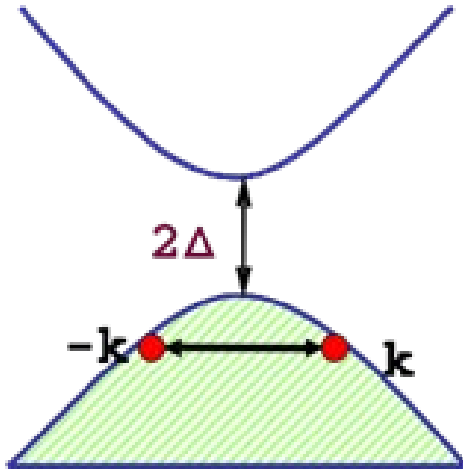
$$\xi_0 = \hbar v_F / \Delta \propto 1/T_c$$

$$H_{c_2}^\perp(0) \propto T_c / d$$

$J_c \propto$ current distribution factor

ratio of $J_c \approx$ ratio of conductivity in normal state

Conventional superconductors



$$\Delta_k = - \sum_{k'} V_{k,k'} \langle c_{-k\downarrow} c_{k\uparrow} \rangle$$

s-wave: $\Delta_k = \Delta$

$$= - \sum_{k'} V_{k,k'} \frac{\Delta_{k'}}{2E_{k'}} \tanh \beta E_{k'}$$

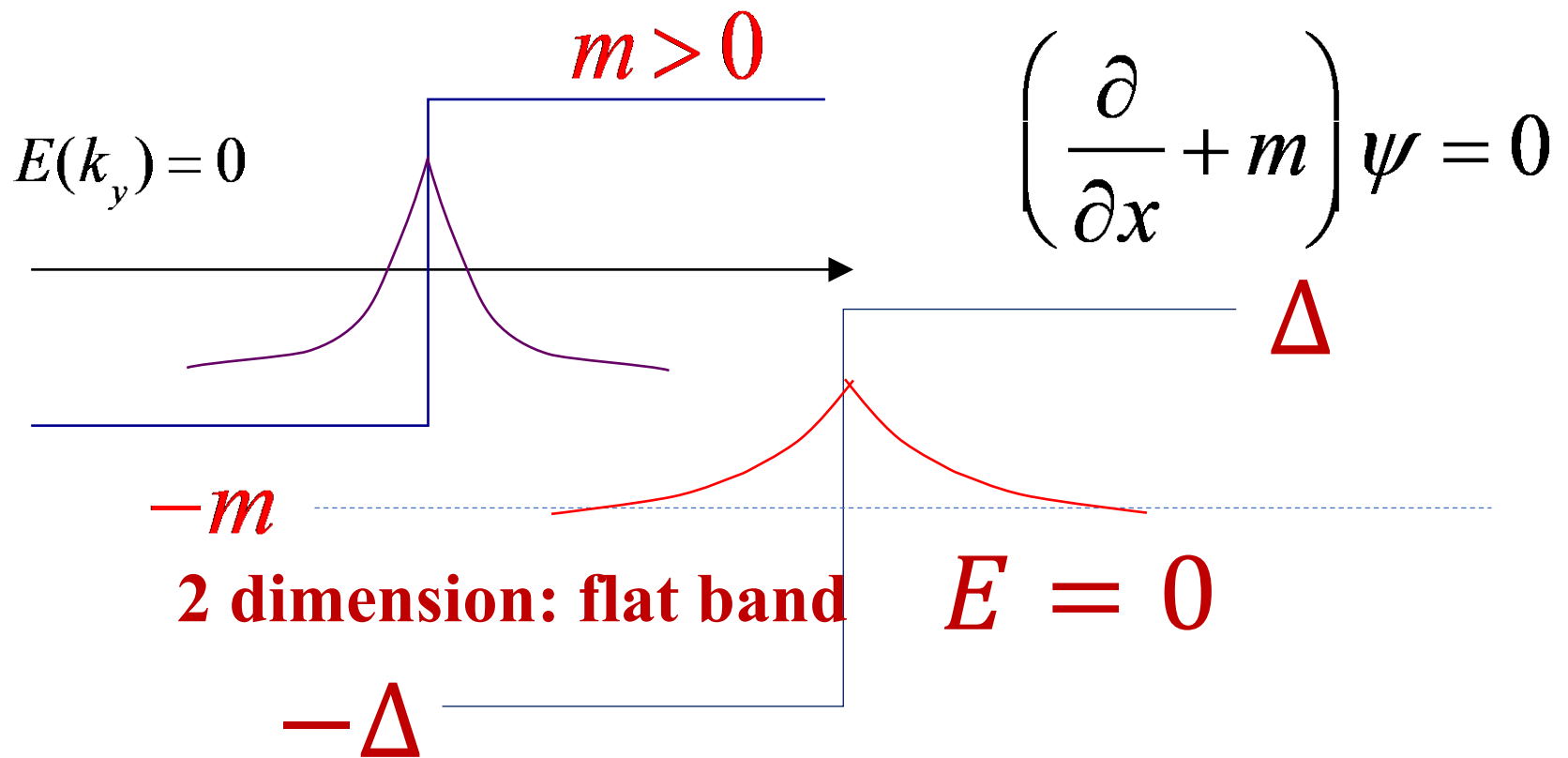
Mean field:

$$H = \sum_{k,\sigma} (\epsilon_k - \mu) c_{k\sigma}^\dagger c_{k\sigma} - \Delta_k c_{k\uparrow}^\dagger c_{-k\downarrow}^\dagger - \Delta_k^* c_{-k\downarrow} c_{k\uparrow}$$

$$k_B T_c = \hbar \omega_D e^{-1/Ng}$$

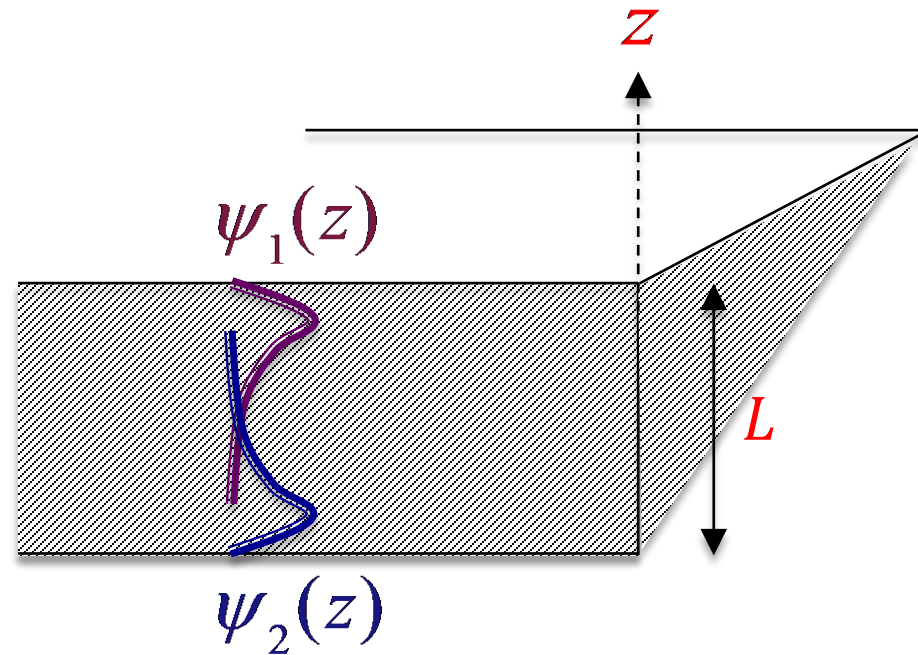
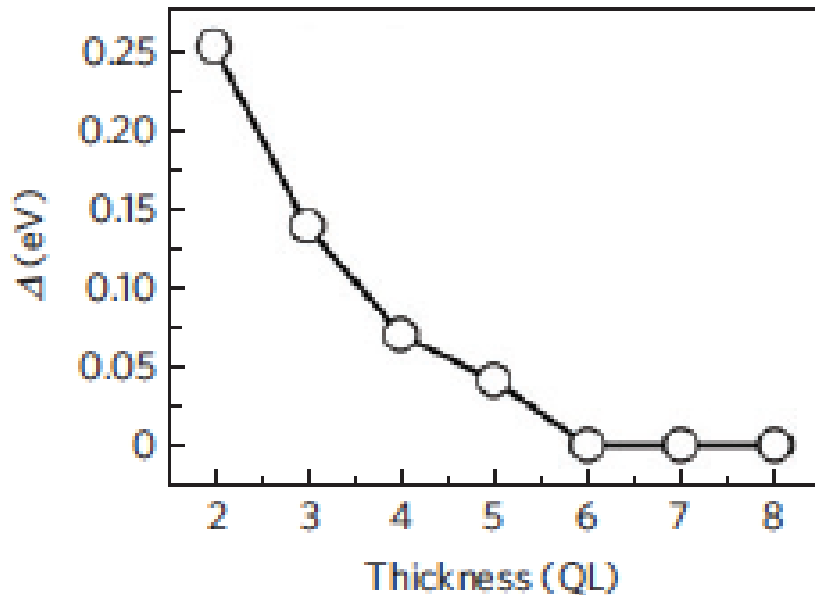
$N(\epsilon_F)$ = density of state

Domain wall fermions and flat-band



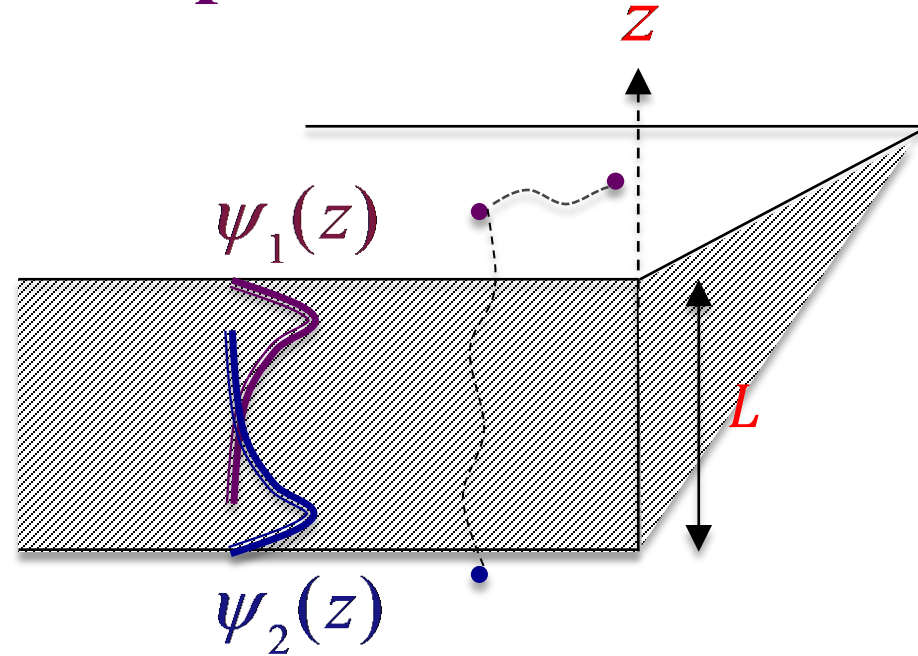
Origin of thickness dependence

Overlap of edge states: hybridization gap arises
 \Rightarrow Change of density of state



Origin of thickness dependence

Coulomb interaction:
 intra surface
 (min separation = 0)
 versus
 inter surface
 (min separation = L)



Fermi-energy dependent screened Coulomb interaction $V_q^C(z, z')$

$$G_q(z - z') = \frac{4\pi e^2}{\kappa} \frac{e^{-q|z-z'|}}{2q}$$

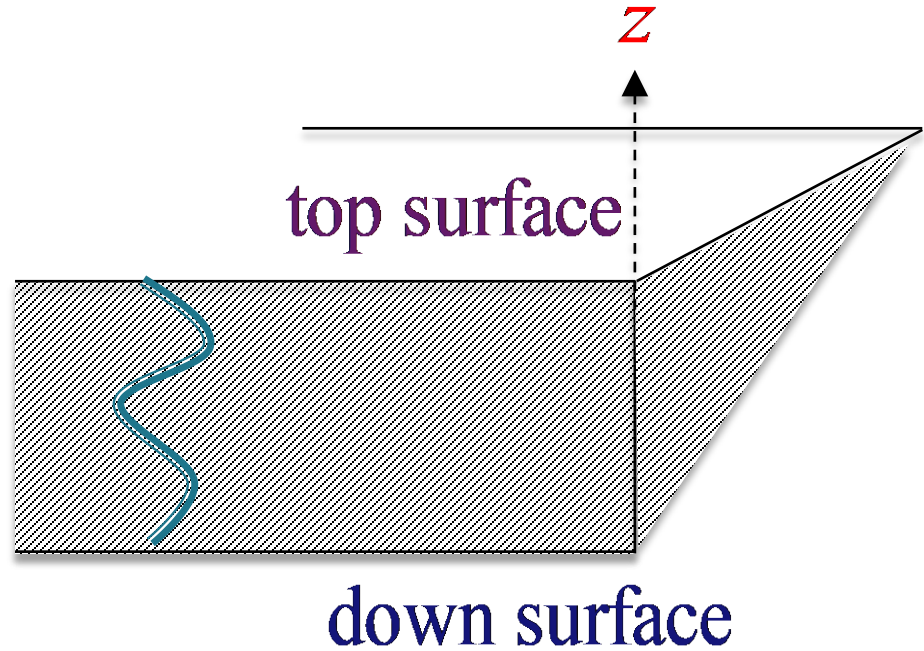
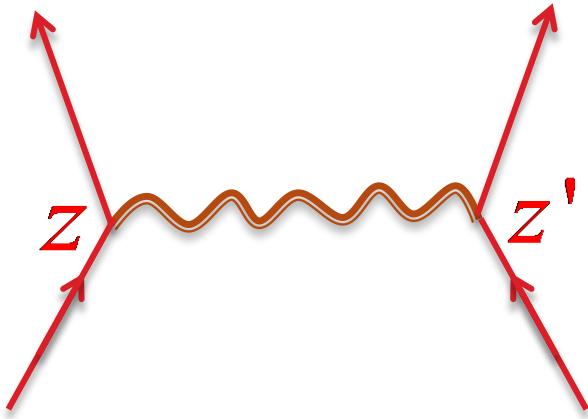
$$\left(\frac{d^2}{dz^2} - q^2\right)V_q^C(z, z') = -\frac{4\pi}{\kappa} \delta(z - z')$$

$$+2q_{TF} |\psi_1(z)|^2 V_1(z') + 2q_{TF} |\psi_2(z)|^2 V_1(z')$$

$$V_n(z) = \int dz' V_q^C(z', z) |\psi_n(z')|^2$$

Origin of thickness dependence

Electron-Phonon interaction



Phonon propagation: intra-surface versus inter-surface

$$V_q^P(z, z') = -\frac{[Z\hbar q \overline{G}_q]^2}{Ma^2} \sum_E \frac{\phi_E(z)\phi_E(z')}{E^2 + (\nu q)^2}$$

$\phi_E(z)$ = phonon wavefunction

$$\overline{G}_q = \iint dz dz' G_q(z, z')$$

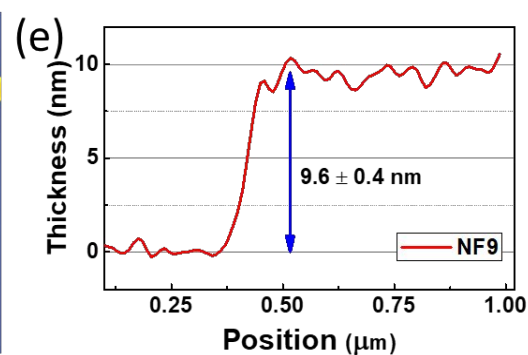
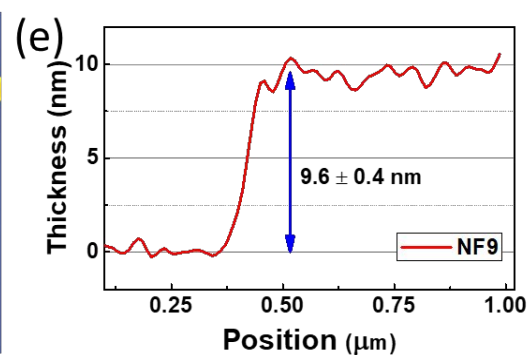
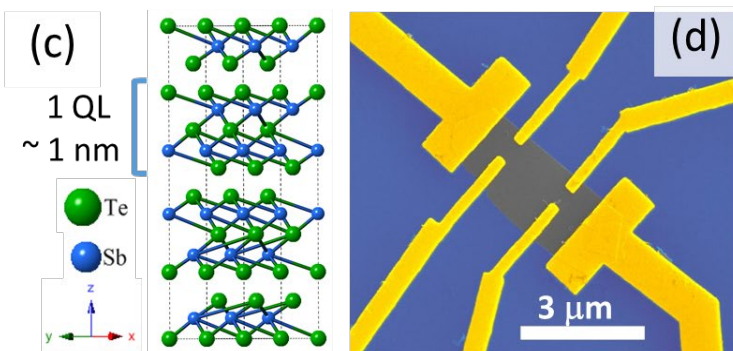
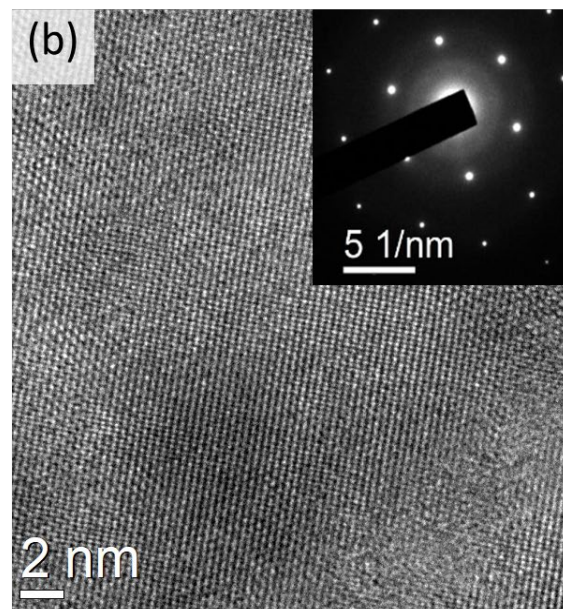
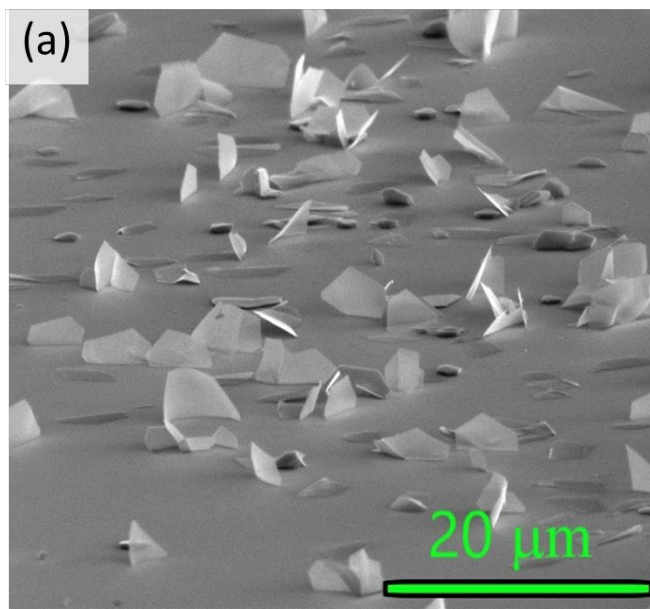
z direction: standing wave



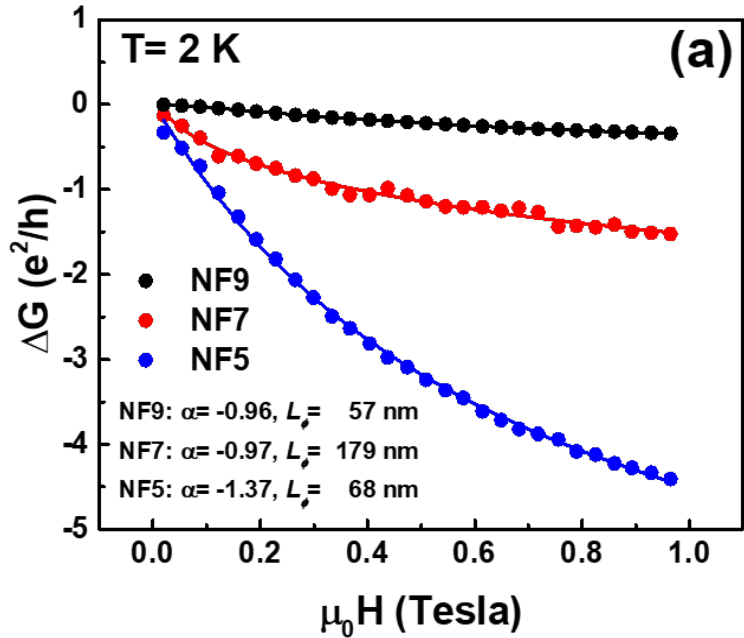
Experimental Evidences in Sb_2Te_3 nanoflakes

Physical vapor deposition (PVD)

Using polycrystalline Sb_2Te_3 on SiO_2/Si substrate



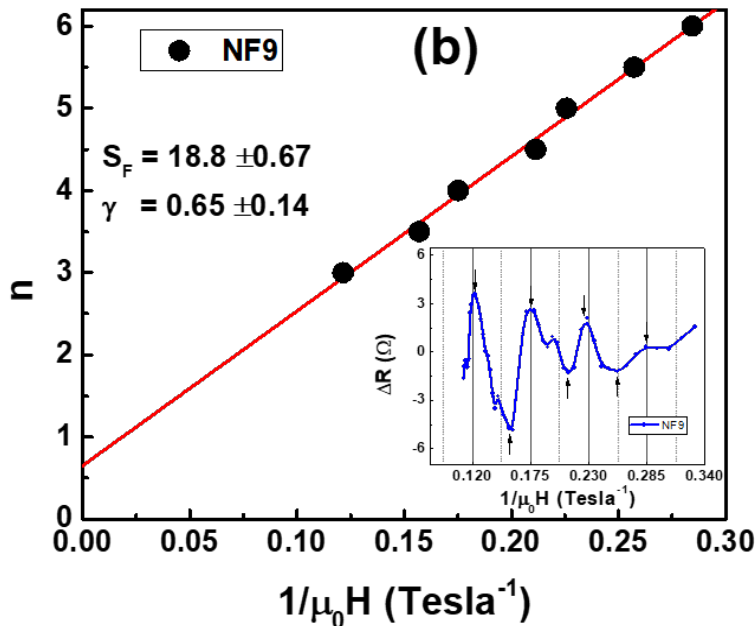
Evidences of surface states



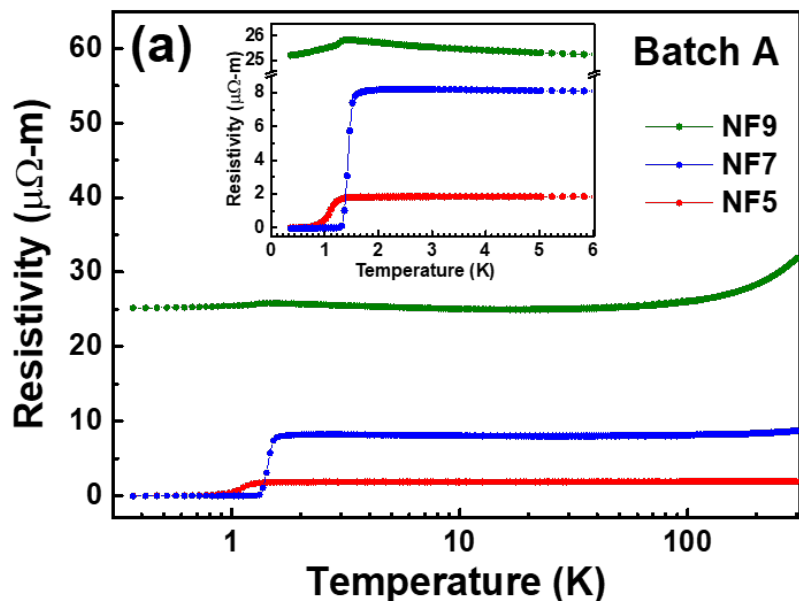
Weak anti-localization

$$\Delta G = -\frac{\alpha e^2}{2\pi^2 \hbar} \left[\ln \left(\frac{\hbar}{4eL_\phi^2 B} \right) - \psi \left(\frac{1}{2} + \frac{\hbar}{4eL_\phi^2 B} \right) \right]$$

Shubnikov-de Haas oscillations due to Landau levels



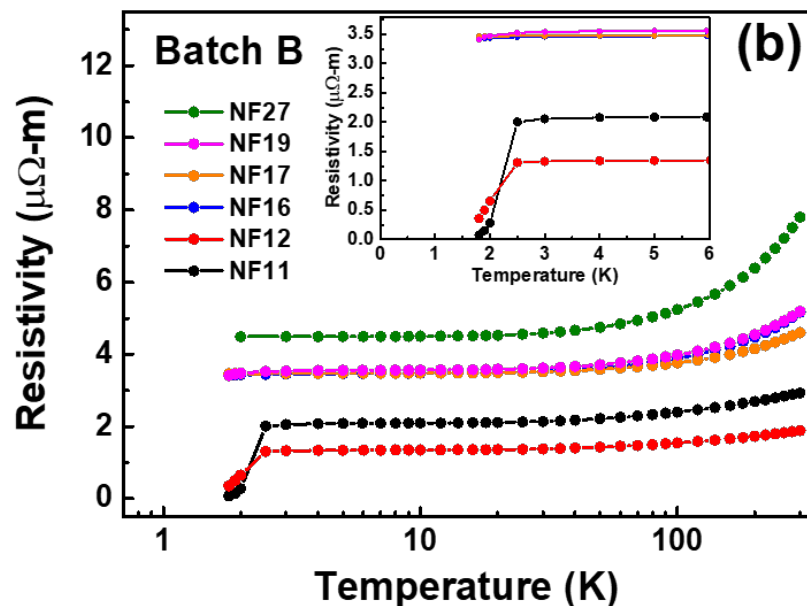
Transport Measurements



Superconducting transition $\leq 2.5\text{K}$

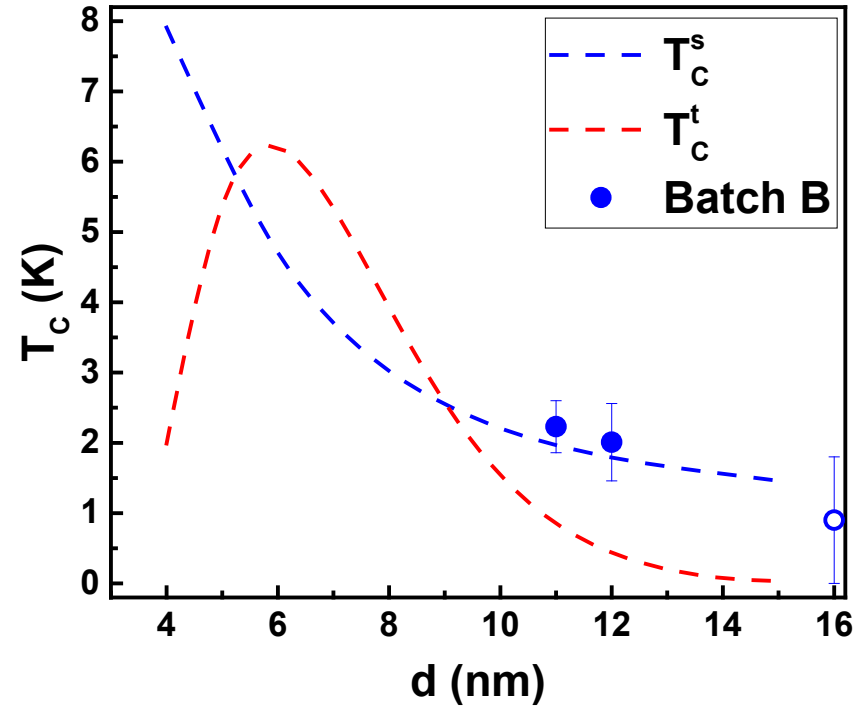
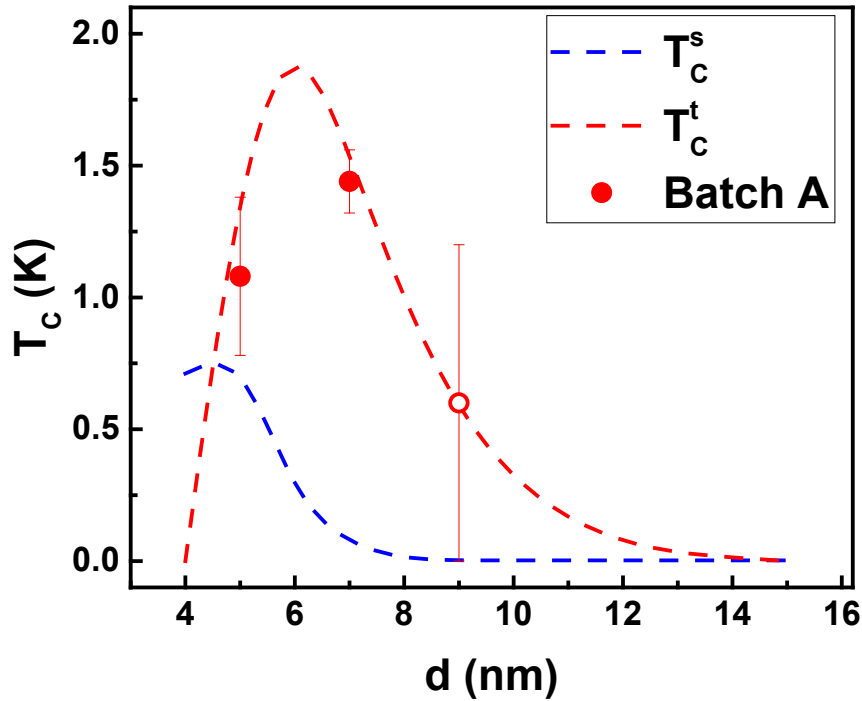
Two batches of samples grown under different condition (Te vapor pressure)

Batch A, smaller k_F



Batch B, larger k_F

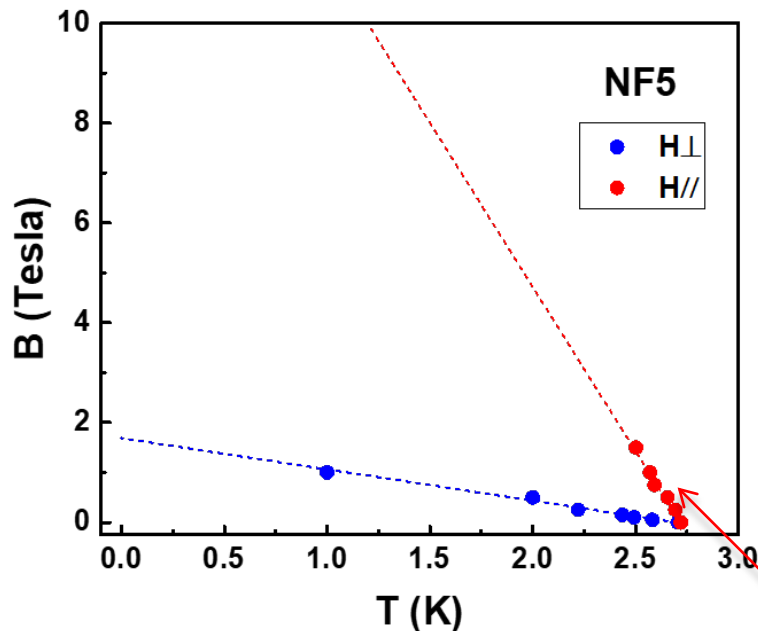
Transition temperatures: theory versus expt



1 quintuple layer $\approx 1nm$

The Debye temperature: 180K, the speed of phonon: $v_p = 2$ km/s, the decay length ξ_d about 1.2nm, the mass of ions: 124.7u, and the charge of ions being taken to be average of 3e and 4e, i.e., 3.53e.

Evidence of triplet pairing



$$\text{clean: } H_{c_2}^{\text{orb}}(0) = -0.73 \left. \frac{dH_{c_2}}{dT} \right|_{T=T_c} \times T_c$$

$$\text{dirty: } H_{c_2}^{\text{orb}}(0) = -0.69 \left. \frac{dH_{c_2}}{dT} \right|_{T=T_c} \times T_c$$

$H_{c_2}^{\square}(0)$ dominated by orbital effects

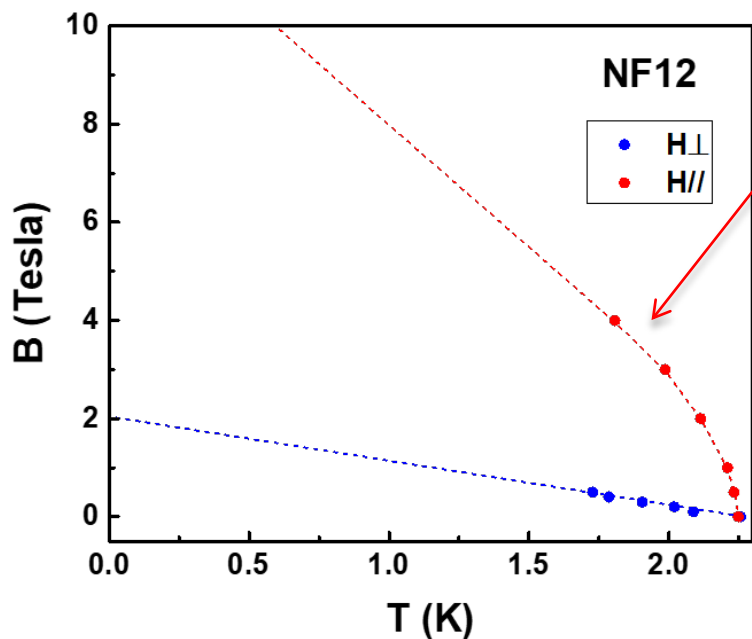
(Paramagnetic limiting is absent)

Estimated $H_{c_2}^{\text{orb}}(0) = 34 - 36$ Tesla

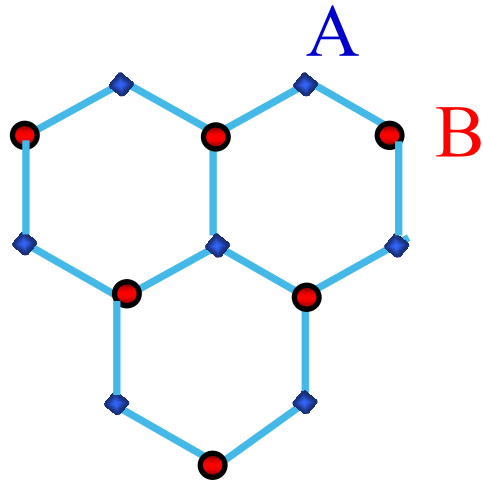
$$H_{c_2}^{\square}(0) \approx 12T \ll \text{Estimated } H_{c_2}^{\text{orb}}(0)$$

$$H_{c_2}^{\square}(0) = \text{Pauli limit}$$

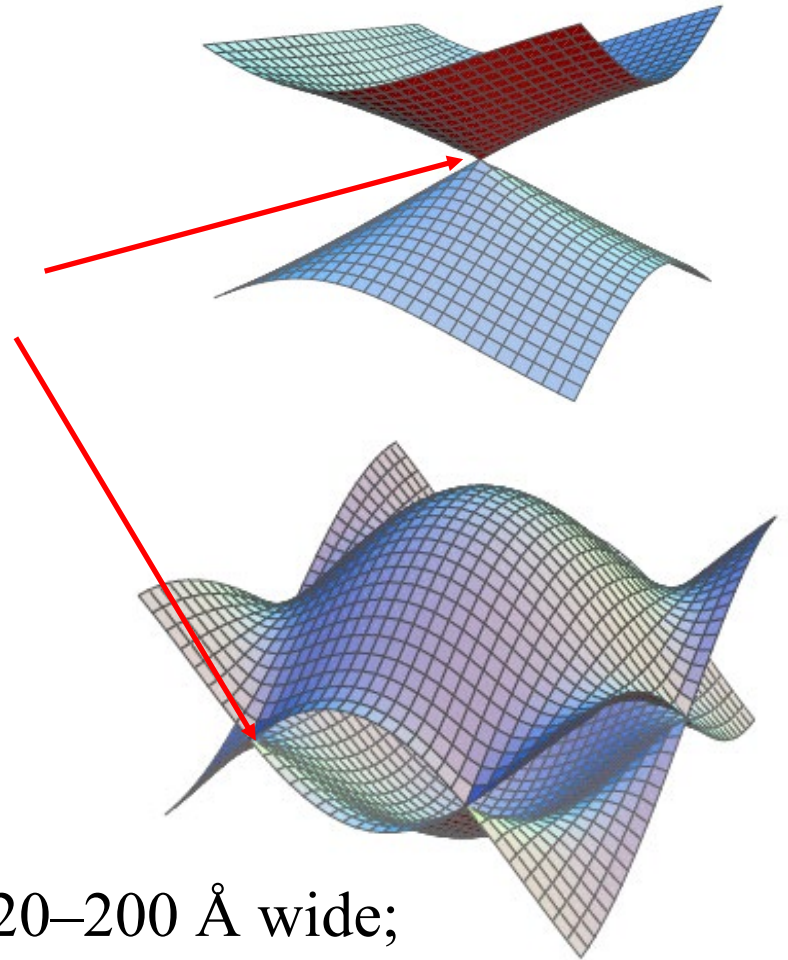
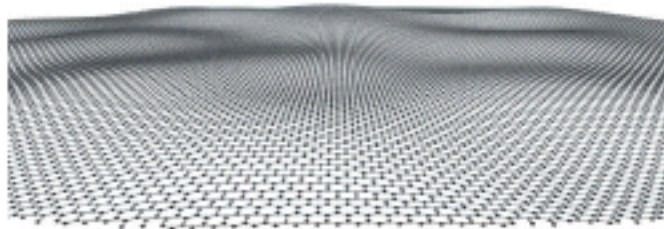
\Rightarrow singlet pairing dominates



2D Dirac Fermions in Graphene



Dirac points



Ripples are of order 2–20 Å high and 20–200 Å wide;
Meyer et al., Nature 446, 60, (2007);
Fasolino et al., Nature Materials 6, 858 (2007)

